



International Symposium
on
Ligaments & Tendons - IX

The Westin Casuarina Hotel

Las Vegas, NV

February 21, 2009

Edited by: Savio L-Y. Woo, PhD, DSc

Guoan Li, PhD

Gail Thornton, PhD

Rui Liang, MD

Ho-Joong Jung, MD

Matthew B. Fisher, BS

Volume 9

Symposium Sponsors

We gratefully acknowledge our kind sponsors. Without which, the symposium could not have taken place.



Department of Bioengineering
Swanson School of Engineering
University of Pittsburgh



Asian + American Institute for Research
and Education



FlexCell International Corporation



Musculoskeletal Research Center



Steadman + Hawkins Research
Foundation



Let People Move



Nicola's Foundation



DonJoy Orthopedics



National Science Foundation
Engineering Research Center for
Revolutionizing Metallic Biomaterials

Wyeth

Wyeth

International Symposium on Ligaments & Tendons-IX

The Westin Casuarina Hotel
Las Vegas, NV

Welcome!

Welcome to sunny Las Vegas and the Ninth International Symposium on Ligaments and Tendons (ISL&T-IX)!

Once again, we have reunited with our friends and colleagues for another lively scientific discussion of state-of-the-art research on ligaments and tendons. We are pleased that this meeting continues to be a place where students as well as junior and senior level biologists, engineers and clinicians can get together to exchange ideas, learn from one another, and establish collaborations.

Consistent with that theme, this year's program features multidisciplinary topics starting with an in-depth discussion on the ACL and Joint Kinematics followed by a look at Tissue Healing & Mechanics. Then, the focus will shift to the latest findings in the area of Tendinopathy, followed by exciting results on Biology & Biochemistry of Ligaments and Tendons. Keeping with the high energy, we will discuss the Biomechanics of the Shoulder. Wrapping up the discussion will be topics on Scaffolds for Functional Tissue Engineering Approaches.

We would especially like to thank our sponsors, the International Program Committee, and the International Advisory Committee, for supporting and maintaining the high quality of this meeting. Since this will be the final ISL&T meeting organized at the MSRC, we are a little saddened. However, we are enthusiastic at the bright, young talent in the ligament and tendon field and look forward to an exciting ISL&T next year. Finally, we would like to thank you for your enthusiastic participation year after year.

Please enjoy the day!

With our very best wishes,

The ISL&T-IX Organizing Committee

Savio L-Y. Woo, PhD, DSc
Rui Liang, MD
Ho-Joong Jung, MD
Matthew B. Fisher, BS
Diann DeCenzo, M.S.



Musculoskeletal Research Center, Department of Bioengineering, Swanson School of Engineering,
University of Pittsburgh

General Information

Aims of the Symposium

The *International Symposium on Ligaments & Tendons* provides a forum to discuss state-of-the-art ligament and tendon research. By bringing together some of the best minds in our field, we hope to address challenging problems in ligament and tendon biomechanics and biology, and set new research directions that hold great potential for the future.

Planning Committee

Savio L-Y. Woo, PhD, DSc, Chair
Rui Liang, MD
Ho-Joong Jung, MD
Matthew B. Fisher, BS
Diann DeCenzo, MS - Treasurer

International Program Committee



Guoan Li, PhD, Co-Chair

Bioengineering Laboratory, Department of
Orthopaedic Surgery, Massachusetts General
Hospital/Harvard Medical School, USA

Paul Ackermann, MD (Europe)
Chih-Hwa Chen, MD (Asia)
Kathy Derwin, PhD (North America)
Vincent Wang, PhD (North America)
Toru Fukubayashi, MD (Asia)
Jo Hannafin, PhD (North America)
Zong-Ming Li, PhD (North America)
Martha Murray, MD (North America)
Roger Smith, PhD (Europe)
Kurt Spindler, MD (North America)
Harukazu Tohyama, PhD (Asia)
Kazunori Yasuda, MD (Asia)
Cy Frank, MD (North America)



Gail Thornton, PhD, Co-Chair

McCaig Institute for Bone and Joint Health,
Department of Surgery and Civil Engineering,
University of Calgary, Canada

Michael Bey, PhD (North America)
David Corr, PhD (North America)
Braden Fleming, PhD (North America)
Hiromichi Fujie, PhD (Asia)
Ranjan Gupta, MD (North America)
Catherine Kuo, PhD (North America)
Helen Lu, PhD (North America)
Graham Riley, PhD (Europe)
Louis Soslowsky, PhD (North America)
Stavros Thomopoulos, PhD (North America)
Michael Torry, PhD (North America)
Ray Vanderby, PhD (North America)

Instructions to Presenters

I. Podium Presenters

The time for presentations has been limited, in favor of discussion. Please see the presentation formats listed below. Your moderators have been asked to adhere to the time allotted for your presentation as well as the number of slides.

Important: All speakers are asked to check-in with the session moderators 15 minutes before the session in which they will present to meet the projectionist and the moderator.

Presentation Requirements

- *For 15 minute time slots*
 - ◊ 10 min. presentations each immediately followed by a 5 min. discussion.
 - ◊ Maximum **10 PowerPoint slides** for computer presentation.

- *For 5 minute time slots*
 - ◊ 5 min. presentations followed by a 5 min. group discussion of 2-3 papers.
 - ◊ Maximum **5 PowerPoint slides** for computer presentation.

An Important Note on Slides

Kindly note that all speakers must be prepared to present their paper using PowerPoint projection. We ask that you send your PowerPoint presentation file to us by **February 13, 2009** so that we can load all talks into a master computer prior to the symposium. Please make sure that you clearly label your file with the author's name and the title of your presentation.

Note: In view of time and the large number of talks, there will be no opportunity to use your personal computer or load your PowerPoint file during the symposium.

II. Poster Presenters

All posters should be no larger than 34 inches x 45 inches (86.4 cm x 114.3 cm). Poster boards will be available in the lobby. Your poster space will be indicated by the corresponding page number of the poster in the program book. Please set up your poster between 7:30 - 8:00 am and take them down at 6:00 pm.

Note: An opportunity has been provided for you to present your posters orally during different breaks. You will be given 2 minutes to present and this will be coordinated by the poster moderators. Please be sure to attend to your poster at the assigned time.

Symposium Awards

We are proud to continue to recognize our outstanding papers presented at the ISL&T. All these awards are designed to stimulate high quality scientific research by investigators in the study of ligaments and tendons. The awardees will be selected by members of the program committee based on the quality of the abstract and presentation as well as the overall merit of the study.

To acknowledge the work by students, fellows, and residents, we will provide the following two awards:

Best Student Paper Award

Best Research Fellow Paper Award

To be eligible, the presenters must be the first author of the abstract. Each award consists of a certificate and a check for \$200 (donated by FlexCell International Corporation).

Best Poster Award

For the fourth year, a poster award will also be presented. This award consists of a certificate as well as a check for \$200 (donated by FlexCell International Corporation).

Banquet

Joyful House Chinese Cuisine

4601 Spring Mountain Road

Las Vegas, NV 89102

6:45-7:30 pm Reception & Cocktail Hour (Cash Bar)

7:30-9:30 pm Dinner & Award Ceremony

The restaurant is 2.5 miles away from the Hotel. Please take a taxi for transportation to the restaurant.

PROGRAM

7:30 AM **Registration/Check-In and Continental Breakfast**

8-8:20 AM **Opening Remarks**
Savio L-Y. Woo

Podium Session 1: ACL Reconstruction

Moderators: Mario Lamontagne, PhD & Giuliano Cerulli, MD

8:20-8:35 AM **Invited Lecture** 12
My clinical and experimental challenges to develop ideal ACL reconstruction
K Yasuda

8:35-8:50 AM Lengthening at the fixations and increase in anterior laxity are small during the 14
first four months of implantation after soft-tissue allograft anterior cruciate
ligament reconstruction
CK Smith, ML Hull, SM Howell

8:50-8:55 AM The relationship between graft tunnel position and in vivo knee kinematics 15
after ACL reconstruction
JH Wang, S Tashman

8:55-9:00 AM The relationship between closed kinetic chain strength of the lower limb and 16
jumping performance in ACL-deficient subjects and ACL-reconstructed
subjects using anatomical double-bundle reconstruction
H Tohyama, M Ueda, T Chiba, M Yuri, K Ikoma, K Yasuda

9:00-9:05 AM **Discussion**

Podium Session 2: Knee Kinematics & Mechanics

Moderators: Michael Torry, PhD & Harukazu Tohyama, PhD

9:05-9:20 AM Estimation of the upper bound of the in-vivo forces in the anterior cruciate 17
ligament
A Hosseini, TJ Gill, G Li

9:20-9:25 AM Total knee and ACL force for a stimulated in-vivo motion: A comparative 18
study between human and ovine
ST Herfat, DV Boguszewski, JT Shearn, DL Butler

9:25-9:30 AM Force contributions in an ovine knee during simulated in-vivo motion 19
DV Boguszewski, ST Herfat, JT Shearn, DL Butler

9:30-9:35 AM	Discussion	
9:35-9:40 AM	In-vitro evaluation of suture augmentation techniques after ACL injury <i>MB Fisher, HJ Jung, PJ McMahon, SL-Y Woo</i>	20
9:40-9:45 AM	Ex-vivo knee kinematics in ACL-deficient knee. A stereophotogrammetric study <i>F Margheritini, A Cereatti, M Donati, PP Mariani, A Cappozzo</i>	21
9:45-9:50 AM	Discussion	
9:50-9:55 AM	Quantitative clinical assessment of tibial rotation using an electromagnetic tracking system <i>JE Tibone, MT Vercillo, MH McGarry, TQ Lee</i>	22
9:55-10:00 AM	The three slopes of the tibial plateau: Impact on knee biomechanics <i>J Hashemi, N Chandrashekar, B Gill, J Slauterbeck, R Schutt, H Mansouri, E Dabezies, B Beynnon</i>	23
10:00-10:05 AM	Discussion	
10:05-10:35 AM	Break and Poster Session 1 Moderators: Sinan Karaoglu, MD & Christos Papageorgiou, MD	
	The influence of the knee hydrarthrosis on the muscle recovery after anterior cruciate ligament reconstruction <i>T Sakurai, T Fukubayashi, M Fukano, S Sasaki</i>	24
	Ligament creep and fatigue responses are similar for different rabbit breeds <i>GM Thornton, SJ Bailey, NM Chamberland</i>	25
	Mechanical testing of engineered fibers derived from human dermal fibroblasts: methods and feasibility <i>NR Schiele, RA Koppes, DM Swank, DB Chrisey, DT Corr</i>	26
	Gene expression and protein analysis in calcific tendinopathy of human rotator cuff <i>F Oliva, A Grasso, N Maffulli</i>	27
	Effect of Dihydrotestosterone on cultured human tenocytes form intact supraspinatus tendon <i>L Ruzzini, UG Longo, F Franceschi, A Cittadini, A Sgambato, N Maffulli, V Denaro</i>	28

Transglutaminases expression in mice tendons and humans supraspinatus tendon ruptures <i>F Oliva, U Tarantino, M Celi, N Maffulli</i>	29
Influence of fasting plasma glucose levels in the pathogenesis of rotator cuff tears <i>UG Longo, F Spiezia, F Franceschi, F Forriol, N Maffulli, V Denaro</i>	30
Response of a stem cell-based self-assembled tissue (scSAT) to cyclic tension <i>A Ogawa, K Saito, W Ando, N Nakamura, H Fujie.</i>	31
Local vitamin C injection reduced tendon adhesion in a chicken model of injured flexor digitorum profundus tendon injury <i>SC Fu, LK Hung, A Shum, YW Lee, TY Mok, PYY Lui, KM Chan</i>	32
Bioengineered cambial layer progenitor cell sheets transplantation for tendon-bone healing <i>CH Chang, CH Chen, HW Liu, SW Whu, SH Chen, JC Yeh, MY Wu, IH Lin, HJ Sun, GH Hsiue</i>	33

Podium Session 3: Ligament & Tendon Healing & Mechanics

Moderators: Louis Soslowsky, PhD & David Butler, PhD

10:35-10:50 AM	The effects of surface treatment with lubricin after flexor tendon repair <i>C Zhao, YL Sun, KN An, GD Jay, SL Moran, PC Amadio</i>	34
10:50-11:05 AM	Healing ligaments rupture consistently faster during fatigue loading than creep loading over a range of functional stresses <i>GM Thornton, SJ Bailey</i>	35
11:05-11:20 AM	An ultrasound technique to evaluate axial properties of ligament/tendon <i>H Kobayashi, R Vanderby</i>	36
11:20-11:25 AM	A short loading episode per day improves tendon healing <i>P Eliasson, T Andersson, P Aspenberg</i>	37
11:25-11:30 AM	The influence of genetic ablation of macrophage migration inhibitory factor on healing of the achilles' tendon: A biomechanical study <i>E Kondo, T Ishikawa, H Fujiki, M Daimaruya, S Onodera, K Yasuda</i>	38
11:30-11:35 AM	Discussion	
11:35-11:40 AM	Multiaxial nanoscale deformation mechanisms in tendon collagen <i>HRC Screen, J Seto, S Krauss, P Boesecke, HS Gupta</i>	39

11:40-11:45 AM	Impact of cyclic loading on the toe-region and linear properties of the patellar tendon graft: Implications for initial graft tension <i>J Hashemi, N Chandrashekar, JR Slauterbeck, BD Beynnon</i>	40
11:45-11:50 AM	Discussion	
11:50-11:55 AM	The influence of growth changes for elastic properties of tendon structures <i>Y Egawa, S Torii, C Nakamura, T Fukubayashi</i>	41
11:55-12:00 PM	A geometrical model of carpal tunnel expansion with ligament stretching and arch narrowing <i>Z-M Li</i>	42
12:00-12:05 PM	Discussion	
12:05-1:05 PM	Lunch and Poster Viewing	

Podium Session 4: Tendinopathy

Moderators: James Wang, PhD & Albert Banes, PhD

1:05-1:20 PM	Invited Lecture Mechanobiological understimulation of tendon cells as the etiopathogenesis of tendinopathy: A proposed scientific rationale for the clinical paradigm <i>S Arnoczky, M Lavagnino</i>	43
1:20-1:35 PM	A molecular analysis of posterior tibialis tendinopathy <i>AN Corps, AHN Robinson, RL Harrall, NC Avery, VA Curry, BL Hazleman, GP Riley</i>	44
1:35-1:50 PM	Glutamate receptors in tendinopathy <i>N Schizas, Ø Lian, F Frihagen, L Engebretsen, R Bahr, PW Ackermann</i>	45
1:50-2:05 PM	Polarization sensitive optical coherence tomography evaluation of intratendinous changes in ruptured and tendinopathic Achilles tendons <i>PO Bagnaninchi, Y Yang, GD Maffulli, AE Haj, N Maffulli</i>	46
2:05-2:10 PM	The pathogenic role of tendon stem cells in tendinosis <i>J Zhang, J Wang</i>	47
2:10-2:15 PM	Development of an in vitro model for tendinopathy <i>J Qi, L Chi, J Wang, R Sumanasinghe, M Wall, M Tsuzaki, AJ Banes</i>	48

2:15-2:20 PM Expression of sensory neuropeptides in tendon proper is associated with failed healing in calcific tendinopathy 49
PP Lui, G Ho, LS Chan, SC Fu, KM Chan

2:20-2:25 PM Discussion

Podium Session 5: Biology & Biochemistry

Moderators: Chih-Hwa Chen, MD & Catherine Kuo, PhD

2:25-2:40 PM Evaluation of myostatin inhibition in preclinical models of muscle atrophy associated with orthopedic injury 50
CA Morris, M St. Andre, P Bialek, J Parkington, A Root, J Zhang, G Bain, S Jelinsky, P Yaworsky, H Seeherman

2:40-2:55 PM Evaluation of osteogenesis of photo-responsive hydrogel encapsulated bone morphogenetic protein-2 and ligamentum flavum cells 51
CH Chang, CH Chen, CB Wong, HW Liu, SW Whu, MY Wu, JC Yeh, IH Lin, SH Chen, HJ Sun

2:55-3:00 PM Nanofiber alignment regulates adhesion and integrin expression of human mesenchymal stem cells and tendon fibroblasts 52
SP Kwei, KL Moffat, WN Levine, HH Lu

3:00-3:05 PM Variations in cell morphology in the canine cruciate ligament complex 53
KD Smith, A Vaughan-Thomas, PD Clegg, DG Spiller, JF Innes, EJ Comerford

3:05-3:10 PM Discussion

3:10-3:40 PM Break and Poster Session 2

Moderators: Stavros Thomopoulos, PhD & David Corr, PhD

Fondaparinux does not inhibit tendon repair 54
P Aspenberg, P Eliasson, T Andersson, J Schilcher, T Lindahl

Histological, biomechanical and transcriptional processes during normal rat tendon repair 55
SA Jelinsky, L Li, D Ellis, J Archambault, J Li, J Moreau, C Morris, H Seeherman

Characterizing structure-function relationships in tendon 56
S Toorani, JC Shelton, HRC Screen

Long term follow-up of anterior cruciate ligament reconstruction with an immunohistochemically modified porcine xenograft <i>KR Stone, TJ Turek, AW Walgenbach, U Galili</i>	57
The comparison of in vivo knee kinematics between knee osteoarthritis patient and young healthy subjects during normal gait: Application of point cluster technique <i>K Naito, Y Nagano, M Fukano, H Ida, S Torii, K Nakazawa, M Akai, T Fukubayashi</i>	58
Effect of lubricin on the attachment and proliferation of tenocytes <i>YL Sun, C Zhao, GD Jay, KN An, PC Amadio</i>	59
Mechanical function of the three bundles of the anterior cruciate ligament in response to externally applied loads <i>S Fukano, H Otsubo, T Suzuki, K Shino, H Fujie</i>	60
Biomechanical evaluation of three different subscapularis tendon repairs <i>FC Wang, GS Van Thiel, V Wang, S Nho, D Piasecki, A Romeo</i>	61
Determination of the mechanical property of the patellar tendon from biglycan knockout mice: Application of a novel all-in-one micro tensile test system <i>T Imai, H Amano, W Ando, N Nakamura, H Fujie</i>	62
MRI of the posterolateral corner of the knee using microscopy coil <i>H Ishigooka, T Sugihara, T Satoh, S Miyamoto, Y Kawana, H Fujiya, K Kitsukawa, T Lee, M Beppu</i>	63

Podium Session 6: Shoulder

Moderators: Evan Flatow, MD & Zong-Ming Li, PhD

3:40-3:55 PM	Invited Lecture Rabbit subscapularis model for studying rotator cuff pathology and repair <i>Thay Q Lee</i>	64
3:55-4:00 PM	Mesenchymal stem cells in the bursa subacromialis- Implications for a rotator cuff repair mechanism <i>AF Steinert, J Stehle, O Rolf, F Jakob, U Nöth, F Gohlke</i>	65
4:00-4:05 PM	A biomechanical analysis of anterior bankhart repair with capsular plication using suture anchors <i>RM Frank, GS Van Thiel, SJ Nho, FC Wang, VM Wang, MT Provencher, AD Mazzocca, AA Romeo, NN Verma</i>	66
4:05-4:10 PM	Discussion	

4:10-4:15 PM Shoulder rotational properties of throwing athletes with and without arm injury history 67
N Zheng, K Eaton

4:15-4:20 PM Effect of internal rotator muscles on shoulder internal impingement: a cadaveric study 68
T Mihata, BJ Jun, YJ Chen, MH McGarry, SE Galle, M Kinoshita, TQ Lee

4:20-4:25 PM Discussion

Podium Session 7: Functional Tissue Engineering-Bioscaffolds

Moderators: Martha Murray, MD & Helen Lu, PhD

4:25-4:40 PM Nanofiber composite for tendon-to-bone interface tissue engineering 69
KL Moffat, Y Kim, SD Subramony, SB Doty, HH Lu

4:40-4:55 PM The influence of aligned polycaprolactone nanofibre meshes on the gene expression and cellular orientation of tendon fibroblasts 70
SE Taylor, L Bosworth, A Vaughan-Thomas, S Downes, RKW Smith, PD Clegg

4:55-5:10 PM In vivo study of ACL regeneration using silk scaffolds in a pig model 71
H Liu, H Fan, SL Toh, JCH Goh

5:10-5:15 PM Novel 3D tensile culture system for ligament tissue engineering with mesenchymal stem cells 72
DM Doroski, ME Levenston, JS Temenoff

5:15-5:20 PM Cyclic tensioning culture strengthens a stem cell-based self-assembled tissue (scSAT) derived from synovium 73
K Saito, A Ogawa, W Ando, N Nakamura, H Fujie

5:20-5:25 PM Discussion

5:25-5:30 PM Effect of native ligament extracellular matrix on human adipose stem cells 74
D Little, AN Blount, F Guilak, DS Ruch

5:30-5:35 PM Electrospun scaffolds to support cellular differentiation for ligament tissue engineering 75
RD Shaffer, LA Dahlgren, AS Goldstein

5:35-5:40 PM Discussion

5:40-5:50 PM Closing Remarks
Savio L-Y. Woo, PhD

My Clinical and Experimental Challenges to Develop Ideal ACL Reconstruction

Kazunori Yasuda, MD, PhD

Professor and Chairman, Department of Sports Medicine & Joint Surgery

Hokkaido University School of Medicine, Sapporo, Japan

E-mail: yasukaz@med.hokudai.ac.jp

In my 30-year clinical experience, I performed single-bundle ACL reconstruction (Open technique) with the quadriceps and patellae tendon graft (1, 2) between 1980 and 1989. To improve disadvantages of this procedure, I started clinical and basic studies to rediscover utility of hamstring tendon graft, which was discarded in those days, in 1989. I developed a technique to strongly fix the tripled or quadrupled hamstring tendon graft to the bone with polyester meshed tapes and spiked staples in 1990 (3, 4), and performed arthroscopy-assisted single-bundle ACL reconstruction with the hamstring tendon graft between 1990 and 1999. Thus, I have clarified isolated graft site morbidity (3), intraosseous graft healing (5-7), effects of initial tension for the hamstring tendon graft (8), and so on.

Thus, single-bundle ACL reconstruction with the hamstring or BTB graft has been established as a standard strategy to treat the ACL-deficient knee in the 2000s. However, I have found several problems in the clinical results after ACL reconstruction from the viewpoint of pursuing ideal ACL reconstruction. For example, the postoperative knee stability was insufficient, restoration of the graft properties was too slow, and various degrees of tunnel enlargement frequently occurred after ACL reconstruction. An aim of this presentation is to introduce my clinical and experimental challenges to improve ACL reconstruction.

To improve the knee stability after single-bundle ACL reconstruction, we have developed a new surgical procedure in which 4 intraarticular tunnel outlets were created at the center of each anatomic attachment of the AMB and the PLB, respectively, since 2000 (9-12). We intra-operatively measured the graft tension-versus-flexion angle curve for each graft, and confirmed that we could reconstruct the AMB and the PLB having nearly normal functions in each patient, using the arthroscopy-assisted procedure (13). Recently, we performed a prospective comparative cohort trial with 328 patients followed up for 2 years or more (14). The anatomic double-bundle procedure was significantly better in knee stability than our single-bundle procedure. There was no difference in the complication ratio between the double- and single-bundle procedures. However, clinical utility of the anatomic double-bundle procedure remains controversial. Further long-term follow-up studies are needed in the near future

Slow restoration of the graft properties is a major cause of slow return to the sports activities and occasional graft failure during the rehabilitation phase. We have clarified that the slow restoration is caused by functions of extrinsic fibroblasts that infiltrate in the graft after surgery (15-17). We have experimentally challenged to accelerate restoration of the graft properties using a biological strategy. We clarified that a local application of VEGF significantly increased revascularization in the graft, although it did not significantly inhibit or accelerate the deterioration of the graft after implantation (18,19). Recently, we elucidated that cell-based therapy using TGF-beta1-supplemented synovium-derived cells significantly improved graft properties (20).

Tunnel enlargement is a serious problem in revision ACL reconstruction, although significant correlation between the degree of tunnel enlargement and postoperative knee stability has not been detected in previous clinical studies. Orthopaedic surgeons have had great concern about tunnel enlargement. Mechanism of tunnel enlargement remains unclear. To obtain fundamental knowledge, first, we clarified the natural course of intraosseous healing of the flexor tendon graft (5, 6, 7).

Perpendicular collagen fibers formed by 6 weeks particularly mainly in the anterior space. Recently, we have experimentally challenged to enhance the intraosseous healing of the flexor tendon graft using a biological strategy. Application of TGF-beta1 within a bone tunnel enhanced formation of bone and Sharpey-like collagen fibers around the flexor tendon graft (21)

In conclusion, there remain many problems in the clinical outcome of ACL reconstruction. To develop ideal ACL reconstruction in the future, I believe that we need not only to improve surgical procedures but also to develop novel biological treatments for extrinsic fibroblasts that infiltrate in the graft after surgery.

References

1. Yasuda, et al: Clin Orthop Relat R, 246: 217-224, 1989
2. Yasuda, et al: Am J Sports Med, 20: 471-475, 1992
3. Yasuda, et al: Am J Sports Med, 23: 706-714, 1995
4. Yamanaka, Yasuda, et al: Am J Sports Med, 27: 772-777, 1999
5. Tomita, Yasuda, et al: Arthroscopy, 17: 461-476, 2001
6. Yamazaki, Yasuda, et al: Am J Sports Med 30: 498-505, 2002.
7. Yamazaki, Yasuda, et al: Knee Surg Sports Traumatol Arthrosc 14: 1086-1093, 2006
8. Yasuda, et al: Am J Sports Med, 25: 99-106, 1997
9. Yasuda, et al: Arthroscopy 20:1015-1025, 2004
10. Yasuda, et al: Arthroscopy 22: 240-251, 2006
11. Kondo and Yasuda: Arthroscopy 23: 1198-1209, 2007
12. Kondo, Yasuda, et al: Arthroscopy 23: 869-876, 2007
13. Yasuda, et al: Arthroscopy 24: 276-284, 2008
14. Kondo, Yasuda, et al: Am J Sports Med 36:1675-1687, 2008
15. Ohno, Yasuda, et al: Clin Biomech, 11: 207-213, 1996
16. Tohyama and Yasuda: J Biomech Eng-T ASME, 122: 594-599, 2000
17. Tohyama, Yasuda, et al: Knee Surg Sports Traumatol Arthrosc 14: 1270-1277, 2006
18. Ju, Yasuda, et al: Am J Sports Med. 34: 84 – 91, 2006.
19. Yoshikawa, Yasuda, et al: Am J Sports Med. 34:1918-1925, 2006
20. Kondo, Yasuda, et al: Trans Orthop Res Soc 32, 0808, 2007
21. Yamazaki, Yasuda, et al: Arthroscopy 21:1034-1041, 2005

LENGTHENING AT THE FIXATIONS AND INCREASE IN ANTERIOR LAXITY ARE SMALL DURING THE FIRST FOUR MONTHS OF IMPLANTATION AFTER SOFT-TISSUE ALLOGRAFT ANTERIOR CRUCIATE LIGAMENT RECONSTRUCTION

C.K. Smith*, M.L. Hull*^, and S.M. Howell^

*Biomedical Engineering Program and ^Department of Mechanical Engineering, University of California at Davis, Davis, CA USA

INTRODUCTION

Anterior laxity has been shown to increase after soft-tissue allograft anterior cruciate ligament reconstruction because of lengthening at the fixations from interference screw fixation.¹ The purpose of the present study was to evaluate lengthening-resistant fixation methods and determine at 1, 2, 3, and 4 months the lengthening at each fixation, when lengthening at the fixations ceases, the increase in anterior laxity, and whether there is an association between the lengthening at the fixations and anterior laxity before lengthening at the fixations ceases.

METHODS

In a longitudinal in vivo study, Roentgen stereophotogrammetric analysis was used to measure lengthening at the fixations and an increase in anterior laxity during the first 4 months following ACL reconstruction in 20 subjects. The subjects were treated with fresh-frozen, non-irradiated, non-chemically treated tibialis allografts fixed with an EZLoc on the femoral side and with a WasherLoc on the tibial side. Tantalum markers were implanted into the bones, graft, and fixation devices. Radiographs were exposed of the knee on the day of surgery and at 1, 2, 3, and 4 months postoperatively as a 150-N anterior force was applied to the tibia. Subjects were prescribed brace-free, aggressive rehabilitation.

RESULTS

Although small, the greatest lengthening at 4 months was between the femoral fixation and femur (1.2 ± 0.7 mm) followed by lengthening between the graft and tibial fixation (0.4 ± 0.8 mm). Lengthening between the graft and femoral fixation and between the tibial fixation and tibia were negligible (Figure 1). After 1 month there were no significant increases in lengthening at the fixations (Table 1). The average increase in anterior laxity at 1 month was 0.4 ± 1.8 mm. There was no association between the increase in anterior laxity and combined lengthening of both fixations after 1 month ($r^2 = 0.00$). The average increase in anterior laxity at 4 months was 1.7 ± 2.3 mm.

DISCUSSION

The cessation of lengthening at the fixations after 1 month suggests that the biologic incorporation of the graft was fairly well established. The lack of association between the increase in anterior laxity and lengthening at the fixations at 1 month indicates that early lengthening, when small, is not a determinant of anterior laxity. An increase in the stiffness of the bone-graft-fixation device construct from biologic incorporation might explain the lack of any association. The continued increase in anterior laxity up to 4 months presumably is due to a decrease in graft stiffness as a result of graft remodeling.

1. Khan, R., A. Konyves, et al. (2006). "RSA can Measure ACL Graft Stretching and Migration: Development of a New Method." *Clin Orthop Relat Res* 448: 139-45.

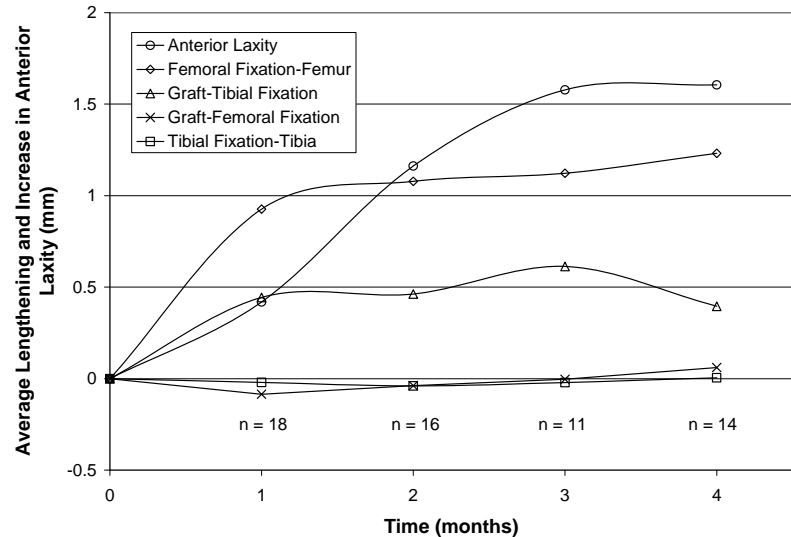


Figure 1: Average increase in anterior laxity and slippage. The n values indicate the number of subjects tested at each time interval.

Table 1: P-values for lengthening and anterior laxity. Significant changes were between the femoral fixation and femur and between the graft and tibial fixation at 1 month.

Month	Femoral Fixation-Femur	Graft-Femoral Fixation	Graft-Tibial Fixation	Tibial Fixation-Tibia
0-1	<0.0001	0.96	0.02	0.93
1-2	0.61	1.00	1.00	0.97
2-3	0.91	0.97	0.98	0.78
3-4	0.98	1.00	0.82	1.00

THE RELATIONSHIP BETWEEN GRAFT TUNNEL POSITION AND IN VIVO KNEE KINEMATICS AFTER ACL RECONSTRUCTION

J.H. Wang, S. Tashman
Biodynamics Laboratory, University of Pittsburgh, Pittsburgh, PA

INTRODUCTION

Anterior cruciate ligament (ACL) reconstruction can reduce knee instability, but it cannot restore normal rotational knee motion¹. Cadaveric biomechanical studies, using simplified loading schemes, have shown that the ACL graft tunnel position can affect knee kinematics^{2,3}. Effects of tunnel position on *in vivo* knee kinematics are unknown. The purpose of this study was to evaluate the effect of the tibial and femoral ACL graft tunnel positions on knee kinematics during a high-loading, functional task.

METHODS

Twenty-four patients with primary ACL reconstruction underwent kinematic tests during downhill treadmill running (2.5m/s; 10° slope) using dynamic radiostereophotogrammetric analysis (D-RSA; 250 frames/s) one year after surgery. Tibio-femoral kinematics were determined as previously described¹. Descriptive variables (min, max, mean, range) were extracted for two translation parameters (anterior-posterior, medial-lateral) and two rotational parameters (internal/external rotation, abduction /adduction) during the period from heel strike to mid-stance. CT scans were acquired and reconstructed into 3D bone surface models. Tibial and femoral tunnel positions were interactively identified and marked on the 3D bones, and expressed in bone-fixed anatomical coordinate systems, as shown in Figure 1. Pearson's correlations were determined for each kinematic variable relative to the six tunnel positions (tibia and femur; X,Y,Z). P-value was set <0.05.

RESULTS

Significant correlations were found for the anterior/posterior tunnel positions (Z-axis in Figure 1) relative to internal/external rotation. Anterior position of the femoral tunnel was correlated with *increased* internal rotation (max: $r=0.486$, $p=0.014$; mean: $r=0.425$, $p=0.039$). Anterior position of the tibial tunnel was correlated with *reduced* internal rotation (max: $r=-0.558$, $p=0.003$; min: $r=-0.566$, $p=0.004$; mean: $r=-0.581$, $p=0.003$).

DISCUSSION

Anteriorly (arthroscopically, superiorly) located femoral tunnels and posteriorly located tibial tunnels were associated with greater internal rotation of tibia during the running. The AP positions of the tibial and femoral tunnels define the sagittal direction of the graft (graft angle) when the knee is in full extension. A more anterior femoral tunnel and a more posterior femoral tunnel both create more vertically directed grafts, which may impair ACL function for controlling internal/external rotation of the knee.

There are two primary limitations of this study. First, there are many other factors with an *in vivo* analysis that might influence the relationships between tunnel position and kinematics. Second, correlations only investigate linear relationships, and it is likely that the effects of tunnel position on kinematics would be nonlinear. Further analyses are underway to better characterize these complex relationships, as well as investigate alternative reconstruction techniques (e.g. anatomical/double-bundle grafts).

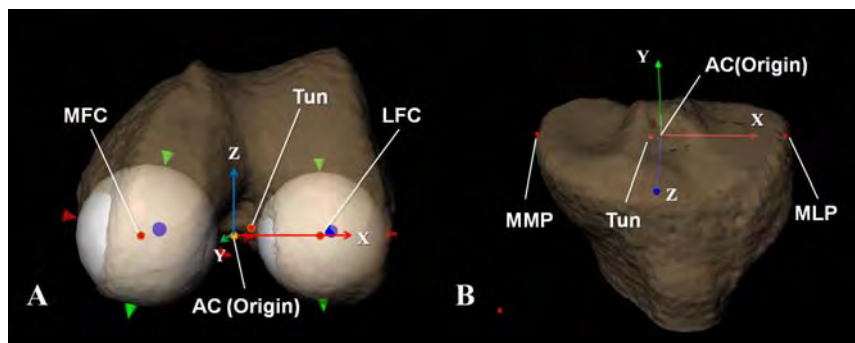


Figure 1: A. The medial femoral condyle (MFC) and lateral femoral condyle (LFC) centers were determined by fitting spheres to the outer contour of the posterior condyles. Tunnel position (Tun) was described relative to the midpoint between MFC and LFC (femur anatomic origin; AC). B. For the tibia, tunnel position (Tun) was expressed relative to the anatomic origin (AC), defined as the midpoint between the most medial (MMP) and most lateral (MLP) points of the tibial plateau.

REFERENCES:

1. Tashman et al. (2004) *Am J Sports Med.* 32(4):975-983
2. Loh et al. (2003) *Arthroscopy.* 19(3):297-304.
3. Musahl et al. (2005) *Am J Sports Med.* 33(5):712-718.

THE RELATIONSHIP BETWEEN CLOSED KINETIC CHAIN STRENGTH OF THE LOWER LIMB AND JUMPING PERFORMANCE IN ACL-DEFICIENT SUBJECTS AND ACL-RECONSTRUCTED SUBJECTS USING ANATOMICAL DOUBLE-BUNDLE RECONSTRUCTION

H. Tohyama¹, M. Ueda², T. Chiba², M. Yuri², K. Ikoma², K. Yasuda¹
 Departments of ¹Sports Medicine and ²Rehabilitation Medicine, Hokkaido University School of Medicine, Sapporo, Japan

INTRODUCTION

Several studies show that decreased jumping performance accompanies the rupture of anterior cruciate ligament (ACL) of the knee. Closed kinetic chain (CKC) exercise has become popular in rehabilitation partly due to the belief that it is more closely related to function than open kinetic chain (OKC) resistance. Blackburn and Morrissey (1) found that lower limb extensor CKC muscle strength is more highly related to jumping performance than knee extensor OKC strength. However, no studies have examined the relationship between CKC strength of the lower limb extensors and jumping performance in the subjects after an ACL injury. The purpose of the present study was to compare the relationship between CKC strength of the lower limb extensors and jumping performance in ACL-deficient subjects with that in the subjects after double-bundle anatomical ACL reconstruction.

MATERIALS AND METHODS

We measured the isokinetic strength measurement and the jumping performance in a group of ACL-deficient (n=22) patients, a group of healthy controls (n=16) and a group of ACL-reconstructed patients with double-bundle anatomical ACL reconstruction using hamstring tendon grafts (2) (n=16). All ACL-reconstructed patients were evaluated at 12-18 months after the surgery. Isokinetic peak strength for the knee extensors in OKC was measured using KIN-COM AP (TN, USA). Isokinetic peak strength for the hip, knee, and ankle extensors in CKC was measured using Strengthergo.240 (Mitsubishi Electric Co., Tokyo, Japan). The one-leg vertical jump and the one-leg long jump tests were also assessed. Pearson's correlation analysis were performed for statistical analysis.

RESULTS AND DISCUSSION

The correlation between kinetic strength and jump performance were weaker in the ACL-deficient group than in the control and ACL-reconstructed groups (Fig. 1). In the control and ACL-reconstructed groups, lower limb extensor CKC muscle strength is more highly related to jumping performance than knee extensor OKC strength, but CKC strength in the ACL-deficient group is not highly related to jumping performance. Demont et al. (3) reported that the muscular activity in ACL-deficient leg during functional activities was different from that in the normal control subjects. Therefore, the change in muscular activity in ACL-deficient leg during jumping performance may result weak correlation between CKC strength and jumping performance in the ACL-deficient subjects. In addition, the present study suggests that double-bundle anatomical ACL reconstruction restores the correlation between CKC strength and jumping performance.

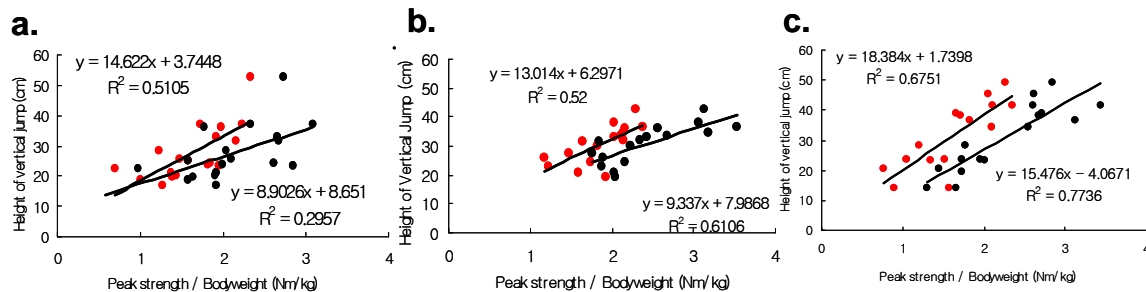


Figure 1: Correction between OKC (red) and CKC (black) peak strengths and the height of vertical jumping performance (a. ACL-deficient, b. control, c. ACL-reconstructed).

REFERENCE 1) Blackburn JR, Morrissey MC. (1998). J Orthop Sports Phys Ther., 27430-5. 2) Yasuda K, et al. (2004). Arthroscopy. 1015-25. 3) Demont RG, Lephart SM, Giraldo JL et al. (1999). J Athl Train., 115-20.

ESTIMATION OF THE UPPER BOUND OF THE IN-VIVO FORCES IN THE ANTERIOR CRUCIATE LIGAMENT

Hosseini A, Gill TJ and Li G

Bioengineering Laboratory, Massachusetts General Hospital/Harvard Medical School, Boston, MA

INTRODUCTION

The knowledge of in-vivo ACL forces is instrumental for understanding ACL injury mechanisms and for improvement of surgical ACL reconstruction. Numerous in-vitro investigations have measured ACL forces in response to various loads applied to the knee. However, in-vivo ACL forces in response to controlled loading are still unknown. The objective of this study was to estimate the force of healthy ACL as well as the possible upper bound of ACL forces under an increasing axial tibial loading in living subjects using a non-invasive method.

METHODS

This study was planned in three major steps. In the first step, the kinematics of one knee of 10 healthy subjects (randomly selected, 5R/5L) were determined using a previously described dual fluoroscopic technique [1]. This kinematics data was obtained (at 15°, 30° and 45° of flexion) and different controlled weightbearing: minimal load (<10N), 0.25, 0.50, 0.75 and 1.0 body weight (BW). At each flexion angle, the elongation of the ACL under different load bearing was measured. The curves of *in-vivo ACL elongation-weightbearing* were created for each subject. In the second step, the *in situ force-elongation* curves of the ACL were determined at each flexion angle in 6 cadaveric human knees using a robotic testing system. In the last step, the in-vivo elongation data from 1st step was mapped into the force-elongation curves from 2nd step at the corresponding flexion angles and the *in-vivo ACL forces* were statistically estimated. For this purpose, the force-elongation curves of 6 specimens were averaged on each flexion angle and a *Toe Region* (TR) was defined as part of the force-elongation curve, where the slope of the curve is almost horizontal and the force is under a certain value of F_0 . Then, the in-vivo weightbearing-elongation curve of the ACL of each living subject at each flexion angle was matched with the in-situ force-elongation curve and the in-vivo ACL tension of each subject under weightbearing condition was determined by a mean value F_i and a standard deviation σ_i (i = number of living subject). Finally, a *weighted mean statistical method* was used to estimate the in-vivo ACL tension of all subjects. The weighted mean of in-vivo ACL force and standard error of the mean ($F \pm \sigma$), was calculated using:

$$F = \left(\sum_{i=1}^{10} \frac{F_i}{\sigma_i^2} \right) * \left(\sum_{i=1}^{10} \frac{1}{\sigma_i^2} \right)^{-1} \quad \text{and} \quad \sigma^2 = \left(\sum_{i=1}^{10} \frac{1}{\sigma_i^2} \right)^{-1}$$

RESULTS

The estimated changes in the ACL force due to axial tibial weightbearing at 15°, 30° and 45° of flexion are shown in fig. (1A-1C). Force estimation was based on toe regions of $F_0 = 0$ and 50 N. At 15° of flexion, the ACL force under full BW was 131.4 ± 16.8 N at TR 0N (*i.e.*, toe region at 0 N), and it increased to 209.4 ± 29.5 N at TR 50N. At 30° and under full BW, the ACL tension was 106.7 ± 11.2 N at TR 0N and 193.5 ± 24.6 N at TR 50N. Finally, at 45° of flexion, the force was determined as 34.6 ± 4.5 N at TR 0N and 103.4 ± 12.9 N at TR 50N under full BW. In addition, the effect of different value of toe region on the ACL force under full body weight tibial load at different flexions is shown in fig. 1D. The patterns of the ACL force shows that beyond a toe region (> 10 N initial tension), the estimated in vivo ACL force is approaching an asymptote in each flexion angle.

DISCUSSION

The in-vivo tension in the ACL under varying weightbearing (zero to full body weight) at different flexion angles in living subjects. The results showed that under full body weight, the ACL would be loaded mildly (below 250 N). The ACL tension is significantly higher at 15° and 30° compared to 45°.

Since, ACL had a complicated 3D structure, different fibers of the ligament could be loaded at different flexion angles. So, it is challenging to determine the zero length of the ACL. In this study, if the ligament was tight at its initial length (under no weightbearing) during the in-vivo activity, the estimated ACL force is an underestimation of the actual force. However, by increasing the toe region, the ACL force is changing asymptotically. This behavior suggests that 50N toe region can be used to define an upper bound for force estimation. If under no ‘axial tibial loading’ the ACL tension was under 50 N, full body weight caused just less than 250 N tension in the ACL, which is much lower than the ACL failure tension of about 1500 N [2]. Future study should investigate ACL forces during other daily activities such as gait, stair climbing, etc.

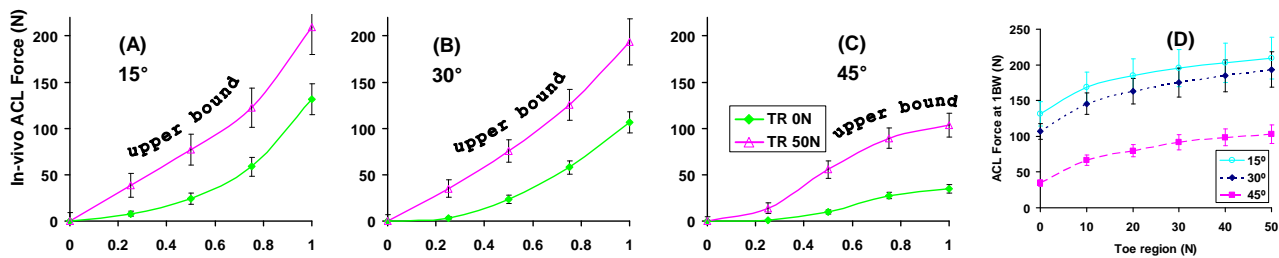


Figure (1): (A-C) Change of the in-vivo ACL tension as a function of axial tibial weightbearing at 15°, 30° and 45° of flexion during a single-legged lunge. Forces are estimated using *weighted mean method* based on different Toe Regions (TR) of 0 and 50N. (D) The effect of toe region on the ACL force, when the knee is under full body weight.

REFERENCES

- [1] Li G., *et al.* J Biomech. Eng, 2004. [2] Woo S., *et al.* Am J Sports Med. 1991.

TOTAL KNEE AND ACL FORCE FOR A SIMULATED IN VIVO MOTION: A COMPARATIVE STUDY BETWEEN HUMAN AND OVINE

ST Herfat, DV Boguszewski, JT Shearn, DL Butler

Department of Biomedical Engineering, University of Cincinnati, Cincinnati, OH;

INTRODUCTION. A suitable animal model is needed to establish functional tissue engineering parameters (FTEPs) under physiologic conditions to provide design criteria for new and novel orthopaedic repairs [1,2]. The objective of this study was to examine the differences in knee joint and ACL reaction forces between the ovine and human for a simulated ovine in vivo walking motion. We hypothesize that while joint force patterns may be similar between species, the ovine joint provides a more demanding environment for the ACL than does the human.

MATERIALS AND METHODS. Seven skeletally mature female sheep (age: 3 to 4 years old; weight: 100 – 150 lbs) and four human cadaveric knees were used in this study. Each limb was dissected free of all tissues except the 4 knee ligaments and joint capsule. The distal half of the tibia was then removed and the proximal half secured in a specially-designed fixture with bone cement. This fixture, which aligned the joint axes with the robot axes, was then attached to the 6-axis load cell on our 6 DOF Robot (KR210; KUKA) end effector. Once aligned, the femur was fixed to the base, the forces and moments were minimized to less than 5 N and 1 Nm, respectively, and knee

flexion angle was set to the midpoint for the selected motion path (60.5°). We chose the center of the ACL insertion site on the tibia (between the tibial spines) as the joint center point, and all rotations and translations were imposed about this point. The joints from both species were subjected to an identical 10-cycle sequence of a 6 DOF gait path determined from data collected by Tapper et al [3] in the sheep model. We first recorded reaction forces and torques during this simulated activity. We then removed all tissues but the ACL including the distal portion of the femoral condyles, so that the ACL was the only structure transmitting force across the joint. The specimen was then subjected to the same 6 DOF motion path to determine resultant ACL reaction force. For the intact and ACL-only conditions, we examined forces in all 3 directions and calculated a total resultant ligament force. Gait cycles were normalized (%) to compare species.

RESULTS. The simulated in vivo motion generated significantly greater total joint reaction force in the sheep knee compared to the human ($p < 0.001$), particularly during the stance phase (Fig. 1A). However, the shapes of both curves were similar during the full gait cycle. The ovine ACL generated significantly greater force than the human ACL during stance ($p < 0.05$), the latter remaining essentially unloaded (Fig. 1B). ACL force was highest during the swing phase for both species. During swing phase, both the magnitude and shape of the force curves were similar between species for both the intact and ACL-only conditions.

DISCUSSION. By imposing identical knee motions and then recording similar patterns of joint reaction force, one could conclude that both knees exhibit similar knee ligament

architecture and interactions. However, isolating the ACL reveals a stiffer sheep ligament that generates a greater percentage of the total knee force during stance phase. Thus for the applied motions, the sheep knee provides a more challenging environment and possibly more effective test platform for judging ACL reconstructions. Of course, future studies will need to be conducted on cadaveric human knees using simulated in vivo human motions and results compared across species to determine which model(s) provides the greatest information about the potential utility of treatments for ACL repair and reconstruction.

REFERENCES. [1] Butler et al. CORR, 2004. [2] FTE Conference Group, Tissue Engineering, 2008. [3] Tapper et al. JOR, 2006.

ACKNOWLEDGMENTS. Partial support from NIH grants EB004859-01 and AR46574-06.

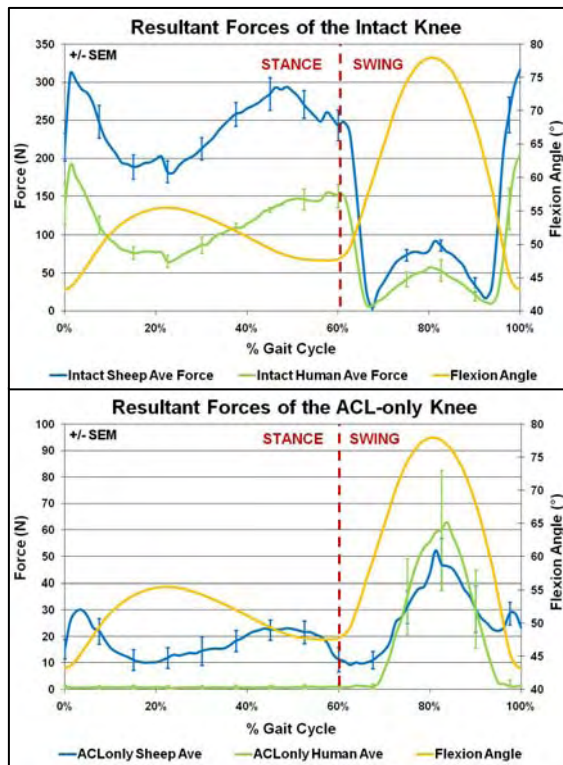


Figure 1. A. Resultant sheep and human knee reaction forces during gait. **B.** Resultant forces for both models after isolating the ACL.

FORCE CONTRIBUTIONS IN AN OVINE KNEE DURING SIMULATED *IN VIVO* MOTION

DV Boguszewski, ST Herfat, JT Shearn, DL Butler

Department of Biomedical Engineering, University of Cincinnati, Cincinnati, OH;

INTRODUCTION. The role of soft tissue function and bony interaction in the knee during gait is vital to injury prevention and treatment. However, our current understanding of the restraining action of these structures is usually limited to non-physiologic tests. In this study, we examine the contributions of knee soft tissue structures and bony

contact during a simulated *in vivo* motion using a robot.

MATERIALS AND METHODS. Seven skeletally mature female sheep (age: 3-4 yrs; weight: 100–150lbs) were used in this study. Each limb was dissected free of all tissues except the 4 major knee ligaments, the menisci, and the joint capsule. The tibia was secured in a specially-designed fixture and attached to a 6-axis load cell on the end of a 6 DOF Robot (KR210; KUKA). The fixture aligned the anatomical axes of the joint with the corresponding robot axes. All rotations and translations were made to occur about the joint center point (ACL insertion site between the tibial spines). We first cycled the intact knee 10 times using a 6 DOF gait path determined from normal sheep data collected by Tapper et al [1]. We then performed a selective cutting sequence using a stiffness-based, displacement controlled, test methodology [2]. One structure (e.g. MCL) was then cut and the motion path repeated. Each of the remaining structures (ACL, LCL, PCL, Medial Meniscus, Lateral Meniscus, Medial Capsule, Lateral Capsule, and bony contact) were sectioned in random order (except the ACL was always the last structure removed) [2]. The section-induced change in 3-D forces and moments represented the contribution of that structure to the overall intact knee reaction force.

RESULTS. Stance Phase: Bony interaction contributed more to joint reaction forces than did other structures. It accounted for $95\% \pm 14\%$ (Mean \pm SEM), $73\% \pm 5\%$ and $59\% \pm 4\%$ of the posterior- (Fig 1A), medial- (Fig 1B), and compressive-directed forces in the knee (Fig 1C), respectively. Bony contact also contributed $56\% \pm 4\%$ and $50\% \pm 4\%$ of total adduction and internal rotation moments, respectively. The ACL and menisci also provided important contributions during the stance phase. The ACL supplied the only medial force other than bone ($20\% \pm 2\%$; Fig 1B), and only significant anterior force ($p < 0.05$; Fig 1A). The medial meniscus contributed the only compressive force other than bone ($37\% \pm 4\%$; Fig 1C), and only significant lateral force ($p < 0.05$; Fig 1B). **Swing Phase:** The ACL and MCL served as the primary restraining structures during swing.

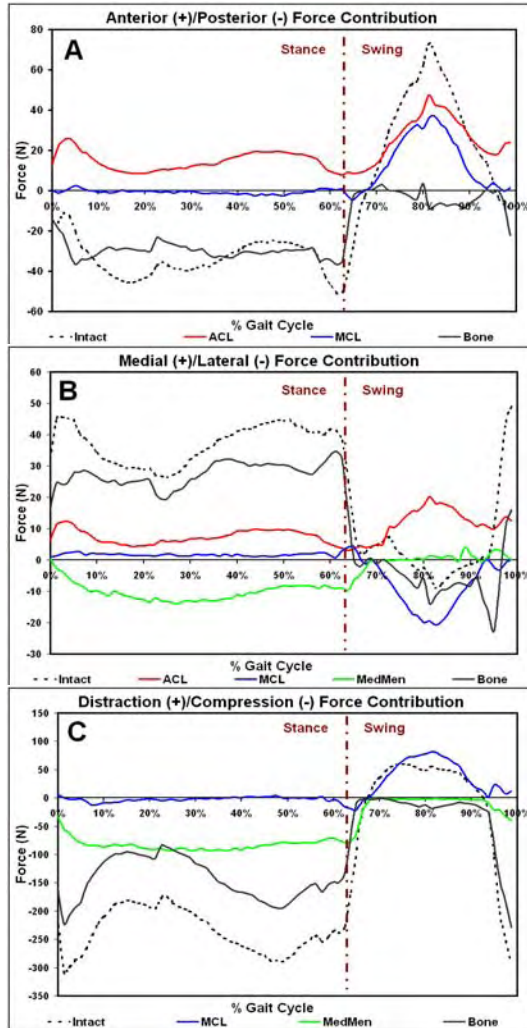


Fig 1. Sheep knee joint reaction loads for A) Ant/Post, B) Med/Lat, and C) Dist/Comp

Combined, they provided the primary anterior force accounting for $118\% \pm 2\%$ at peak flexion (Fig 1A). In swing the ACL resisted medial loading (average of $10.6\text{N} \pm 3.5\text{N}$; Fig 1B) while the MCL resisted lateral loading (average of $-8.5\text{N} \pm 2.8\text{N}$; Fig 1B). The MCL also provided the only resistance to distraction (Fig 1C), abduction, and external rotation. All other structures provided negligible force and moment contributions during this motion.

DISCUSSION. During stance the bony interaction between the femur and tibia provides the major force contribution to the intact knee, with the medial meniscus having an important role in compression while also resisting lateral motions. During the swing phase the ACL and MCL are the key structural contributors. The motion characteristics during gait depend on the soft tissue structures and bony interaction. The force contributions of these structures are useful in understanding mechanisms of joint motion as well as in developing functional tissue engineering design criteria for new and novel therapies for the prevention and treatment of injury [3,4].

REFERENCES 1. Tapper et al, JOR 2006 2. Butler et al, JBJS 1980 3. FTE Conf, 2008 4. Butler et al, JBE 2000

IN-VITRO EVALUATION OF SUTURE AUGMENTATION TECHNIQUES AFTER ACL INJURY

Matthew B. Fisher, B.S., Ho-Joong Jung, M.D. Patrick J. McMahon, M.D., and Savio L-Y. Woo, Ph.D., D.Sc.
Musculoskeletal Research Center, Department of Bioengineering, Swanson School of Engineering,
University of Pittsburgh, Pittsburgh, PA

INTRODUCTION: With the advancement of functional tissue engineering (FTE), healing of the anterior cruciate ligament (ACL) of the knee has regained significant interest¹. However, these new biological approaches coupled with suture repair of the ACL still require augmentation in order to restore initial knee stability¹. One type of augmentation uses additional sutures passed through tunnels drilled in the femur and tibia. On the femoral side, tunnels have been drilled through [2, 3] or placed anterior to [4] the ACL origin. Thus, the objective was to evaluate the location of these femoral bone tunnels for suture augmentation in terms of restoration of knee kinematics and in-situ force in the augmentation sutures compared to the intact knee. We hypothesized that a femoral tunnel placed through the ACL origin will better restore kinematics compared to a more anterior femoral tunnel because the placement better replicates the natural insertion site of the ACL [6, 7].

METHODS: Six goat knee specimens were tested using a robotic/universal force-moment sensor testing system. Two external loading conditions were applied to the intact knee at 30°, 60°, and 90° of flexion: (1) a 67-N anterior tibial load (ATL), and (2) a 5-N-m varus torque. The 5 DOF kinematics of the intact knee were recorded. Then, the ACL was fully transected. The kinematics of the intact knee were replayed to determine the in-situ force of the ACL [8]. Afterward, the same loading conditions were applied to the ACL-deficient knee and the 5 DOF knee kinematics were measured. Suture augmentations were performed using #2 Fiberwire sutures (Arthrex, Inc.) and were created by passing two sutures directly from a femoral bone tunnel to a tibial bone tunnel and tied under tension. Two different femoral tunnels were created (1) anterior to, or (2) through the ACL insertion (Fig. 1). One tibial tunnel (medial to the ACL insertion) was used. After each augmentation, the same 2 external loading conditions applied to the intact knee were repeated on the augmented knee. The force in the augmentation sutures were obtained by removing the sutures and replaying the knee kinematics [8]. The order of the repairs was randomized. The anterior tibial translation (ATT) between experimental conditions, and the corresponding forces in the sutures were compared to the ACL using repeated measures ANOVA ($p < 0.05$).

RESULTS: In response to the 67-N ATL, the augmentations placed anterior and through the femoral origin of the ACL were able to restore ATT to within 0.5-3.0 mm and 0.6-2.3 mm, respectively, of the intact knee, through the range of flexion ($p > 0.05$), and were 10-11 mm lower than the ACL-deficient knee ($p < 0.05$) (Fig. 2). There were no significant differences in ATT between the augmentations ($p > 0.05$). The in-situ forces in both groups were within 8 N of the ACL ($p > 0.05$).

Under the 5 N-m varus torque, both suture augmentations were able to restore the ATT to within 0.8-4.2 mm and 0.8-3.9 mm, respectively, of the intact knee ($p > 0.05$), and were 6-9 mm lower than the ACL-deficient knee ($p < 0.05$). No significant difference in ATT between the augmentations could be detected ($p > 0.05$). The overall in-situ forces for both augmentation procedures were comparable to the intact ACL, except at 30°, in which they were 17 and 14 N lower, respectively ($p < 0.05$).

DISCUSSION: Our findings suggest that suture augmentation of an injured ACL could restore knee kinematics under both a 67 N ATL and a 5 N-m varus moment in the goat model. The augmentation through the femoral origin of the ACL was found to be not significantly better than the anterior femoral tunnel augmentation (i.e., only 0.7 mm maximum difference). Thus, the data did not support our hypothesis. Placement of the femoral tunnel anterior to the ACL origin may be advantageous because this simpler approach would reduce the risk for injury to the tissue. This information should be helpful to guide future investigation on the effects of FTE techniques to heal of a torn ACL.

ACKNOWLEDGEMENTS: Financial support from the Commonwealth of Pennsylvania and NSF Engineering Research Center Grant are acknowledged. Fiberwire sutures were kindly donated by Arthrex, Inc.

REFERENCES: 1. Murray M, et al. JOR 2008. 2. Fleming B, et al. JOR 2008. 3. Abramowitch S, et al. JOR 2003.

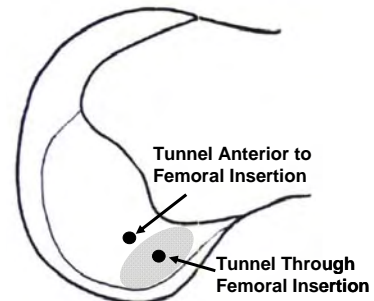


Figure 1. Femoral tunnel position

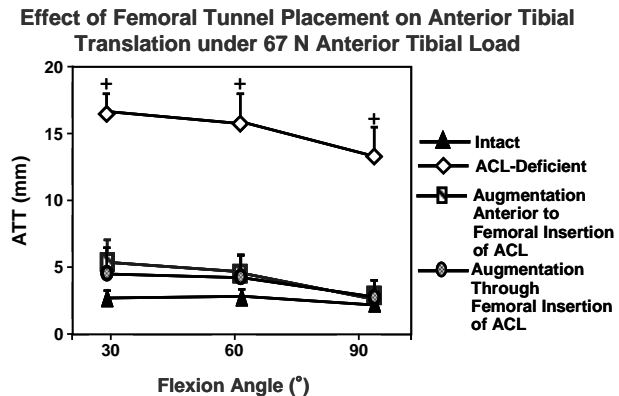


Figure 2. ATT under 67 N ATL (+ indicates significant difference from all other groups, $p < 0.05$)

Ex-vivo knee kinematics in ACL-deficient knee. A stereophotogrammetric study

Fabrizio Margheritini, Andrea Cereatti, Marco Donati, Pier Paolo Mariani, Aurelio Cappozzo
University of Rome "Foro Italico", Unit of Sports Traumatology, Piazza Lauro de Bosis 6, 00195 Rome, Italy

INTRODUCTION

It is well known that the anterior cruciate ligament (ACL) is the primary restraint to tibial anterior translation. However, in addition to flexion and extension, the human knee also allows tibial internal–external rotations due to the lack of congruency between the femoral condyles and the tibial plateau. The section of ACL has been described as a primary cause of rotational instability but this view is still controversial. On the opposite other studies showed the role of peripheral ligaments as the PMC in controlling the internal rotation. The objective of this study was to develop an experimental set up for the determination of knee joint kinematics under controlled loading in the intact cadaver and to assess the role played by the ACL and the PMC in opposing tibial internal-external rotation. The starting hypothesis was that both ACL and PMC do play a role in controlling tibial rotation

METHODS

Experiments were carried out on four intact adult cadavers with no detectable damages to the knee joints. Two clusters made of four retro-reflective markers (the redundancy allows for reliability assessment) were fixed to each of the following bones: pelvis, femur, and tibia. Transosseous bi-cortical steel pins (6 mm diameter) were used. Anatomical calibration was carried out and the anatomical frames suggested in [1] were used. The location of the hip joint centre was estimated using a functional approach. The instantaneous position of the markers in a global frame during movement was reconstructed using a nine camera stereophotogrammetric system (VICON MX) at a sampling rate of 120 samples per second. Recordings were made while an operator applied a torque about the longitudinal axis of the tibia (y_t) with the knee flexed at 30°. The load was measured using a specifically designed boot instrumented with a six component load cell. Position and orientation of the load cell axes were tracked by means of a marker cluster. After the inertia parameters of both the leg-foot system and the instrumented boot were assessed, the y_t joint torque component acting at the knee was estimated through inverse dynamics. Knee joint kinematics was represented using the Cardan convention. The knee joints were tested using a Lachman and maximum tibial internal/external rotation (IR, ER) in different conditions: intact, ACL- and PMC-deficient knee. A pivot-shift as described by MacIntosh has been also performed in the ACL-deficient knee.

RESULTS

After section of both the ACL and the PMC, the anterior tibial translation increased significantly ($p < 0.05$). Concerning the tibial rotation, an example of load-displacement response of the human knee joint about the y_t axis, is shown in Fig. 1. Under an ER torque, sections produced virtually no change. When an IR 3 Nm torque was applied, the relevant movement increased by about 1.5° after ACL and 4.5° after PMC section. Six out of eight knees examined showed no sign of a clinically detectable pivot-shift.

DISCUSSION

The description of the knee kinematics has always been challenging. The amount of rotation varies greatly among individuals depending on age, sex, body build, physical development, and general ligamentous laxity. The use of robotic systems guarantees a fine control of both force and position [2] but limits the analysis to the knee specimen excluding the role of extra-articular structures such as the iliotibial tract or the thighs' muscles. On the contrary, the experimental apparatus presented in this work allows accounting for the influence of secondary knee joint restraints. The measurement inaccuracies affecting the knee kinematics estimate were shown to be compatible with the objective of the study. Results showed that ER is not controlled by ACL and PMC. ACL does not play a significant role in controlling IR whereas PMC has an effect on it. In our series the pivot-shift was not present in all knees after ACL section, even in presence of positive Lachman test, suggesting that structures other than the ACL can have a role in limiting this form of rotational instability. As suggested by Lane et al. [3] the pivot-shift phenomenon (at list when is graded as +) can occur as a result of the combination of increased anterior tibial translation with rotation that is within normal limits. We believe that these results, if confirmed by further studies with a larger number of specimens, can provide useful data for the management of knee joint instability due to ligamentous deficiency.

REFERENCES

- [1] Cappozzo A. et al, Clin Biomech 1995; 10: 171-178.
- [2] Woo S.L.Y. et al, Am J Sports Med 1999; 27:533-543.
- [3] Lane J.G. et al. Am J Sports Med. 1994; 22:289-93.

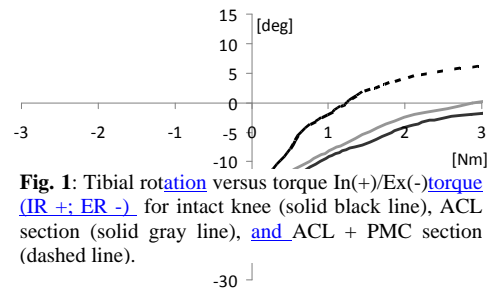


Fig. 1: Tibial rotation versus torque In(+)/Ex(-)torque (IR +; ER -) for intact knee (solid black line), ACL section (solid gray line), and ACL + PMC section (dashed line).

Quantitative Clinical Assessment of Tibial Rotation Using an Electromagnetic Tracking System

^{1,2}Tibone, J E; ²Vercillo, M T; ¹McGarry, M H; ⁺Lee, T Q

⁺Orthopaedic Biomechanics Laboratory, Long Beach VA Healthcare System, Long Beach, CA and University of California, Irvine, CA

²Kerlan-Jobe Orthopaedic Clinic, Los Angeles, CA

Senior author tqlee@med.va.gov

INTRODUCTION:

The importance of assessing rotational knee laxity is well established in both the evaluation and treatment of knee injuries, particularly those involving the anterior cruciate ligament. Use of a system of cutaneous electromagnetic position sensors (Polhemus FASTRAK, Colchester, VT) for quantitative assessment of joint motion has been described previously in several studies.¹⁻⁵ Recently, this technology was adapted to allow for quantitative assessment of tibial rotation. This was validated in the laboratory setting and found to have an accuracy of $1.6 \pm 1.3^\circ$ and repeatability of $0.8 \pm 0.4^\circ$ in comparing cutaneous measurements with actual movement of the osseous structures as measured through use of a transosseous sensor. The system has yet to be validated in the clinical setting.

The ability to quantitatively assess tibial rotation in a simple fashion in the clinical setting would aid in the diagnostic evaluation of knee rotational stability and provide a means for objective clinical assessment of knee kinematics after ACL reconstruction. The purpose of this study was to validate the use of a system of cutaneous electromagnetic position sensors to quantitatively assess side-to-side differences in tibial rotation in the clinical setting. Our hypothesis was that reliable comparison of side-to-side differences in tibial rotation is possible utilizing a simple, portable testing arrangement in an office or training room setting.

METHODS:

Ten healthy collegiate male subjects were studied. Institutional Review Board approval was obtained along with each subject's written consent. The mean subject age was 20.5 years (range 19 – 24). All subjects had clinically normal, symmetric knee examinations and were without evidence of prior knee injury by history.

Each subject was placed in the prone position. A bump was placed between the distal thighs to provide separation for the legs. Two 2 inch wide belts were then placed about the distal thighs and secured into place while the subject maximally adducted the legs (Figure 1A). A custom Plexiglass sensor mount allowed the tibial cutaneous sensor to be reliably aligned over the anterior tibial crest (Figure 1B). A second cutaneous sensor was placed over the lateral epicondyle of the distal femur.

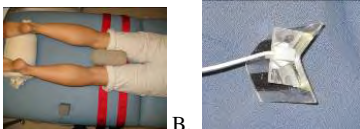


Figure 1. A: Clinical testing arrangement. B: Plexiglass sensor mount.

Assessment of knee rotational laxity was performed by two examiners during separate sessions by applying maximal manual internal and external rotation torques with the subject in the prone position and the knee at 30° and 90° of flexion (Figure 2A, B). Quantitative assessment of tibial rotation was performed using cutaneous electromagnetic position sensors (Polhemus FASTRAK, Colchester, VT). Hand position was kept constant during testing.



Figure 2. Clinical testing arrangement. A: 30° of flexion. B: 90° flexion

Means, standard deviations, and 95% confidence intervals were calculated for both knees of each subject at 30° and 90° of flexion. Intraexaminer reliability was defined as the average side-to-side difference across all trials for a single examiner. Interexaminer reliability was defined as the average difference of side-to-side

measurements made by the two examiners. Statistical significance was set at $p < 0.05$. Statistica v6.0 (StatSoft, Inc., Tulsa, OK) was used for statistical analysis.

RESULTS:

The testing protocol was tolerated well by all subjects with no adverse effects noted. Total testing time per subject for each examiner was between 15 and 20 minutes. Each examiner was able to reliably measure side-to-side differences in tibial rotation. Although a small variation in absolute rotation is noted, the side-to-side comparison remains the same between sessions.

Across all sessions, the overall average intraexaminer side-to-side difference was 2.12 (range, 0.17-6.33; SD 1.83; 95% CI, 0.57). Overall, the average intraexaminer side-to-side difference between session 1 and 2, or intraexaminer reliability, was 1.14 (range, 0.15-4.60; SD 1.16; 95% CI, 0.51). At 30° knee flexion, it was 1.78 (range, 0.49 – 4.60; SD 1.35; 95% CI, 0.84). At 90° knee flexion, it was 0.49 (range, 0.15-1.18; SD 0.33; 95% CI, 0.20) (Figure 3).

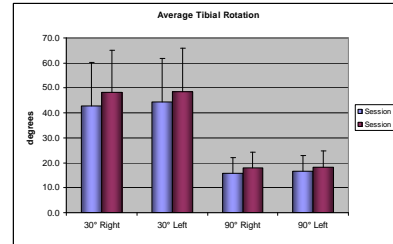


Figure 3: Intraexaminer average tibial rotation.

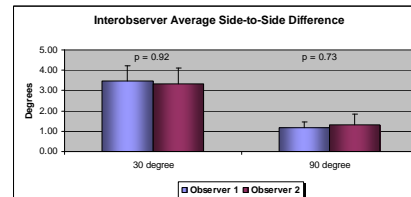


Figure 4. Interobserver side-to-side difference in tibial rotation.

Overall, the average interexaminer side-to-side difference in tibial rotation, or intraexaminer reliability, was 1.38 (range, 0.25-3.78; SD 1.25; 95% CI, 0.55). At 30° knee flexion, it was 1.57 (range, 0.31 – 3.78; SD 1.58; 95% CI, 0.84). At 90° knee flexion, it was 1.06 (range, 0.25-2.17; SD 0.82; 95% CI, 0.51) (Figure 4).

DISCUSSION:

A simple clinical testing arrangement utilizing cutaneous electromagnetic position sensors reliably compared side-to-side knee rotational laxity within acceptable limits for use in the clinical setting. The use of electromagnetic position sensors for evaluation of tibial rotation is a promising method of assessing pathologic knee rotational laxity and subsequent surgical correction in the clinical setting.

REFERENCES:

1. Tibone JE et al. *Clin Orthop. Relat Res.* 2002;400:93-97.
2. Reis MT et al. *Clin Orthop Relat Res.* 2002;400:88-92.
3. Sethi PM et al. *Am J Sports Med.* 2004;32(7):1711-1715.
4. Magit DP et al. *Am J Sports Med.* 2008;36(7):1389-96.
5. Magit DP et al. *Am J Sports Med.* 2008;36(5):971-7.

ACKNOWLEDGEMENTS:

VA Rehabilitation Research & Development, VA Medical Research, and California Orthopaedic Research Institute.

THE THREE SLOPES OF THE TIBIAL PLATEAU: IMPACT ON KNEE BIOMECHANICS

J. Hashemi¹, N. Chandrashekar², B. Gill¹, J. Slauterbeck³, R. Schutt¹, H. Mansouri¹, E. Dabezies¹, B. Beynon³
Texas Tech University (HSC); University of Waterloo; University of Vermont

INTRODUCTION

The geometry of the tibial plateau is complex and asymmetric. The subject to subject differences in tibial plateau geometry could play crucial role in the biomechanical response of the tibiofemoral joint to loads. Prior research has characterized the geometry of the tibial plateau with a single posterior slope in a lateral x-ray. However, it is more prudent to characterize the tibial plateau with three slopes including medial slope (MTS), the lateral slope (LTS), the coronal slope (CTS) as well as the depth of the medial tibial plateau (MTD). We hypothesize that 1) large subject-to-subject variations of slopes and depths of concavity on the medial plateau exist; 2) MTS and LTS are different within subjects; 3) there exist sex based differences in the slopes as well as the depth of concavity the tibial plateau.

METHODS

In a blinded study, the MTS, LTS, CTS, and MTD of the bony portion of the tibial plateau were measured using sagittal and coronal MRI images. The MRIs were obtained from 33 female and 22 male subjects. Student t-tests were performed to test for the significance of differences between sexes. Paired t-tests were performed to assess side to side differences between MTS and LTS within subjects.

RESULTS

The average MTS and LTS of female subjects were greater than those of the male subjects ($p < 0.05$) while the average CTS of females was lower than that of the males ($p < 0.05$). The correlation coefficient between MTS and LTS was 0.5. The within subject difference between MTS and LTS was significant ($p < 0.05$). A difference in the MTD between sexes existed but was not significant with a power of 34%.

DISCUSSION

The geometry of the tibial plateau is more vigorously explained by three slopes and the depth of the medial tibial condyle. The subject-to-subject differences in the geometry of the tibial plateau may influence the biomechanics of the tibiofemoral joint during loading. For instance subjects with large lateral to medial CTS will create a component of the joint compressive force (red arrow) that will promote adduction of the knee Figure 1a (CTS=6°) and 1b (CTS=0°). Those subjects with high MTS and LTS (Figure 1c and 1d) will have larger anteriorly directed shear component of the joint compressive force (red arrow) than those with mild slopes (Figure 1e and 1f).

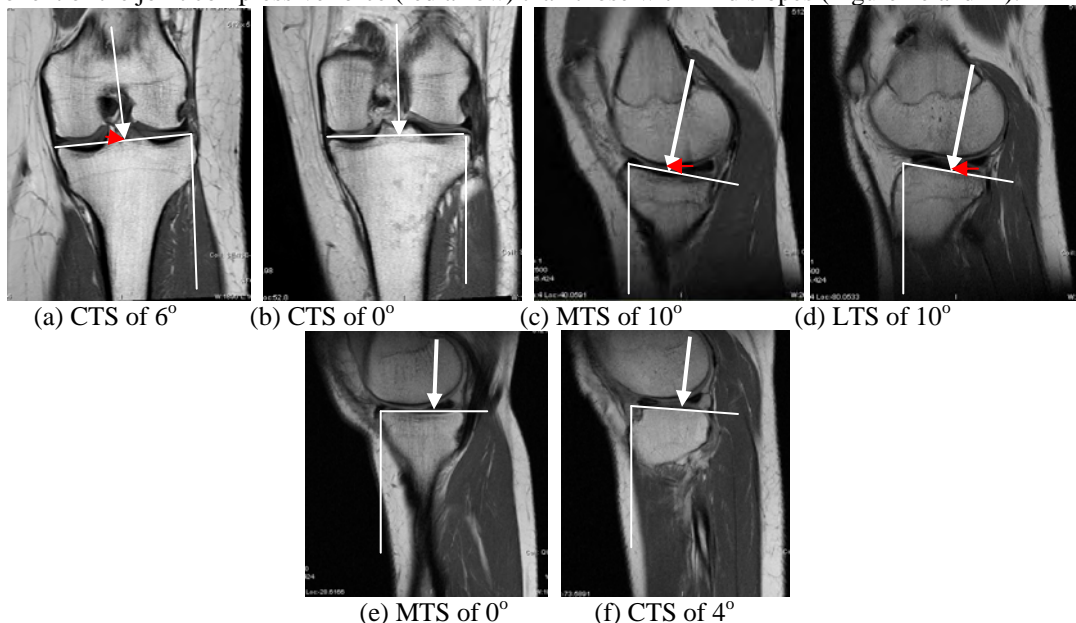


Figure 1. Joint compressive force differences in subjects with various CTS, MTS, and LTS.

The within subject differences between MTS and LTS (depending on the extent of difference) could produce affinities toward extensive internal tibial rotation or mild external tibial rotation. Because of the systematic differences in MTS, LTS, and CTS between sexes, it is possible that biomechanical responses of the male and female tibiofemoral joints will also be different. Therefore, the sex and subject-to-subject based differences in the tibial plateau geometry could be important to consider in knee injury risk assessment.

THE INFLUENCE OF THE KNEE HYDRARTHROSIS ON THE MUSCLE RECOVERY AFTER ANTERIOR CRUCIATE LIGAMENT RECONSTRUCTION.

Takakuni Sakurai^{1,3}, Toru Fukubayashi², Mako Fukano¹, Sogo Sasaki³

¹Graduate School of Sports Science, University of Waseda, Saitama, Japan, ²Faculty of Sports Science, Waseda University, Japan

³Foundation for Oriental Medicine Research and Attached Clinic, Japan

INTRODUCTION:

Periarticular swelling which often accompanies edema or hydrarthrosis is appeared after anterior cruciate ligament (ACL) reconstruction. However, the effect of the hydrarthrosis on the functional muscle recovery occurring after surgery has unknown.

Therefore, the purpose of this study was to examine the influence of hydrarthrosis on recovery of the muscle activation, the knee extension torque and the volume of the quadriceps femoris.

METHODS:

23 patients who were to have ACL reconstruction with quadrupled semitendinosus tendon by same orthopaedic doctor TF participated in this study. Each subject gave IRB approved informed written consent. Subjects were divided into two prognostic groups: hydrarthrosis group (HA) and no hydrarthrosis group (N) or absence of hydrarthrosis for three months after surgery.

Bioelectrical Impedance (BI) of the both lower extremities were measured (Physion XP) at every month for six months after surgery. Isokinetic knee extension torque was measured in seated position at 60 and 180 deg/sec (BIODEX SYSTEM III.) at every month from three months to six months after surgery.

Simultaneous surface electromyograms (EMG) of the rectus femoris (RF), the vastus lateralis (VL) and the vastus medialis (VM) were recorded at 1000Hz (bio-monitor ME6000) in isometric knee extension at 75 degree at every month from three months to six months after surgery. The EMG data was integrated (I-EMG) and normalized by the value of I-EMG on the ipsilateral side at 90 degrees of knee flexion for one second. T1, weighted resonance images (MRI) of both thighs were obtained using first spin echo imaging sequence (TR: 700 msec, TE: 15 msec). The individual muscle volume of the RF, the VL, the VM and the vastus intermedius (VI) were calculated based on the MR images.

An unpaired t-test was performed to determine differences due to the hydrarthrosis. Significance was set at $p < 0.05$.

RESULTS:

After surgery, the BI of the lower extremity decreased in both groups at post operative one month. The BI with hydrarthrosis compared to the contralateral side was significantly lower than that of the no hydrarthrosis (Fig. 1).

Recovery of the knee extension torque was tending to be delayed with hydrarthrosis (Fig. 2). The knee extension torque with hydrarthrosis was smaller than that of the no hydrarthrosis. The differences had statistically significance until five months after surgery.

With regard to the volume of the quadriceps femoris, the VM, the VL and the VI with hydrarthrosis showed considerable reduction in three and six months after surgery (Fig. 3).

The normalized I-EMG of VM in hydrarthrosis side was significantly smaller than that of the no hydrarthrosis in three, four and five months after reconstruction. The VL in hydrarthrosis

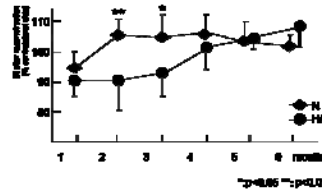


Fig. 1 : Postoperative change in BI

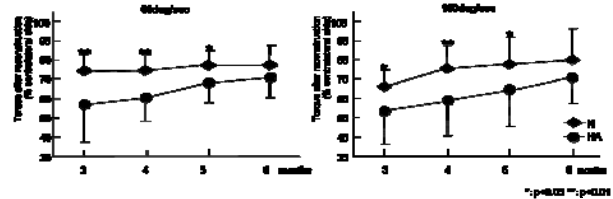


Fig. 2: Postoperative change in extension torque

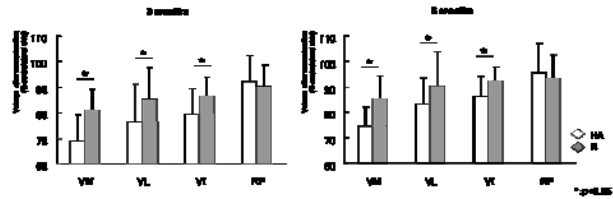


Fig. 3: Postoperative change of the volume of quadriceps femoris

	3months		4months		5months		6months	
	HA	N	HA	N	HA	N	HA	N
VM	66.2±9.4	74.2±13.4 *	67.8±14.4	77.3±16.3 **	77.1±13.3	85.7±17.2 *	85.7±10.2	89.4±12.3
VL	73.3±17.2	79.2±14.8 *	78.9±12.5	86.4±10.8 *	86.3±13.6	90.1±16.8	93.4±15.5	95.6±12.9
RF	82.9±8.3	81.2±12.5	83.9±14.3	89.5±12.1	90.1±10.8	94.4±9.7	96.1±13.4	98.6±9.4

Table 1: Postoperative change in I-EMG (% of contralateral side)

side was significantly smaller than that of the no hydrarthrosis in three and four months after surgery (table 1).

DISCUSSION:

The reduction of BI of the affected side might be caused by the periarticular swelling due to the invasion of operative treatment at one month after surgery. With regard to the patients with hydrarthrosis, the BI compared to the contralateral side was decreased by dropsy in two and three months after surgery. On contrary, BI was larger than no hydrarthrosis group because of the muscle atrophy after five months.

This study found that the regaining the muscle volumes was delayed due to the obstruction of rehabilitation by continuing hydrarthrosis. For this reason, normal muscle contraction might be disturbed by the expanded articular capsule and the compressed quadriceps femoris with the hydrarthrosis.

Another important factor we speculated was that the feedback from mechanoreceptor in the knee might be disturbed due to swelling. These results suggest that normal physiological response is a key factor of the regaining the muscle strength and volume.

As a result, this study indicates the importance of early remission of hydrarthrosis for regaining the muscle functions after ACL reconstruction.

LIGAMENT CREEP AND FATIGUE RESPONSES ARE SIMILAR FOR DIFFERENT RABBIT BREEDS

G.M. Thornton, S.J. Bailey, N.M. Chamberland
 McCaig Institute for Bone and Joint Health, University of Calgary, Calgary, Alberta

INTRODUCTION

Rabbits are a common model for studying ligament and tendon mechanics, with a variety of breeds being studied: Japanese White [1], New Zealand White [2-4], and Burgunder [5]. The rabbit medial collateral ligament (MCL) is often used to study normal and healing ligament mechanical properties. While we had previously reported the similarity of the ultimate tensile strength (UTS) of MCLs from two of these breeds: New Zealand White 95.4 ± 12.3 MPa ($n=15$) and Burgunder 97.7 ± 12.6 MPa ($n=5$) [5], we have yet to compare their creep-rupture and fatigue-rupture responses. Our purpose in this study was to evaluate the creep and fatigue response of MCLs at high stress from two rabbit breeds to determine if data collected previously for skeletally-mature, female Burgunder rabbits is comparable to that for skeletally-mature, female New Zealand White rabbits.

METHODS

Five skeletally-mature, female New Zealand White rabbits were used in this study approved by the institutional animal care committee. One MCL from each rabbit was assigned to creep and the other MCL to fatigue. After standardized preparation and mounting in an MTS system, the knee joint underwent two cycles from -5N to +2N, stopping at +1N to establish ligament zero. After measuring MCL geometry, an environment chamber equilibrated at 37°C and 99% relative humidity before re-establishing ligament zero. The MCL underwent 30 cycles at 1Hz from 1N to a force corresponding to 4.8MPa (5% of 95.4MPa). Fatigue-tested MCLs underwent cyclic loading at 1Hz from 1N to a force corresponding to 57.2MPa (60% of 95.4MPa). Creep-tested MCLs experienced sustained loading at the same force as in the fatigue tests, but the creep test was occasionally interrupted with unloading-loading cycles. Time-to-rupture (T_R) was the last time the MCL held 99% of the test force. Strain was calculated as the deformation divided by the undeformed MCL length. Parameters were compared between creep and fatigue using Wilcoxon signed-rank test for paired data (significance at $p<0.05$). The MCL creep and fatigue data from New Zealand White rabbits were compared to previously-published data for Burgunder rabbits [5] using Mann-Whitney U tests.

RESULTS

At 60%UTS, creep time-to-rupture was greater than fatigue time-to-rupture for MCLs from New Zealand White rabbits (Table 1; $p=0.04$). Initial strain (ϵ_i) and strain-at-rupture (ϵ_R) were not different comparing creep and fatigue for this breed. While the length of the MCLs from Burgunder rabbits were less than that of the New Zealand White rabbits (fatigue $p=0.01$ and creep $p=0.05$), the initial deformation and initial strain at 60%UTS were not statistically different (Table 1). The creep time-to-rupture and fatigue time-to-rupture were not different comparing the two breeds when tested at the same %UTS. Likewise, the strain-at-rupture was not statistically different between breeds.

DISCUSSION

Fatigue-tested MCLs ruptured faster than creep-tested MCLs when tested at 60%UTS for New Zealand White rabbits. This is consistent with the observation that fatigue loading causes faster rupture than creep loading of MCLs from Burgunder rabbits [5]. Additionally, creep and fatigue tested MCLs had similar initial strains and strains-at-rupture for both the New Zealand White and Burgunder rabbits. Testing at a percentage of breed-specific UTS appears to have created similar initial conditions for the creep and fatigue tests because no breed differences in applied test force, initial elongation, or initial strain were observed despite a difference in MCL length between breeds. The similarity in MCL failure, creep-rupture and fatigue-rupture responses between breeds suggests that previously-published long-term creep and fatigue data, where the longest test lasted 168 hours [5], may not have to be repeated but rather may be considered normal rabbit MCL response regardless of breed.

ACKNOWLEDGEMENTS: NSERC, McCaig Fund

REFERENCES: [1] Yamamoto N, Hayashi K. 1998 *Biomed Mater Eng* 8:82-90 [2] Woo SLY et al. 1992 *J Biomech* 25:377-386 [3] Danto MI, Woo SLY. 1993 *J Orthop Res* 11:58-67 [4] Thornton GM et al. 2002 *J Orthop Res* 20:967-974 [5] Thornton GM et al. 2007 *Clin Biomech* 22:932-940

Table 1: Properties of MCLs tested at 60% UTS from New Zealand White (NZW) and Burgunder (BRG) rabbits.

Group	CREEP					FATIGUE				
	n	T_R (hrs)	MCL Length (mm)	ϵ_i (mm/mm)	ϵ_R (mm/mm)	n	T_R (hrs)	MCL Length (mm)	ϵ_i (mm/mm)	ϵ_R (mm/mm)
NZW	5	6.2 ^	24.17 *	0.090	0.180	5	0.68	25.27 *	0.070	0.151
		(0.8-17.4)	(23.01-26.40)	(0.082-0.116)	(0.138-0.248)		(0.08-3.20)	(23.83-26.42)	(0.069-0.118)	(0.116-0.174)
BRG [5]	4	5.9 ^	21.70	0.104	0.177	5	0.51	21.35	0.094	0.158
		(2.8-11.3)	(20.80-23.50)	(0.080-0.132)	(0.111-0.201)		(0.09-1.01)	(20.05-22.05)	(0.089-0.111)	(0.147-0.207)

Data are shown as median (range). ^ Creep different than fatigue ($p<0.04$). * NZW different than BRG ($p<0.05$).

MECHANICAL TESTING OF ENGINEERED FIBERS DERIVED FROM HUMAN DERMAL FIBROBLASTS: METHODS AND FEASIBILITY

N.R. Schiele¹, R.A. Koppes¹, D.M. Swank², D.B. Chrisey³, D.T. Corr¹

Departments of (1) Biomedical Engineering (2) Biology (3) Material Science and Engineering, Rensselaer Polytechnic Institute, Troy, NY

INTRODUCTION

Fibroblast cells are crucial for the maintenance of extracellular matrix proteins and for the synthesis of collagen, a major building block of tendon, ligament, and skin [1]. By directing fibroblast cell growth, and guiding the production of their own extracellular scaffold, we aim to exploit the behavior of these cells to develop a bottom-up engineering approach for customized replacements of collagenous soft tissues. As an important first step, the objective of this study was to establish a method to create and mechanically evaluate engineered fibers, grown from human dermal fibroblasts, on the scale of a single collagen fiber.

METHODS

An UV excimer laser (ArF, 193 nm, TeoSys, Crofton MD) was used to micromachine 3D features in 2% agarose gel. Channels were created with a 1-cm length, a 100- μm width, and a 60- μm depth. Human fibronectin (BD Bioscience) was pipetted (20 μl of 0.3 mg/ml) into the channel and after drying in a laminar flow hood for one hour, human dermal fibroblast cells (1 ml of 5×10^4 cells/ml) in culture media (89.5% DMEM, 10% FBS, 0.5% penicillin-streptomycin) were pipetted over the channels. Fibroblast fibers were incubated for 72 hours (37 $^{\circ}\text{C}$, 5% CO_2 , 95% RH) then removed using a dissecting needle and tweezers. Each fiber was placed into glycerol, sectioned into test specimens $\sim 300 \mu\text{m}$ in length, and each test specimen was secured at both ends using T-clips, laser cut from aluminum foil (MicroConnex Snoqualmie, WA), (**Fig. 1**). The resulting preparation (250 μm gage length) was evaluated using a custom microscope-based single fiber mechanics rig. Load is measured using a force gauge, AE-800 Series sensor element, (SensorOne technologies, Sausalito, CA) with a resonance frequency of ~ 10 kHz. The T-clips were attached to the hooks of the testing rig in a temperature controlled (± 0.25 $^{\circ}\text{C}$ of 15 $^{\circ}\text{C}$) bath of relaxation solution. Each fiber specimen was uniaxially elongated to failure, quasi-statically, using the rig's micrometer/micromanipulator: a slight tensile preload was applied, then force was recorded every 10 μm increase in length until specimen failure.

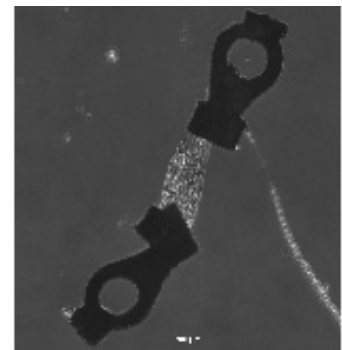


Fig. 1. Micrograph of representative fibroblast fiber (gage length \hat{A} 250 μm), T-clipped in preparation for mechanical testing (phase contrast, 10x).

RESULTS

Engineered fibroblast fibers possessed sufficient structural integrity to permit significant manipulation during dissection, handling, T-clip attachment and mounting to the test rig. Preliminary testing has shown that a single fibroblast fiber can withstand elongations of approximately 300% with failure occurring due to slippage at the fiber/T-clip interface.

DISCUSSION

We have demonstrated the ability to grow and mechanically evaluate fibers of human dermal fibroblasts, on the scale of small collagen fibers. Once single fibers have been fully characterized, their mechanical properties can be altered to more closely resemble those of native tendon or ligament through (a) geometric modifications of the agarose channels, (b) chemical manipulation using growth factors, and (c) mechanical stimulus during growth using a bioreactor. Encouraging collagen production can strengthen the fibers while variations in fiber geometry (*e.g.* width, crimp geometry; **Fig. 2**) may allow tailored mechanical responses to be created in an attempt to replicate toe-in regions of tendon and ligament. Additionally, the dynamic stiffness of each modification can be evaluated using the motor on the fiber mechanics rig - a piezo translator, P-841.20 (Pysik Instrumente, Karlsruhe, Germany) with 30- μm throw and less than 0.5 millisecond response time when used with position feedback. These developments help provide the foundation necessary for our future research in tendon/ligament tissue engineering.

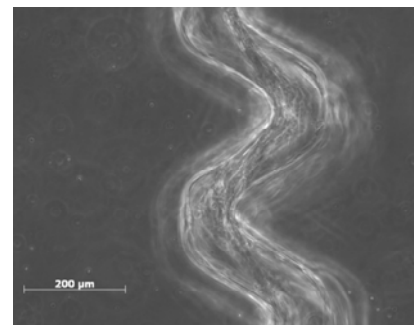


Fig. 2. Crimp pattern that has been micromachined into agarose gel and seeded with fibroblasts.

REFERENCE

1. Martin P. Wound Healing-Aiming for Perfect Skin Regeneration. Science 276 (1997) 75-81.

Gene Expression and Protein Analysis in Calcific Tendinopathy of Human Rotator Cuff.

Francesco Oliva, Andrea Grasso*, Nicola Maffulli**

Department of Trauma and Orthopaedic Surgery University of Rome "Tor Vergata", School of Medicine Viale Oxford 81, 00133 Rome, ITALY.

*Department of Shoulder Surgery Villa Valeria Hospital, Piazza Carnaro 18, 00141, Rome, ITALY.

**Department of Trauma and Orthopaedic Surgery, Keele University School of Medicine, North Staffordshire Hospital, Thornburrow Drive, Hartshill, Stoke on Trent, Staffordshire, ST4 7QB, ENGLAND.

Purpose

Calcific tendinopathy is a common disease of unknown aetiology. Two different pathogenetic theories have been developed. According to Codman, disruption of tendon fibers precedes calcium deposits. Uthoff, on the other hand, proposed that a viable environment allows an active process of cell-mediated calcification . 1 The aetiopathogenesis of the association of calcium deposits with the process of failed healing response typical of tendinopathy is at present unknown .

Material and Methods

We compared biopsies of pathological rotator cuff tendons and specimens harvested from an apparently healthy area in the same tendon of 10 patients. As control, we examined 10 normal tendons from patients with shoulder instability.

RNA was extracted from snap-frozen biopsies using a modification of the guanidium-thiocyanate method (Trizol reagent) and retrotranscribed using random primer hexamer (CDNA Archive kit, Applied Biosystems). RNA levels were measured using quantitative PCR; BMP2, 4 and 6 were analyzed using the Taqman Gene Expression Assays, whereas collagen V, VEGF, Cathepsin K, TG2, osteopontin and osteonectin were evaluated using the Sybr green method. Relative quantification was performed using the $2^{-\Delta\Delta C_t}$ method.

Results

There was greater gene expression of osteopontin, Cathepsin K and TG2 in calcific tendons, while collagen V, VEGF and BMP 2 do not show any significant differences. BMP 4 and 6 show lower level in pathological tendons compared with the healthy area.

Conclusion

The tissue in the area of tendinopathy undergoes marked rearrangement at molecular levels, and support the role of Cathepsin K and Osteopontin during the phases of formation and resorption of the calcific tendinopathy.

Bibliography

1. [Uthoff HK](#), [Loehr JW](#). Calcific Tendinopathy of the Rotator Cuff: Pathogenesis, Diagnosis, and Management. J Am Acad Orthop Surg. 1997; 5:183-191.
2. [Riley GP](#), [Harrall RL](#), [Constant CR](#), [Cawston TE](#), [Hazleman BL](#). Prevalence and possible pathological significance of calcium phosphate salt accumulation in tendon matrix degeneration. Ann Rheum Dis. 1996;55:109-115.
3. [Archer RS](#), [Bayley JI](#), [Archer CW](#), [Ali SY](#). Cell and matrix changes associated with pathological calcification of the human rotator cuff tendons. J Anat. 1993;182:1-11.

EFFECT OF DIHYDROTESTOSTERONE ON CULTURED HUMAN TENOCYTES FROM INTACT SUPRASPINATUS TENDON.

+¹Ruzzini L.; ¹Longo UG.; ¹Franceschi F.; ²Cittadini A.; ²Sgambato A.; ³Maffulli N.; ¹Denaro V.
+¹Campus Biomedico University, Rome, Italy ²Catholic University, Rome, Italy ³Keele University, Stoke on Trent, UK

INTRODUCTION

Rotator cuff tears are one of the most common causes of shoulder pain and disability in the upper extremity.

Many factors have been reported to be associated with tendon pathology such as gender, age, body composition and genetics.

The role of hormones in the pathogenesis of tendinopathy is not well recognized even though the use of steroids is correlated with an higher incidence of spontaneous tendon ruptures. However, little information exists regarding the effect of endogenous testosterone on human tenocytes cell function.

The aim of our study was to investigate the biological effects of dihydrotestosterone (DHT) on human tenocyte cultures from intact supraspinatus tendon o male subjects.

METHODS

Cultured human tenocytes were seeded into six-well culture plates at a density of 5×10^4 cells per well and incubated for twenty-four hours to allow for attachment of cells. 10^{-9} M to 10^{-7} M DHT or DMEM only (control) was added to the cultureplate wells. The cells were incubated for 48 hrs, 72 hrs and 96 hrs before being subjected to cell proliferation test.

Cell morphology was observed under an inverted phase-contrast light microscope after 48 hrs, 72 hrs and 96 hrs of DHT treatment. Cells from the second and third passages were used for the experiments.

Comparisons between control and DHT-exposed groups were analyzed using paired student's t-test; p values less than 0.05 were considered significant.

RESULTS

DHT-treated tenocytes showed an increased proliferation rate when treated to DHT concentration higher than 10^{-8} M. Differences in cell numbers between control and DHT-treated cells were statistically significant ($p < 0.05$) after 48h and 72 h of treatment with DHT concentrations of 10^{-8} M and 10^{-7} M. The tenocytes treated with DHT (10^{-8} M and 10^{-7} M) were seen to had become more flattened and polygonal compared to control cells that maintained their fibroblast-like appearance during the experiment at each observation time.

DISCUSSION

Testosterone has previously been shown to play a detrimental role on the function of cells from many different tissues. For this reason we aimed to investigate effects of testosterone in human tenocytes.

The results of our in vitro experiments showed that progressive increasing concentration of dihydrotestosterone (DHT) at doses of $> 10^{-8}$ M had direct effects on male human tenocytes, increasing cell number after 48h and 72 h of treatment and leading to a more dedifferentiated phenotype after 48 h, 72 h and 96 h of treatment.

As the tenocyte is the major cell type in tendons and is responsible for the production and maintenance of extracellular matrix, such an effect is especially important during tendon-healing and repair, when active proliferation is required.

These data can therefore be taken as preliminary evidence for a relationship between testosterone and rotator cuff tendinopathy.

TRANSGLUTAMINASES EXPRESSION IN MICE TENDONS AND HUMANS SUPRASPINATUS TENDON RUPTURES

Francesco Oliva, Umberto Tarantino, Monica Celi, Nicola Maffulli.

Department of Trauma and Orthopaedic Surgery University of Rome "Tor Vergata", School of Medicine, Rome, Italy.

Department of Trauma and Orthopaedic Surgery, Keele University School of Medicine, Staffordshire, England.

AIMS

The diversity of tendon injuries spans from acute traumatic tendon rupture to chronic overuse injuries such as tendinopathy and calcific tendinosis. Treatment mainly is based on triggering the natural healing process, but the outcome of healing often is unsatisfactory. Transglutaminase (TGs) enzymes and proteins crosslinking have for long time been implicated in the formation of hard tissue development, matrix maturation and mineralization. Among the TGs family members, TG2 and factor XIII are the more studied in the context of connective tissue formation and stabilisation. We investigate the TGs expression pattern of Achilles tendons of TG2 knock-out and wild type mice and both in normal and injured shoulder's suprapinatus tendon biopsies.

MATERIAL AND METHODS

Tendon samples were harvested from 5 individuals (2 men, 3 women; age, 60 +/- 1 year) who had sustained a rotator cuff tear and underwent miniopen surgery repair of the lesion, and from 5 individuals who died of cardiovascular events (mean age, 65 +/- 1 year). We analyze the consequences of TG2 deficiency, generated by a gene-targeting approach, harvesting normal Achilles tendon of mice at 8 weeks of age TG2 knock-out and wild type (five animals for each group).

RESULTS

The present original basic science study provides a description of the presence of transglutaminases enzymes, never elucidated before, first in TG2 knock-out mice and in wild type mice tendons. Histology revealed no gross anatomy differences between TG2 knock-out and wild type Achilles tendons.

RT-PCR experiments performed on wild type or TG2 knock-out mice reveal that TG1 and TG3 are expressed, at transcriptional level, in WT and TG2 knock-out tendon biopsies. TG5 transcript is not detected

After that the study has been performed also on human surgical specimens of torn supraspinatus tendon from patients with rotator cuff tears. All five patients with a torn supraspinatus tendon showed a lost parallel arrangement of the fibers, the nuclei became progressively rounded, an increased cellularity and vascular bundles were noted. The collagen stainability was decreased. Control tendons show the typical normal histology with fibers arranged close and parallel to each other with slight waviness, vascular bundles running parallel alongside of the collagen fibers, tenocyte nuclei were flattened and spindle-shaped, sometimes arranged in rows.

Factor XIII, TG1 and TG2, unlike TG3 and TG5 are expressed in control group. Injured supraspinatus tendons shows a reduction of TG2 expression in all specimens analyzed.

CONCLUSIONS

The histologic appearance of supraspinatus injured tendons was of poor healing response with absence of acute inflammation. The reduction of TG2 expression in all injured supraspinatus tendons suggest that this ubiquitous transglutaminase could be important in maintaining tendon structural integrity thanks to its mechanical or cross-linking function. We advocate more studies on this topic never before elucidated to add new knowledge on the obscure relationship between the ECM and healing tendons processes.

Bibliography

1. Tallon C, Maffulli N, Ewen SW. Ruptured Achilles tendons are significantly more degenerated than tendinopathic tendons. *Med Sci Sports Exerc* 2001, 33, 1983–1990
2. Vora AM, Myerson MS, Oliva F, Maffulli N. Tendinopathy of the main body of the Achilles tendon. *Foot Ankle Clin* 2005, 10; 293-308
3. Candi E, Oddi S, Paradisi A, Terrinoni A, Ranalli M, Teofoli P, Citro G, Scarpato S, Puddu P, Melino G. Expression of transglutaminase 5 in normal and pathologic human epidermis. *J Invest Dermatol* 2002, 119; 670-677
4. Tarantino U, Oliva F, Taurisano G, Orlandi A, Pietroni V, Candi E, Melino G, Maffulli N. FXIIIa and TGF-beta over-expression produces normal musculo-skeletal phenotype in TG2-/- mice. *Amino Acids* 2008, 2
5. Orlandi A, Oliva F, Taurisano G, Candi E, Di Lascio A, Melino G, Spagnoli LG, Tarantino U. Transglutaminase-2 differently regulates cartilage destruction and osteophyte formation in a surgical model of osteoarthritis *Amino Acids* 2008, 27

Influence of fasting plasma glucose levels in the pathogenesis of rotator cuff tears

Umile Giuseppe Longo *, Filippo Spiezia *, Francesco Franceschi *, Francisco Forriol **,
Nicola Maffulli [†] Vincenzo Denaro *

* Department of Orthopaedic and Trauma Surgery, Campus Biomedico University, Via Alvaro del Portillo, 200, 00128 Rome, Italy

** Department of Orthopaedic and Trauma Surgery, Fremap University, Madrid, Spain

[†] Department of Trauma and Orthopaedic Surgery, University Hospital of North Staffordshire, Keele University School of Medicine, Stoke on Trent, ST4 7LN United Kingdom.

Objective

To determine the plasma glucose levels in non diabetic patients with rotator cuff tear

Materials and Methods

The study included 194 subjects who were operated at our institution. Group 1 included 97 consecutive patients (36 men and 61 women; mean age: 62.9 years, range 37 to 82) who underwent arthroscopic repair of a rotator cuff tear in 2007 and 2008. Group 2 (control group) included 97 patients (36 men and 61 women; mean age: 61.6 years, range 36 to 80) who underwent arthroscopic meniscectomy for a meniscal tear in the same period, and had no evidence of shoulder pathology. These patients were frequency-matched by age (within 3 years) and gender with patients of Group 1.

Main outcome measure

Measurement of fasting plasma glucose levels

Results

Patients with rotator cuff tears (Group1) showed statistically significantly higher fasting plasma glucose levels within the normoglycemic range ($p=0,007$) when compared with patients with meniscal tear (Group 2).

Conclusions

The present study suggests that normal, but in the high range of normal, increasing plasma glucose levels may be a risk factor for rotator cuff tear. An enhanced understanding of these factors holds the promise of new approaches to the prevention and management of rotator cuff tears.

RESPONSE OF A STEM CELL-BASED SELF-ASSEMBLED TISSUE (scSAT) TO CYCLIC TENSION

*Ogawa A., *Saito K., **Ando W., Nakamura N., and +*Fujie H.

+*Biomechanics Laboratory, Department of Mechanical Engineering, Kogakuin University, Tokyo, Japan

** Department of Orthopaedic Surgery, Osaka University Medical School, Osaka, Japan

INTRODUCTION:

Healing capacities of the ligaments and tendons are limited, although they have superior functions. Therefore, it is one of potential options for the repair of such soft tissues to use cell-based therapies. We have been developing a novel tissue-engineering technique for the repair of ligaments and tendons which involves a stem cell-based self-assembled tissue (scSAT) derived from synovium¹⁾. As the scSAT is composed of cells with their native extracellular matrix, it is free from concern regarding long-term immunological effects. The scSAT is expressed as tissue engineered construct (TEC) when it is used for cartilage repair. Our previous studies indicated that the tensile property of the scSAT is dependent on cell density, culture period, and amount of ascorbic acid²⁾. However, we have a hypothesis that the scSAT changes its mechanical property and structure in response to externally applied tensile stress, in the same way as remodeling phenomena occurred in normal ligaments and tendons. The detailed information regarding the remodeling of the scSAT may improve the tissue engineering technique for ligament and tendon repair. Therefore, the effect of tensile stress on the mechanical property of the scSAT was determined in the present study.

MATERIALS AND METHODS:

• Specimen preparation

Mesenchymal stem cells (MSCs) obtained from the synovial membranes of human knee joints were cultured in DMEM in monolayer. After the cell density reached to 4.0×10^5 cells/cm² (6-cm dish), 0.2 mM of ascorbic acid 2-phosphate was injected to promote the bio-synthesis of extracellular matrix. Thirty five days after the injection, synthesized matrices were carefully detached from culture plate and allowed to undergo active contraction for 1 hour to develop scSATs¹⁾.

• Cyclic tensioning

The scSAT specimen of 8 x 10 mm in size were fixed to the chucks of a cyclic tensioning apparatus. The initial length of the specimen between the chucks was set 8 mm. The specimen was subjected to a cyclic tensile load with the range of either 4-8 mN, 6-10 mN, or 8-12 mN at 37 °C in an incubator for 3 days (loaded group). In each day, the cyclic load was applied to the scSAT for 1 hour in DMEM followed by an unloaded condition for 23 hours. For comparison, the scSAT was set unloaded for 3 days in the incubator (control group).

• Tensile test and histological observation

The scSAT was, then, subjected to tensile testing at a rate of 0.05 mm/s in saline solution at 37 °C using a custom-made micro tensile tester developed in our laboratory³⁾. Histological observation of the surface structure of the scSAT was determined using a differential interference contrast microscope (IX71, OLYMPUS, Japan).

RESULTS and DISCUSSION:

Typical stress-strain relationships of the loaded and non-loaded control groups are shown in Figure 1(a). The relationships of all the groups exhibited J-shaped curves. The curves of 4-8 mN-loaded groups consisted of toe-region in low strain and linear region in high strain. The tangent modulus in 5-10% of strain was slightly increased in loaded groups than in control groups. The tensile strength was shown in Figure 1(b). As compared with the control group, the strength was significantly higher in the loaded group of 4-8 mN, but was significantly lower in the loaded group of 8-12 mN. Histological observation indicated that the fibrous structure was aligned parallel to the direction of cyclic load application in the loaded group, while no fibrous structure was observed in the control group. These results imply that cyclic tensioning for 1 hour a day for total 3 days strengthened the scSAT, however, relatively large tensioning caused deterioration of the scSAT possibly because of the failure of collagen structure.

REFERENCES:

- 1) Ando W. et al. Proceedings of the 52nd ORS, 2006.
- 2) Nagai K. et al. Proceeding of the 52nd ISL&T, 2006.
- 3) Fujie H. et al. Proceedings of the 53rd ORS, 2007.

ACKNOWLEDGMENT:

The present study was financially supported in part by Research Project of the MEXT, Japan (BERC, Kogakuin University).

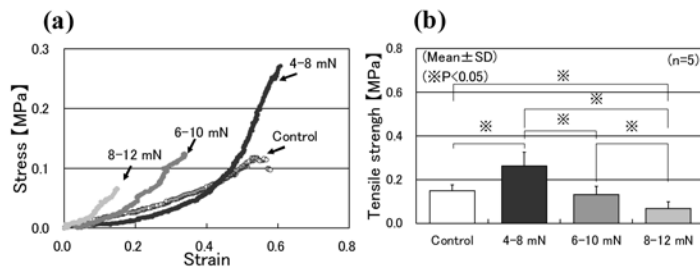


Fig.1 Typical stress-strain curves (a) and tensile strength (b) of the loaded and controls groups in tensile test

LOCAL VITAMIN C INJECTION REDUCED TENDON ADHESION IN A CHICKEN MODEL OF INJURED FLEXOR DIGITORUM PROFUNDUS TENDON INJURY

Fu SC^{1,2}, Hung LK¹, Lee YW^{1,2}, Mok TY^{1,2}, Lui PYY^{1,2}, Chan KM^{1,2}.

¹Department of Orthopaedics & Traumatology, The Chinese University of Hong Kong, Prince of Wales Hospital, Hong Kong.

²The Hong Kong Jockey Club Sports Medicine and Health Sciences Centre, Faculty of Medicine, The Chinese University of Hong Kong, Hong Kong SAR, China

INTRODUCTION:

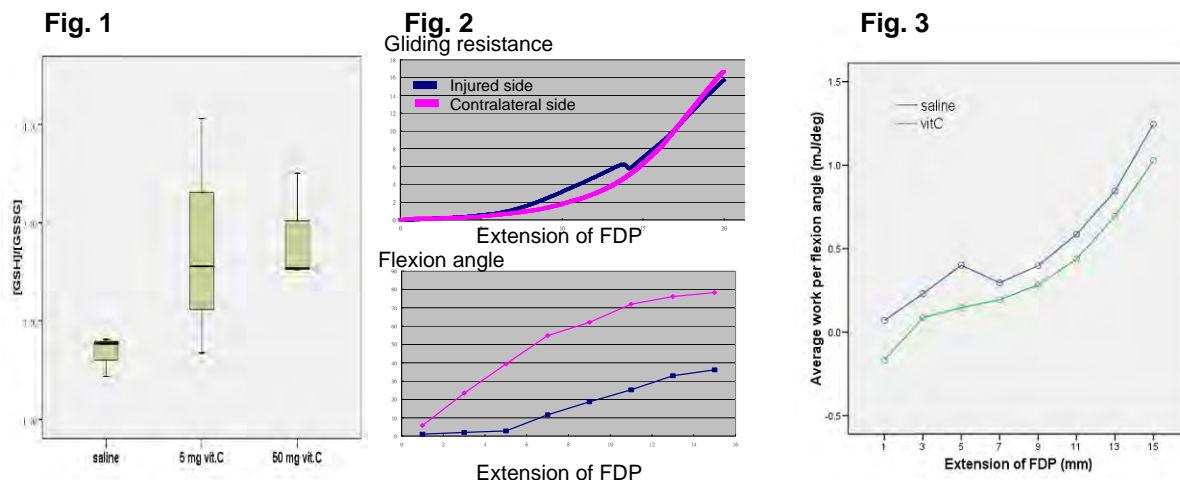
Adhesion formation is a frequent complication of hand flexor tendon repair. Development of excessive fibrotic responses in tendon adhesion is probably related to the extent of local inflammation, tissue damage and hemorrhage; in which overwhelming oxidative stress is inevitably involved. It is possible that antioxidants may be effective to reduce tendon adhesion. In the present study, we investigated the effects of local vitamin C injection to reduce tendon adhesion in a chicken model of Flexor digitorum profundus (FDP) tendon injury.

MATERIALS & METHODS:

A modified chicken model of FDP tendon injury was employed. Immediately after traumatization, vitamin C was injected to the wound in the treatment groups and saline was injected in the control group (n=6). The injured feet were immobilized for 2 weeks. The chicken feet were sampled at 2 or 6 weeks post injury for mechanical testing of gliding resistance and glutathione measurement.

RESULTS:

We found that injection of vitamin C significantly suppressed oxidative stress as revealed by the increase of the ratio of reduced (GSH) to oxidized glutathione (GSSG) (Fig. 1). Injured FDP exhibited significantly increased gliding resistance and decreased flexion angle (Fig.2). Injection of vitamin C significantly reduced work of flexion. (Fig.3)



DISCUSSIONS AND CONCLUSION:

We reported that local injection of vitamin C immediately after surgical repair could reduce the development of oxidative stress, and the gliding properties of FDP were improved. The results suggested that oxidative stress may contribute to the development of tendon adhesion, and anti-oxidation would be a promising strategy to reduce post-surgical tendon adhesion.

BIOENGINEERED CAMBIAL LAYER PROGENITOR CELL SHEETS TRANSPLANTATION FOR TENDON-BONE HEALING

Chih-Hsiang Chang,¹ Chih-Hwa Chen,¹ Hsia-Wei Liu,^{1,2} Shu-Wen Whu,¹ Shi-Hui Chen,¹ Jih-Chao Yeh,^{1,3} Mei-Yun Wu,¹ I-Hsuan Lin,¹ Hsiang-Jou Sun,¹ and Ging-Ho Hsiue⁴

¹Department of Orthopaedic Surgery, College of Medicine, Chang Gung Memorial Hospital-Keelung, Chang Gung University, Keelung, Taiwan

²Material and Chemical Research Laboratories, Industrial Technology Research Institute, Hsinchu, Taiwan

³Department of Biomedical Engineering, Chung Yuan Christian University, Chung Li, Taiwan

⁴Department of Chemical Engineering, National Tsing Hua University, Hsinchu, Taiwan

INTRODUCTION:

Our previous study has reported the results of tendon-bone healing using periosteum wrapped around tendon grafts. The cambium layer of periosteum contains osteochondral progenitor cells that can differentiate into osteoblasts and chondrocytes during tendon-bone healing.¹ For the purpose of healing, we developed a scaffold-free method using polymerized fibrin-coated dishes for making functional cambium layer progenitor cell sheets that may be used as periosteum-like tissue transplants. Naturally derived submucosal layer and acellular tissue matrices from small intestines can be as cell sheets delivery vehicle for tendon-bone healing on anterior cruciate ligament reconstruction (ACL) in a rabbit model.

METHODS:

Polymerized fibrin-coated PE dishes were fabricated with fibrinogen monomers mixed with thrombin.² Cambium layer progenitor cells (CPCs) derived from rabbit tibia periosteum were cultivated on a fibrin-coated surface for 1 week at 37°C. The laminated cell sheets were dissociated intact from the polymerized fibrin layer by proteases secreted from cells. The small intestinal submucosa (SIS) was prepared from the intestines of rabbit by mechanical and chemical processing. CPCs sheets were seeded onto the SIS layer. Bilateral ACL reconstructions using the long digital extensor tendon grafts were performed on mature rabbits. A 2.3-mm diameter femoral and tibial tunnel was created according to the ACL footprints. The CPC-SIS layers wrapped around the tendon grafts were pulled manually from tibial outlet through the drill hole to the joint and then to the femoral tunnel. The rabbits were sacrificed at 4 and 8 weeks postoperatively.

RESULTS:

CPC sheets could be non-invasively harvested as intact, transplantable sheets by intrinsic protease. After peeling from culture surfaces, the CPC sheets remained viable (shown as Figure 1). Harvested cell sheets were slightly disrupted in order to observe the basal surface, and Confocal microscopy assays showed that cultured CPCs did indeed deposit ECM on the basal surface (shown as Figure 2). Transmission electron micrographs of the cells showed the abundant cytoplasmic organelles. *In vivo* study, histological staining showed there was further matrix deposition with fibrocartilage formation in the tendon-bone junction at 4 and 8 weeks.

DISCUSSION:

These preliminary results suggest that a well-organized and functional CPC monolayer maintain their differentiated capacity and keep their *ex vivo* osteochondral potential. Bioengineered CPC sheets and SIS co-layer can feasibly offer a new therapeutic strategy for novel approaches to augment tendon-bone junction healing.

REFERENCES

1. Chen CH, Chen WJ, Shih CH and Chou SW, Arthroscopic anterior cruciate ligament reconstruction with periosteum-enveloping hamstring tendon graft. *Knee Surg Sports Traumatol Arthrosc.* 2004 Sep;12(5):398-405.
2. Itabashi Y, Miyoshi S, Kawaguchi H, Yuasa S, Tanimoto K, Furuta A, Shimizu T, Okano T, Okano T, Fukuda K and Ogawa S, A new method for manufacturing cardiac cell sheets using fibrin-coated dishes and its electrophysiological studies by optical mapping. *Artif Organs*, 2005 Feb;29(2):95-103.

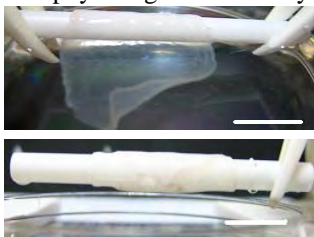


Figure 1. Appearance of CPCs sheets. Scale bar was 1 cm.

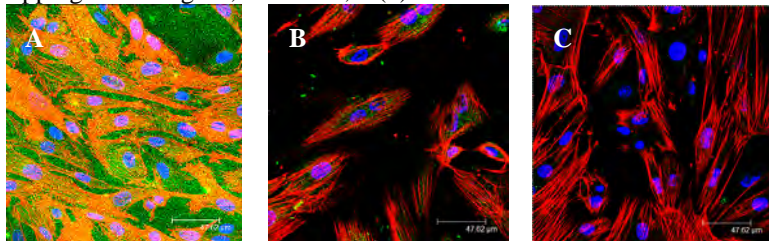


Figure 2. Confocal microscopy assays of CPCs sheets. A:Fibrin; B:Collagen type I; C: Alkaline phosphatase. Red: α -actin; Blue:

The Effects of Surface Treatment with Lubricin after Flexor Tendon Repair

*Zhao, C; *Sun, YL; *An, KN; **Jay, GD; *Moran, SL; *Amadio, PC

*Biomechanics Laboratory, Division of Orthopedic Research, Mayo Clinic College of Medicine, Rochester, MN, USA

** Brown University Providence, RI, USA

INTRODUCTION

Improvement of flexor tendon gliding with boundary lubricants, such as carbodiimide derivatized hyaluronic acid, (cd-HA)(1), can decrease postoperative adhesions. Lubricin, an important component of synovial fluid further decreases tendon gliding resistance when it is combined with cd-HA (2). Although previous studies were conducted using a flexor tendon graft model, the same principle may be applied to the flexor injury and primary repair model, which has more clinical relevance. The purpose of this study was to investigate the combination of lubricin with cd-HA after flexor tendon repair in a canine in vivo model.

METHODS

Sixty mixed-breed dogs weighing 20 to 25 kg were used. The study was approved by of our Institutional Animal Care and Use Committee. Each dog had flexor tendon repair in one paw, with the dogs randomly assigned to have the repairs treated either with cd-HA + lubricin (cd-HA-lubricin group, n=30) or no treatment (control group, n=30). Animals were sacrificed at 10 days (n=20), 21 days (n=20), and 42 days (n=20). The contralateral unoperated tendons were also analyzed (normal group, n=10). The 2nd and 5th flexor digitorum profundus (FDP) tendons from each dog were fully lacerated in zone II, and repaired with a modified Pennington technique with 3/0 Ethibond (Ethicon, Inc., Somerville NJ). A simple running circumferential epitenon suture of 6/0 nylon (Ethicon Inc., Somerville, NJ) was used to reinforce the repair. Therapy started at day 5 postoperatively, and continued until the dogs were sacrificed. Following sacrifice, the repaired tendons were randomly assigned for work of flexion (WOF), gliding resistance (GR), or repair strength (RS) testing.

Measurement of Digit Work of Flexion (WOF): The repaired FDP tendons were carefully exposed at the proximal metacarpal level, transected, and sutured to a cable connected to a load transducer. The repair site, surrounding tendon sheath and overlying skin were all preserved. A K-wire was inserted longitudinally through the metacarpal bone to fix the metacarpophalangeal (MCP) joint in extension. Reflective markers were fixed to the proximal, middle, and distal phalanges, respectively. The prepared digit was then mounted on the testing device by fixing the proximal K-wire to a custom jig. The actuator pulled the tendon proximally a rate of 2 mm per second, causing digit flexion. Digit motion was recorded by a video camera and the marker motion was analyzed by motion analysis software (Motion Analysis Corporation, Santa Rosa, CA). Work of flexion data were calculated from the tendon displacement vs loading curve during digit flexion, and then normalized (nWOF) as described previously (3).

Tendon Gliding Resistance (GR) Measurement: After motion analysis, the repaired tendons were further dissected, keeping the proximal pulley intact. The gliding resistance between the tendon graft and proximal pulley was then measured using a custom tendon-pulley friction testing device, as previously described (4).

Measurement of Repair Strength (RS): To measure breaking strength, the repaired tendons were secured in a servohydraulic testing machine and distracted to failure at a rate of 20 mm/min. A differential variable reluctance transducer (DVRT, Microstrain, Williston, VT) was attached to the tendon spanning the repair site to measure gap formation during testing. Tensile force, grip-to-grip displacement, and gap displacement measured by the DVRT transducer were collected at a rate of 20 Hz. Maximum breaking force was recorded. In addition, a regression line was fit to the linear region of the force versus gap formation (as measured by the DVRT) to measure the resistance to gap formation.

Statistical Analysis: Two-way ANOVA was used to analyze the differences between normal FDP tendons, repaired FDP tendons with cd-HA-lubricin treatment, and repaired tendons without treatment. Fisher's Exact Test was used for the tendon rupture and gap comparisons. A significance level of $p < 0.05$ was used.

RESULTS

Two (3.3%) tendons ruptured in the control group and 14 (23%) in the cd-HA-lubricin group. Gap formation occurred in 13 (21%) control tendons and 20 (33%) tendons in the cd-HA-lubricin group. The difference was significant for rupture, but not for gap formation.

Grossly, there were adhesions noted in all the control repairs, but in few of the unruptured cd-HA-lubricin repairs. The control nWOF was significantly higher than the cd-HA-lubricin and normal tendon nWOF at all three time points ($p < 0.05$). There was no significant difference in nWOF between cd-HA-lubricin and normal tendons at any time period (Figure 1). The GR of the normal tendons was significantly lower than both cd-HA-lubricin and control repairs ($p < 0.05$), but there was no significant difference between cd-HA-lubricin and control repairs at any time point (Figure 2). The maximal strength and stiffness of the control repairs was significantly higher than the cd-HA repairs at day 42 ($p < 0.05$), but not at the other time periods (Figures 3 and 4)

DISCUSSION

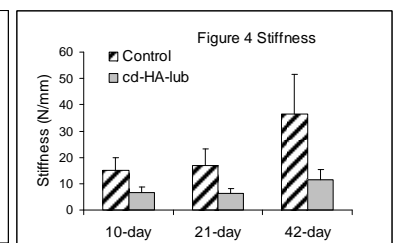
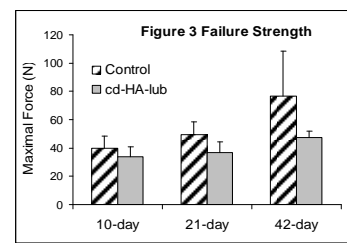
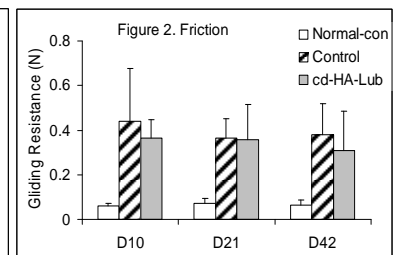
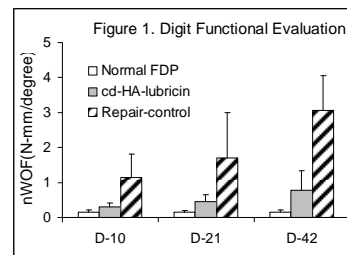
In addition to its lubricating effects, lubricin also inhibits cell adhesion (5). In the current study, we found that repaired tendons treated with lubricin had similar friction to untreated repaired tendons, suggesting little effect of cd-HA-lubricin on tendon lubrication in vivo. However, lubricin treatment improved the digit function by a decreased nWOF due to less adhesion. However, lubricin treated tendons also had more post-repair ruptures and had less repair strength and stiffness. If the adverse effects on healing can be overcome, cd-HA-lubricin could be a useful treatment to reduce adhesions and improve motion after tendon repair.

ACKNOWLEDGEMENTS

This study was supported by Mayo Foundation and NIH (AR44391).

REFERENCES

1. Zhao C, et al. J Bone Joint Surg Am. 2006; 88:2181-2191.
2. Taguchi M, et al. J Bone Joint Surg Am. 2008; 90:129-135.
3. Zhao C, et al. J Hand Ther. 2005; 18:322-329; quiz 329.
4. Uchiyama S, et al. J Bone Joint Surg Am. 1997; 79:219-224.
5. Englert C, et al. Arthritis Rheum. 2005; 52:1091-1099.



HEALING LIGAMENTS RUPTURE CONSISTENTLY FASTER DURING FATIGUE LOADING THAN CREEP LOADING OVER A RANGE OF FUNCTIONAL STRESSES

G.M. Thornton, S.J. Bailey

McCaig Institute for Bone and Joint Health, University of Calgary, Calgary, Alberta

INTRODUCTION

When a ligament is healing from an injury, the failure strength of that healing ligament is decreased from its normal, un-injured strength [1]. In this situation, normal functional loading may expose a healing ligament to damaging loads because of its compromised strength. Our purpose in this study was to investigate the response of healing ligaments to fatigue loading or creep loading at a variety of stresses that correspond to normal functional stresses (approximately 5-10% of the failure strength of a normal ligament [2]). Our hypothesis was that fatigue loading would cause rupture faster than creep loading over the range of functional stresses examined.

METHODS

In this study approved by the institutional animal care committee, 22 female New Zealand White rabbits underwent bilateral medial collateral ligament (MCL) gap surgery. After 14 weeks of healing, the two MCL scars from each rabbit were assigned one to fatigue and the other to creep. Creep and fatigue tests were performed at a range of stress levels normalized to the ultimate tensile strength (UTS) of 14-week MCL scars [3]: 30%, 45%, 60%, 80%. The test stresses corresponding to 30-60% UTS of 14-week MCL scars were equivalent to 6-11% UTS of normal MCLs and, therefore, represented functional stresses.

After standardized preparation and mounting in an MTS system, the knee joint underwent two compression-tension cycles from -5N to +2N, stopping at +1N to establish "ligament zero". After measuring MCL scar geometry, an environment chamber (37°C and 99% relative humidity) was installed and allowed to equilibrate. Then, all MCL scars underwent 30 preconditioning cycles from +1N to a force corresponding to 5% UTS of 14-week MCL scars. *Fatigue*: MCL scars were cycled until rupture, using a sine wave at 1Hz from +1N to a force corresponding to the desired stress level: 30%, 45%, 60%, 80% UTS of 14-week MCL scars. *Creep*: MCL scars were loaded from +1N to a force corresponding to the desired stress level using a half sine wave at 1Hz, and were then held at that force until rupture or for a maximum of 24.0 hours or 48.4 hours. Time-to-rupture was defined as the last time the MCL scar supported 99% of the desired test force. Fatigue and creep time-to-rupture were compared using either a paired t-test or a random effects regression model to account for incomplete pairing (significance set at $p < 0.05$).

RESULTS

When tested at stresses that corresponded to 30-60% UTS of 14-week MCL scar (6-11% UTS of normal MCL), healing ligaments had shorter time-to-rupture when exposed to fatigue loading compared to creep loading ($p < 0.01$; Table 1). At 80% UTS of 14-week MCL scar (15% UTS of normal MCL), rupture occurred shortly after the initial loading and time-to-rupture was not statistically different comparing fatigue and creep (Table 1). Two MCL scars were excluded due to technical error and ACL rupture. One of the 21 fatigue-tested MCL scars had time-to-rupture greater than 24 hours; whereas, 12 of the 21 creep-tested MCL scars had time-to-rupture greater than 24 hours.

Table 1: Time-to-rupture of 14-week MCL scars exposed to fatigue or creep loading.

Test Stress as % UTS of 14-week MCL Scar	Test Stress as % UTS of Normal MCL	Fatigue Time-to-Rupture (hours)	Creep Time-to-Rupture (hours)	P-value Fatigue vs. Creep
30%	6%	15.8 ± 8.5 (n=5) ^^	47.9 ± 1.0 (n=4) **	0.001
45%	9%	5.9 ± 6.4 (n=4)	31.0 ± 8.7 (n=4)	0.001
60%	11%	8.0 ± 6.1 (n=10) ^	20.7 ± 14.4 (n=11) *	0.010
80%	15%	0.003 ± 0.004 (n=2)	0.0002 ± 0.0001 (n=2)	nsd

Data are shown as mean ± standard deviation and "nsd" indicates not statistically different.

^^ includes 1 stopped test (1 at 21.0 hours) and ** includes 3 stopped tests (3 at 48.4 hours).

^ includes 1 stopped test (1 at 8.5 hours) and * includes 3 stopped tests (1 at 48.4 hours and 2 at 24.0 hours).

DISCUSSION

At stresses that would be considered within the functional range, healing ligaments exposed to fatigue loading ruptured faster than those exposed to creep loading. The implications of these findings are important when undertaking exercises to rehabilitate a ligament injury, suggesting that particular attention must be paid to repeated exercises that load the healing ligament even at functional levels.

ACKNOWLEDGEMENTS: NSERC, McCaig Fund

REFERENCES: [1] Frank C et al. Am J Sports Med 11:379, 1983 [2] Butler DL et al. Chapter 16 In: Functional Tissue Engineering Eds: Guilak et al. pp. 213-226, 2003 [3] Bailey SJ and Thornton GM, 54th ORS, 33:0818, 2008

AN ULTRASOUND TECHNIQUE TO EVALUATE AXIAL PROPERTIES OF LIGAMENT/TENDON

Hirohito Kobayashi and Ray Vanderby

Department of Orthopedics and Rehabilitation, University of Wisconsin-Madison

INTRODUCTION

In vivo evaluation of tissue properties in tendons/ligaments is difficult yet has the potential clinically significant. The proper evaluation of tissue parameters could, for example, distinguish normal versus pathological tissues. Published reviews of ligament/tendon biomechanics [1,2] recently concluded that a simple, real-time method to measure ligament/tendon properties is needed. Pursuant of this, we developed an ultrasound method called Acoustoelastic Strain Gauge (ASG) [3~5]. We adapted the theory of Acoustoelasticity(AE)[6] so that the changes in acoustic characteristics could be related to tissue deformation and stiffness. This phenomenon was observed in tendon [7], but never rigorously described. By assuming tissue incompressibility, we derived an Improved ASG (I-ASG) to quantify the axial properties in addition to the axial strain and transverse properties evaluated by ASG.

CONCEPT

For proof of concept, we stretched porcine tendons ex vivo. A target tissue is subjected to both stretch and ultrasound (Fig.1) and a region of interest (element) is evaluated. In a non-stretched state (0), the element has volume $Vol_0 = \pi \frac{D_0^2}{4} L_0 = \pi \frac{T_0^3}{4} v_{110} v_{330}^2$ (thickness $D_0 = T_0 v_{330}$ length $L_0 = T_0 v_{110}$). T_0 represents measurable wave travel time. The wave velocities in transverse and axial directions are represented by v_{330} and v_{110} . With tissue incompressibility, the element volume is stretched to state(1) where $Vol_1 = \pi \frac{T_1^3}{4} v_{111} v_{331}^2 = \pi \frac{T_0^3}{4} v_{110} v_{330}^2 = Vol_0$. The normalized axial stiffness is give by $\frac{v_{111}}{v_{110}} = \frac{\sqrt{C_{11}(e)+t_{11}(e)}}{\sqrt{C_{11}(e=0)}} = (1+e)^{3/2} \frac{\sqrt{C_{33}(e)}}{\sqrt{C_{33}(e=0)}}$. The applied strain and the term on right hand side are given by ASG [4].

METHOD & RESULTS

Porcine flexor tendons (N=8) are stretched (0~3% strain) scanned with ultrasound (A-mode 2.25MHz) in a PBS tank mounted on MTS test machine. The normalized stiffness-force relations are evaluated for data from both mechanical testing and echo measurements (alone) and compared (Fig.2). The average normalized axial stiffnesses evaluated from both mechanical testing and I-ASG are very close.

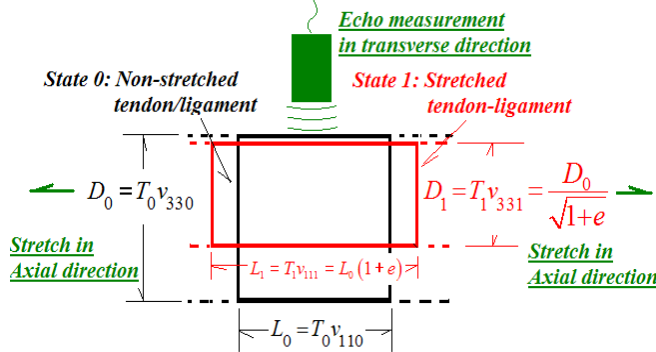


Fig.1 Tissue incompressibility & I-ASG.

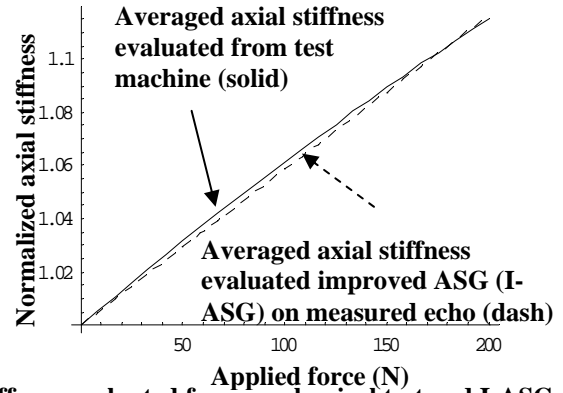


Fig.2 Axial stiffness evaluated from mechanical test and I-ASG.

REFERENCE

- [1] Fleming, B.C., Beynon, B.D., 2004. Ann. Biomed. Eng. **32**, pp.318-328.
- [2] Raverey B., et al., 2004, Clin. Biomech., **19**, pp.433-447
- [3] Kobayashi, H., Vanderby, R., 2007, J. Acoust. Soc. Am. **121** pp.879-887
- [4] Kobayashi, H., et al. APPLICATION OF ACOUSTOELASTICITY TO NONINVASIVE TISSUE STRAIN MEASUREMENT", 53rd ORS meeting (2007)
- [5] Kobayashi, H. Vanderby, R., Submitted to J. Biomech.
- [6] Pao Y. H., et al., 1984, *Physical Acoustics*, Academic Press, Orlando, Vol. XVII, Chap.2
- [7] Pourcelot, P., et al., 2005. J. Biomech. **38**, pp.2124-2129.

A SHORT LOADING EPISODE PER DAY IMPROVES TENDON HEALING

¹P. Eliasson; ¹T. Andersson; ¹P. Aspenberg
⁺¹University of Linköping, Linköping, Sweden

INTRODUCTION

Short periods of loading are sufficient to maintain strength¹ and stimulate repair in bone². The loading episode is “remembered” by the tissue, so that a single episode per day is sufficient. Loading is also important for tendon healing.³ Does tendon tissue also remember short loading episodes, or is there a need for iterated loading several times a day? We used tail suspension in rats to allow short and controlled periods of loading of the Achilles tendon. The suspended rats were allowed running periods of 15, 30 or 60 min once, or 15 min twice, daily.

MATERIALS AND METHODS

Female Sprague-Dawley rats ~200 g were habituated to a treadmill apparatus for 5 days (12 m/min, 7-30 min/day). Thereafter, the Achilles tendon was transected and left to heal.³ Two days after surgery, 40 rats were subjected to hindlimb unloading by tail suspension and divided into 5 groups: unloading without exercise, 15, 30 and 60 min exercise once/day and 15 min exercise twice/day. The exercise groups were let down from suspension and ran on the treadmill for the designated time. There were also 15 rats with free cage activity. After two weeks the animals were killed and tendon regenerates were tested mechanically. All evaluation was blinded. Results were analysed with a one-way Anova with Tukey’s post hoc test. The experiment was approved by the regional animals ethics committee.

RESULTS

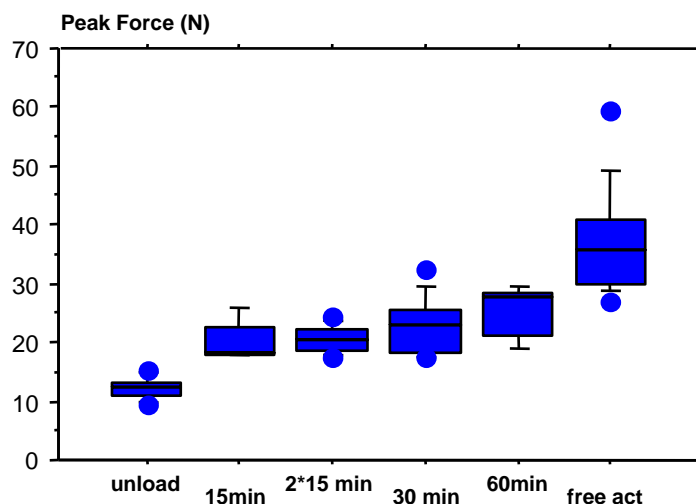
One rat in the unloaded group and one in the free activity group were excluded due to post-operative complications. One rat in the free activity group was excluded due to technical problems.

Peak force was doubled by exercise for 15 min or more compared to the unloaded group ($p=0.001$; Figure 1). There was a tendency to higher peak force with increased exercise time (not significant). The free activity group was in turn almost 50% stronger than the exercise groups ($p\leq 0.002$ for all). The same pattern was found for stiffness.

The cross sectional area was larger in the free activity and 60 min groups compared to the unloaded group ($p<0.003$). There was no significant difference between any of the exercise groups.

The increased cross sectional area with exercise explains the effects on peak force and stiffness: There was basically no difference in peak stress and elastic modulus in any of the groups.

The exercise groups had a shorter distance between the stumps, compared to the free activity group ($p<0.001$ for all except 30 min, where $p=0.049$). The 60 min group also had a shorter distance than the unloaded group ($p<0.001$).



DISCUSSION

Loading had a dramatic effect on cross sectional area, i.e. the quantity of tissue, but not on quality. More than half of the stimulation achieved by free cage activity could be gained from a short period of running. However, dividing 30 minutes of stimulation in two separate periods (8 hours apart) had no additional effect, indicating no benefit from refreshing tissue memory. Thus, the tissue “remembered” the stimulation from one loading period for most of the day.

With daily running periods, the repair tissue could contract as much as the unloaded tendons, or even more, but still gain strength. This would imply that in the clinic, patients might be allowed short training periods without risk of permanent elongation.

Even though all exercise groups increased the strength dramatically, free cage activity still was more effective. The reason could be the total amount of time with activity per day, considering that we see a tendency to a time dependent effect. Another explanation could be that rats with free cage activity can adjust and gradually increase their loading in an optimal way, thereby giving the new tissue an appropriate stimulus. This stimulus might comprise high loading peaks.

1. Rubin et al. *J Bone Joint Surg Am.* 1984
2. O’Sullivan et al. *Clin Orthop Relat Res.* 1994
3. Virchenko et al. *Acta Orthop.* 2006

THE INFLUENCE OF GENETIC ABLATION OF MACROPHAGE MIGRATION INHIBITORY FACTOR ON HEALING OF THE ACHILLES' TENDON: A BIOMECHANICAL STUDY

¹Kondo E, ²Ishikawa T, ²Fujiki H, ²Daimaruya M, ¹Onodera S, ¹Yasuda K

¹Department of Sports Medicine, Hokkaido University School of Medicine, Sapporo, Japan

²Department of Mechanical Systems Engineering, Muroran Institute of Technology, Muroran, Japan

INTRODUCTION

Macrophage migration inhibitory factor (MIF), which was discovered in 1966 as the first lymphokine, has been recognized as a pivotal mediator of inflammation in various pathological conditions. Recent studies have shown that MIF plays an important role in proliferation and differentiation of cells, generation of organs, and wound healing¹⁻³. However, a role of MIF on the tendon healing process has not been elucidated as of yet. A specific hypothesis to be tested in this study using MIF gene-deficient (MIF KO) mice is that the genetic ablation of MIF may inhibit natural improvement of the structural properties of the Achilles' tendon.

METHODS

Thirty Balb/C wild-type (WT) mice and 30 Balb/C background-MIF KO mice (10 weeks) were used. In each group, 20 of the 30 mice were used for evaluation of the injured Achilles' tendon, and the remaining 10 were used for evaluation of the normal (uninjured) Achilles' tendon. For evaluation of the injured Achilles' tendon, in each animal, the right Achilles' tendon was completely transected with a scalpel using a dissecting microscope. Each animal was sacrificed on 3, and 6 weeks after surgery. Tensile tests were performed using a conventional tensile tester with specially designed grips. The structural properties of the Achilles' tendon-calcaneus complex were determined in tensile testing at a cross-head speed of 0.5 mm/min. Statistical analyses were performed between the MIF KO and WT mice using the Student's t-test. The significance level was set at $p=0.05$.

RESULTS

Concerning the uninjured Achilles' tendon, there were no significant differences in the structural properties between the WT and MIF KO mice. Regarding the injured Achilles' tendon, at 3 weeks after surgery, there were no significant differences in the maximum load and the stiffness between the WT and MIF KO mice. At 6 weeks after surgery, the maximum load, and the stiffness were significantly lower ($p<0.0001$, and $p<0.0001$, respectively) in MIF KO mice than in the WT mice.

DISCUSSION

This study clearly demonstrated that the genetic ablation of MIF inhibited natural improvement of the structural properties of the injured Achilles' tendon. This result suggested a possibility that MIF may enhance healing of the injured Achilles' tendon.

REFERENCES

[1] Shimizu T et al. FEBS Lett 381:199-202, 1996. [2] Wistow GJ et al. Proc Natl Acad Sci USA 90:1272-5,1993. [3] Onodera S et al. Immunology 89:430-5, 1996.

MULTIAXIAL NANOSCALE DEFORMATION MECHANISMS IN TENDON COLLAGEN

H. R. C. Screen¹, J. Seto², S. Krauss², P. Boesecke³, and H. S. Gupta¹

1. School of Engineering & Materials Science, Queen Mary University of London, UK. 2. Max Planck Institute of Colloids & Interfaces, Germany. 3. Beamline ID2, European Synchrotron Radiation Facility, France

INTRODUCTION:

Tendon is a hierarchically structured biological composite, in which nanoscale collagen fibrils, surrounded by proteoglycans, assemble into micron scale fibres and macroscopic fascicles. Structurally, tendons are known to be highly anisotropic, and a few studies have demonstrated an equivalent gross mechanical anisotropy [3]. However, very little is known regarding the mechanics of the fibril and fibre levels or how the micro- and nano-scale structure gives rise to these very significant anisotropic properties. By combining tensile loading with *in situ* techniques, it is possible to investigate nano- and micro-scale deformation mechanisms in tissues. Synchrotron small angle X-ray diffraction (SAXD) characterises the fibrillar length scale, providing quantitative information on nanostructural organisation [1], whilst confocal microscopy enables visualisation of the fibre level, using fluorescent dyes to visualise the matrix [2]. Applying novel analysis techniques to X-ray and confocal data collected during stress-relaxation, we were able to investigate concurrently transverse and longitudinal ultra-structural reorganisation.

METHODS:

Fascicles were dissected from the tails of 5 month old male Wistar rats. These were strained to 1, 2, 4, 6 or 8% strain and held at constant displacement whilst recording force, and monitoring mechanics using either synchrotron SAXS detection [1] or confocal microscopy [2]. Shifts in the meridional SAXD reflections of axial collagen stacking gave axial fibril strain, and changes in ultra-low angle intensity in the perpendicular direction measured deformation perpendicular to the fibril axis. For confocal analysis, cell nuclei were stained with Acridine Orange to act as markers of the local matrix strains, within and between fibres (axial), or across the fascicle width (transverse).

RESULTS:

The axial response highlighted a continuous decrease in strain at the nanoscale (fibrils), in direct contrast with the microscale response, where strain within the fibres was negligible (Fig 1a), and fibre sliding played a significant role. Transversely, fibrils showed a consistent increase in diameter during relaxation, which obeyed the same two-stage behaviour as axial strain (Fig 1b). Notably, the increase was greater than would be expected from volume conservation alone. Fibre level structural changes showed a different behaviour, where confocal microscale analysis demonstrated a continual decrease in the distance between fibres during relaxation (Fig 1b).

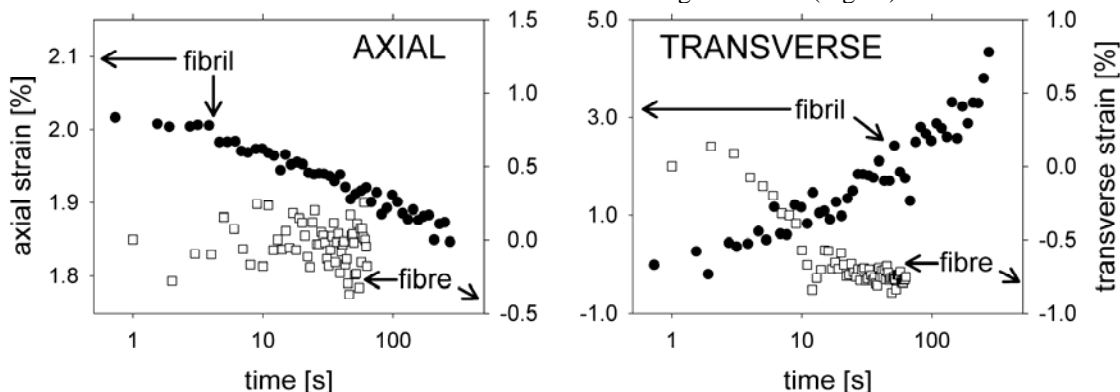


Figure 1. Ultrastructural changes in the a) axial and b) transverse directions during stress relaxation in tendon.

DISCUSSION:

Our results provide a novel picture of the structural mechanisms underlying stress relaxation at the nano- and micro-scale in soft collagenous tissues. At the fibrillar level, we have previously modelled the two-stage axial relaxation behaviour as a series combination of viscoelastic elements [4]. The transverse changes in fibril and fibre level diameters observed in the current work may be explained by the flow of solvent ions between different compartments within the hierarchical structure. Specifically, the fact that fibril diameter increases significantly while fascicles tend to shrink strongly suggests a dynamic interchange of solvent and solute molecules during stress relaxation, from inter-fibre to intra-fibrillar space. The novel data collated using these techniques will enable us to develop a multiscale understanding of the origins of viscoelasticity in this tissue.

REFERENCES:

[1] Gupta HS et al., (2006) *PNAS* 103:17741-6. [2] Screen HRC et al., (2003) *Biorheol.* 40:361-8. [3] Lynch H et al., (2002) *Trans ORS* 27: 243. [4] Screen HRC et al., (2008) *ISLT-8*.

Cyclic Loading of the Patellar Tendon Graft and Graft Properties: Implications for Initial Graft Tension

+¹Hashemi J; ²Chandrashekar N; ³Slauterbeck JR; Beynnon BD

+¹Texas Tech University, Lubbock, TX; ²University of Waterloo, Ontario, CA; ³University of Vermont, Burlington, VT

INTRODUCTION

It has been reported that the low load, toe-region, properties of the patellar tendon are the key properties controlling the biomechanical behavior of the graft¹ after ACL reconstruction. In other words, for activities of daily living (ADL), the graft is almost never strained beyond its toe-region. In addition, the same report suggests that the initial tension applied to the graft must be graft-specific (depending on the stiffness of the graft in the toe-region) and there is no universal tension that would place all grafts in an optimal condition for remodeling. One limitation of this report¹ was that the grafts tested, in tension, had not been cyclically loaded to high levels a-priori. One could argue that moderate cyclic loading of the graft (simulating physical rehabilitation activities immediately after reconstruction) prior to single-cycle loading to failure could significantly affect the properties of the graft including the toe-region properties. This is an especially important consideration in lieu of a recent report that the initial tension in the graft drops by as high as 46% after 1500 cycles of loading² (flexion and extension of the reconstructed knee). The results explain the observed early slackening of the anterior cruciate ligament (ACL) reconstructions. Our objective here is to determine whether the reported drop in initial tension is due to changes in graft properties (for instance tissue relaxation due to cyclic loading). Accordingly, we hypothesize that graft properties (both toe-region properties as well as linear properties) will be impacted by moderate cyclic loading of the graft prior to single-cycle load to failure.

METHODS

Twenty BPTB specimens (average width 4.5mm) were harvested from twenty unpaired healthy knees (10 male and 10 female, average age 38 years, range 17-50 years). The contralateral grafts had been tested in single-cycle to failure tension tests in a previous report¹. In this research, the grafts from the remaining knees in each pair were first loaded cyclically between 20 N (initial graft tension) and 30% of the failure load of the contralateral graft. Thus, each graft was cycled according to the properties of its pair to about 30% of its maximum load. After 5000 cycles, the grafts were loaded to failure at a strain rate of 100%/s. The pre-failure portion of the stress-strain curve was fit to the following bilinear constitutive model using a least squares method

$$\begin{aligned}\sigma &= E_0 \varepsilon \quad \text{where } \varepsilon \leq \varepsilon^* \\ \sigma &= E (\varepsilon - \varepsilon^*) + E_0 \varepsilon^* \quad \text{where } \varepsilon > \varepsilon^*\end{aligned}$$

σ is the engineering stress, ε is the engineering strain, ε^* is the strain at the transition point from the toe-region to the linear region, E_0 is the modulus of elasticity of the toe-region and E is the modulus of elasticity of the linear region. All the linear properties including strain at failure (ε_f), linear modulus of Elasticity (E), failure strength (σ_f), and strain energy density at failure (u) were determined for each BPTB graft. Paired t-tests were performed to determine if the cycled grafts had different toe-region and linear properties than the un-cycled grafts. The alpha value of statistical significance was set to 0.05.

RESULTS

The average and standard deviation of the toe-region and linear properties of the un-cycled/tested-to-failure and cycled/tested-to-failure grafts were compared. The results show that except for strain at failure, the remaining toe-region and linear properties are not significantly different between the two populations.

DISCUSSION

Our results suggest that cyclic loading of the grafts up to 30% of their failure load will not change the properties of the graft. We therefore do not expect that the reported drop in initial tension is because of change in properties of the graft (during the first few days after reconstruction). In their report², the authors assert that there were no graft slippage and bone block positions remained flush. This means that the drop in the initial tension is not due to any of those factors either. We suggest that what causes the initial slackening is the improper initial tension applied to the graft both from a magnitude point of view and method of applying tension. It has been suggested that loading all grafts to a similar initial tension is not appropriate due to differences in properties between grafts¹. We believe that the 40 N initial tension² may be excessive for some grafts with very high toe-region stiffness and too low for other grafts with very low toe-region stiffness. Applying large pre-tensions on very stiff grafts could cause undue stiffness of the knee joint during weight bearing when additional forces due to extension of the knee and exertion of body weight are imposed on the graft. We suggest that graft initial tension should be carefully determined based on the toe-region properties of the graft. Current practices of applying initial tension do not account for changes to initial graft tension due to load bearing. New pre-tensioning procedures should be considered to minimize changes to graft initial tension early during the rehabilitation period.

REFERENCES

1. Chandrashekar et al. *Clinical Biomechanics*. 2008 Aug;23(7):918-25.
2. Arnold et al. *AJSM*. 2004 Feb;33(8):536-42.

The influence of growth changes for Elastic properties of tendon structures.

Yosuke Egawa, Suguru Torii, Chiaki Nakamura, Toru Fukubayashi
Faculty of Sport Sciences, Waseda University, Saitama, Japan

[INTRODUCTION]

Tendons are important for optimal muscle force transfer to bone and play key role in functional ability. The immature tendon structures in children would be less able to cope with repetitive biomechanical stress. Changes in tendon properties with aging could contribute to declines in physical function commonly associated with age. However, the growth changes in elastic properties of tendon structures have not yet been fully understood in humans. The present study aimed to investigate the elastic properties of tendon structures between adult, before the age at peak height velocity (PHV) and after PHV.

[METHODS]

The subjects were 8 elder boys (before-PHV: bone age 13 years or elder), 18 younger boys (after-PHV: bone age 13 years or younger), and 13 young adult men with normal physical appearance, and no history or locomotor complaints who regularly played soccer (Table 1). Bone age was measured by automated system for evaluation of bone age from the computerized scanning of the light hand-wrist X-ray (CASMAS). Elongation of the tendon and aponeurosis of the medial gastrocnemius muscle (MG) during isometric plantar flexion, respectively, were determined using a real-time ultrasonic apparatus (ALOKA-SSD1000 JAPAN) in vivo while torque gradually increased from zero to maximal effort (MVC) within 5 s. The relationship between the estimated muscle force and tendon elongation (L) was fitted to a linear regression, the slope of which was defined as the stiffness of the tendon structures. Kawakami et al. have confirmed the precision and linearity of the image¹.

[RESULTS]

The tibial length were the shortest in YG, and tendon thickness were greatest in YG among the three group. There were no significant difference in tendon length among three groups. However, tendon length / tibial length ratio were similar in both AG and EG, it was significantly greater in YG than in the other two groups. The MVC force was the greatest in AG than in the other two groups. However, there were no significant differences in dL at the MVC force (dLmax) among three groups. Fig1 shows the relationship between Fm and dL. Significant PHV-related differences were found in stiffness. There were no significant differences between EG and AG.

	Adult (n=13)	Elder boys(n=8)	Younger boys (n=18)	
age (y)	21.2 ± 1.1	14.3 ± 0.4	13.8 ± 0.6	a,b
height (cm)	171.9 ± 5.3	170.2 ± 4.0	153.9 ± 7.4	a
weight (kg)	65.1 ± 5.9	58.4 ± 7.4	45.6 ± 10.7	a,b
tibial length (cm)	40.5 ± 2.2	39.2 ± 1.8	36.4 ± 2.7	a
tendon length (mm)	18.0 ± 2.1	18.6 ± 1.7	18.9 ± 1.7	N.S.
tendon length/tibial length	0.45 ± 0.04	0.48 ± 0.05	0.52 ± 0.05	a
tendon thickness (mm)	4.71 ± 0.27	4.97 ± 0.44	5.27 ± 0.55	c
MVC (N)	769.8 ± 130.7	673.0 ± 107.5	543.2 ± 120.1	a
dLmax at MVC (mm)	23.0 ± 5.3	21.3 ± 2.2	21.9 ± 4.4	N.S.
stiffness (N/mm)	42.5 ± 10.4	42.2 ± 9.5	34.4 ± 8.3	a

a: significant difference between YG and other two groups
b: significant difference between EG and AG
c: significant difference between YG and AG

Table 1 Physical characteristics and elastic properties of tendon structures for YG, EG and AG (means ± SD)

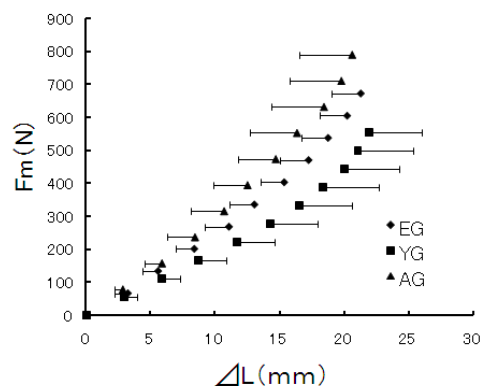


Fig.1 The relationships between Fm and dL for YG, EG and AG.

[DISCUSSION AND CONCLUSION]

The present study showed that the elastic properties of tendon structures are more compliant in before-PHV boys than in after-PHV boys and adults. The observed properties of tendon structures in the pre-PHV boys may play role in protection from athletic injuries.

[REFERENCES]

1. Kawakami, Y., Y. Ichinose, and T. Fukunaga. Architectural and functional features of human triceps surae muscles during contraction. *J Appl Physiol.* 85:398-404, 1998.

A GEOMETRICAL MODEL OF CARPAL TUNNEL EXPANSION WITH LIGAMENT STRETCHING AND ARCH NARROWING

Zong-Ming Li

Hand Research Laboratory, Department of Orthopaedic Surgery, University of Pittsburgh, USA

The carpal tunnel is formed by the interconnected carpal bones at its medial, lateral and dorsal borders, and the transverse carpal ligament (TCL). The TCL inserts radially into the tuberosity of the scaphoid and the ridge of the trapezium and ulnarly into the pisiform and the hook of the hamate. The carpal tunnel is a confined space containing the median nerve and nine flexor tendons, and therefore, the geometry of the tunnel structure is relevant to the compression median neuropathy, i.e. carpal tunnel syndrome. The purpose of this paper is to illustrate the dependence of cross sectional area of the carpal tunnel on arch width and TCL length.

THE GEOMETRIC MODEL

Our experimental data using cadaveric specimens indicated that the TCL was flat without a force applied to it, which means that the arch width (a_0) is equal to the TCL length (l_0) (Figure 1). A carpal arch was formed when a force was applied to the TCL. Theoretically, arch formation can be achieved by elongating the TCL and/or by moving the TCL edges towards each other (i.e. narrowing the arch). The arch height and the arch area are functions of TCL elongation (Δl) or arch width narrowing (Δa).

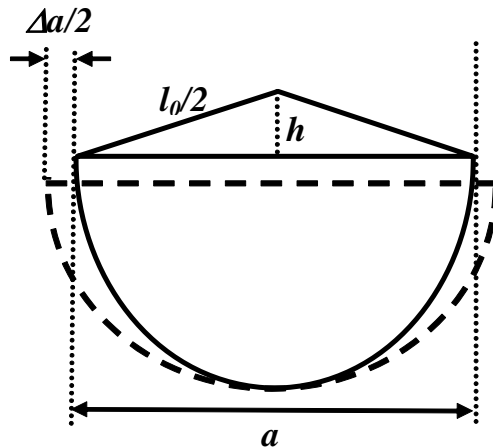


Figure 1. Geometric representation of the cross-section of the carpal tunnel. The enclosed area by the dashed curve and line represents the initial carpal tunnel.

RESULTS

The modeling results show that the arch height and the arch area are sensitive to TCL lengthening or arch width narrowing (Figure 2); with a small change in either produce a relatively large increase in arch height (h) and arch area. For example, a TCL elongation of 0.2 mm ($\Delta l = 0.2$ mm) causes a 1.5 mm arch height and

16.4 mm² arch area. Similarly, a decrease of 0.2 mm in the arch width ($\Delta a = 0.2$ mm) causes 1.5 mm arch height and 16.1 mm² arch area. However, the cross-sectional area composed by the carpal bones is insensitive to the change of a , fluctuating only slightly (within 1.3 mm²) when the tunnel width (a) is decreased by 0-2.5 mm. Therefore, the increase in total area is mainly attributable to the formation of the carpal arch.

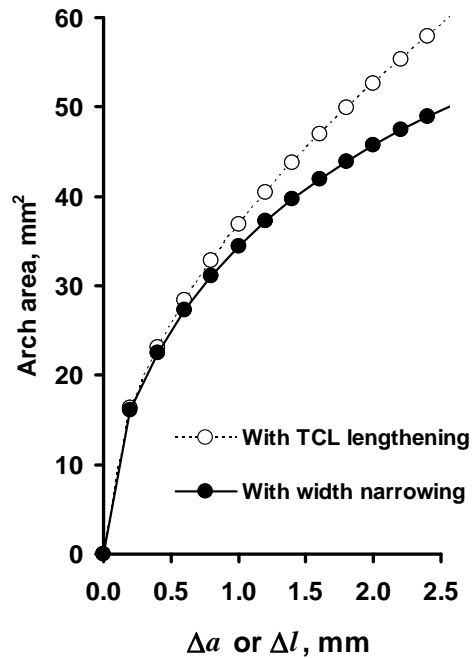


Figure 2. Arch area (iii) due to TCL lengthening (Δl) or arch width narrowing (Δa).

DISCUSSION

The geometrical model captures the relationships among the arch width, TCL length, arch height, and arch area, illustrating that TCL elongation and carpal width narrowing are effective for carpal arch formation and carpal tunnel expansion. The arch area from the modeled geometry matched well with our experimental data. For example, the experimental results showed that when the arch width decreased by 2.0 mm, the arch area was 46.8 mm². The geometrical model predicts an arch area of 45.8 mm².

ACKNOWLEDGEMENTS

NIH R03AR054510

**Mechanobiological Understimulation of Tendon Cells
as the Etiopathogenesis of Tendinopathy:
A proposed scientific rationale for the clinical paradigm**

Steven P. Arnoczky, DVM and Michael Lavagnino, PhD
Laboratory for Comparative Orthopaedic Research
College of Veterinary Medicine, Michigan State University

While there is a significant amount of information available on the clinical presentation(s) and pathological changes associated with tendinopathy, the precise etiopathogenesis of this condition remains a topic of debate. Classically, the etiology of tendinopathy has been linked to the performance of repetitive activities (so-called overuse injuries). This has led many investigators to suggest that it is the mechanobiologic *over-stimulation* of tendon cells that is the initial stimulus for the degradative processes which have been shown to accompany tendinopathy. Although several studies have been able to demonstrate that the *in vitro* over-stimulation of tendon cells in monolayer can result in a moderate increase in the expression of some catabolic genes, the strain magnitudes and durations used in these *in vitro* studies, as well as the model systems, may not be clinically relevant. While different *in vivo* models of “over-use” injuries have been attempted, to date, no animal model has been shown to reproduce the full compliment of pathological changes associated with clinical cases of tendinopathy.

Using a rat tail tendon model, our lab has studied the *in vitro* mechanobiologic response of tendon cells *in situ* to various tensile loading regimes. From these studies we have forwarded the hypothesis that the etiopathogenic stimulus for the degenerative cascade which precedes the overt pathologic development of tendinopathy is the catabolic response of tendon cells to mechanobiologic *under-stimulation* as a result of microscopic damage to the collagen fibers of the tendon. Indeed, many of the catabolic changes seen in clinical cases of tendinopathy have been associated with the under-stimulation of tendon cells. However, to date, there is insufficient evidence to provide a direct link between the mechanical loading conditions of the tendon experienced during repetitive loading and the pathological response (e.g., not everyone involved in repetitive jumping sports will suffer from patellar tendinopathy).

Recently, we have expanded our studies to examine the measured and theoretical loads and strains experienced by the human patellar tendon during jumping activities. The results of these studies suggest that under certain conditions (joint position, tendon strain, etc) experienced during a jump-landing, the area of the patellar tendon commonly associated with patellar tendinopathy can be exposed to localized tissue strains sufficient enough to induce fibril damage. This, in turn, could lead to the mechanobiological understimulation of the tendon cells associated with these damaged fibrils and the initiation of a catabolic cascade. In addition, pilot studies have documented that decelerations reaching 10-15 g's can occasionally occur in jump landings (in the vertical and/or horizontal planes) during routine volleyball maneuvers. When the resulting patellar tendon forces are applied rapidly and at a specific joint position, such loads could be sufficient to induce the aforementioned microdamage in the “at risk” area of the tendon.

Therefore, it is our theory that during repetitive activities one (or more) abnormal (overloading) cycles may occur during which individual collagen fibers can be damaged while the overall biomechanical status of the tendon is not clinically compromised. The outcome of this overloading cycle produces isolated tendon fibril(s) failure and a subsequent altered cell-matrix interaction leading to the mechanobiological understimulation of tendon cells in the damaged area. This, in turn, leads to the initiation of a catabolic cascade that decreases the safety margin of the tendon making it more susceptible to additional damage at lower strains. We theorize that the association of increased frequency of training with the onset of tendinopathy could be related to the “probability” of experiencing an overload event as well as the impact of repetitive loading on the compromised tissue. Additional studies are being planned to further test this hypothesis.

A MOLECULAR ANALYSIS OF POSTERIOR TIBIALIS TENDINOPATHY

A.N. Corps¹, A.H.N. Robinson², R.L. Harrall¹, N.C. Avery³, V.A. Curry¹, B.L. Hazleman¹ and G.P. Riley⁴

¹ Rheumatology Research Unit, Addenbrooke's Hospital, Cambridge, UK

² Department of Trauma and Orthopaedics, Addenbrooke's Hospital, Cambridge, UK

³ Matrix Biology Research Group, University of Bristol, UK

⁴ School of Biological Sciences, University of East Anglia, Norwich, UK.

INTRODUCTION

Pain and dysfunction of the human posterior tibialis tendon (PTT) is associated with adult acquired flat foot problems, particularly in women of middle age. As such, it contributes a significant proportion of tendon problems seen in the clinic. Little is known about the aetiopathogenesis of this condition, which may be treated surgically by tendon transfer using the flexor digitorum longus tendon (FDLT) to restore functional support of the foot arch. Studies of Achilles and supraspinatus tendinopathy have indicated the importance of increased matrix turnover in tendon disease, mediated by changes in the expression of matrix genes and the altered activity of several matrix-degrading metalloproteinases. In this study, we collected PTT and FDLT taken at surgery, and investigated biochemical and molecular markers of matrix turnover, including the expression of mRNA encoding a range of tendon matrix proteins and metalloproteinases. We aimed to determine how the expression patterns in the dysfunctional PTT and the replacement FDLT compared with those in samples of normal PTT, and whether differences in the gene expression patterns were similar to those reported in normal and painful Achilles tendons.

METHODS

Tendon specimens were obtained from tissue discarded during surgery for the repair of PTT using FDLT transfer. The principal specimen group consisted of paired samples of PTT and FDLT tissue from 25 female patients, age 30-77 years, median 60 years. 6 samples of morphologically normal PTT were obtained from female patients with no history of tendon problems, age 29-87 years, median 53.5 years. Tissue glycosaminoglycan (GAG) and collagen content were analysed by standard biochemical analysis. Pentosidine and collagen cross-links were measured by HPLC. Total RNA was isolated from frozen tissue using Tri-Reagent (Sigma) and real-time semi-quantitative RT-PCR reactions were performed using standard techniques. mRNA levels were normalized to 18S RNA. Differences between the tendon groups were described as n-fold differences between the medians, and the statistical significance was assessed using the Mann-Whitney test or the Wilcoxon signed rank test as appropriate.

RESULTS

Diseased PTT contained more than 2-fold higher levels of GAG than normal PTT ($P < 0.05$) and 6-fold higher levels than the FDLT ($P < 0.001$). The total collagen content (% of dry weight) in the three different groups was not significantly different. In normal PTT there was a linear increase of pentosidine content with increasing age and similar levels were found in the paired FDLT. In contrast, diseased PTT contained levels of pentosidine, significantly lower than that predicted by patient age ($P < 0.05$). Diseased PTT showed significantly increased mRNA expression of a number of genes (COL1A1, COL3A1, aggrecan, biglycan, MMP-2, -13 and -23 and ADAM-12) compared with normal PTT or FDLT. ADAMTS-1 mRNA was lower in diseased PTT than in the FDL tendons, while MMP-3 and ADAMTS-5 were lower in both diseased PTT and FDLT than in the normal PT.

DISCUSSION

The molecular changes described here are comparable with previous studies in other tendons, consistent with the hypothesis that there is a similar molecular pathogenesis of tendinopathy at different anatomical sites. The higher GAG content in diseased PTT is similar to that described in chronic tendinopathy of the Achilles and supraspinatus tendon, and increased expression of aggrecan and biglycan mRNA is characteristic of Achilles tendinopathy. The altered proteoglycan content is consistent with cellular changes induced by increased compression and/or shear forces acting at the site of tendon pathology. The increase in pentosidine content of collagen with age in normal PTT and FDLT is similar to that reported in biceps brachii tendons, indicating that each of these tendons normally possess a remarkably stable matrix structure in which Age-related Glycation End-products (AGE) such as pentosidine can accumulate linearly. This relationship is lost in the diseased PTT, where the disease process has led to replacement of the original collagen matrix, as indicated both by the lower pentosidine levels and by the increased levels of mRNA encoding Type I and III collagens. A loss of pentosidine accumulation was noted previously in supraspinatus tendinopathy, and the increase in matrix turnover was confirmed by an analysis of the racemisation of aspartate. The cause of the increased matrix turnover found in tendinopathy is the subject of continuing controversy; the cellular response to an altered mechanical environment is generally agreed to be one of the most important factors, although whether it is a response to too much or too little strain is yet to be determined.

GLUTAMATE RECEPTORS IN TENDINOPATHY

N Schizas¹, Ø Lian², F Frihagen², L Engebretsen², R Bahr², PW Ackermann¹⁺

¹Orthopedic Laboratory, Department of Molecular Medicine and Surgery, Karolinska Institutet, Stockholm, Sweden,
²Oslo Sports Trauma Research Center, Department of Sports Medicine, School of Sport Sciences, Oslo, Norway.

+Paul.Ackermann@ki.se

INTRODUCTION

Tendinopathy entails pain and degenerative tissue proliferation such as tenocyte transformation and increased numbers of sensory nerves and microvessels. Pain and tissue proliferation are suggested to be modulated via nerve transmitters, including substance P (SP) and glutamate, both detected in tendinopathy. Substance P and glutamate are known to activate glutamate receptors in a variety of pain conditions and additionally to be implicated in cell transformation. However, the presence of different glutamate receptors, eg. ionotropic (NMDA) and metabotropic (mGlu), and whether they are up- or downregulated in tendinopathy is still unknown. In this study we assessed the 1) presence, 2) the tissue density and 3) the co-existence of different glutamate receptors together with glutamate in tendinopathic biopsies and controls.

METHODS

All procedures were conducted with local ethical committee approval and patient consent. Human patellar tendon biopsies of tendinopathic patients (n=10) and controls (n=8) were single- and double-stained immunohistochemically for glutamate, glutamate receptors NMDAR1, mGluR1, mGluR5 and mGluR6,7, the nerve marker PGP9.5 and SP and assessed subjectively and semi-quantitatively with image analysis. Images were taken using an epifluorescence microscope with camera and were subjectively assessed by two independent observers blinded with regard to the identity of the slides. Tenocyte density and morphologic characteristics were assessed. Non-parametric Mann-Whitney *U*-tests for independent samples were used, and the level for significance was set at $p < 0.05$.

RESULTS

Of the glutamate receptors tested all except mGluR1 was identified in the tendons, however only NMDAR1 was found significantly altered between both groups. The chronic painful tendons exhibited a significant elevation of NMDAR1 (9-fold) and also of glutamate (10-fold) (Fig.1). This up-regulation of NMDAR1 and glutamate was found to be co-localized on sensory nerve fibers, blood vessels as well as on transformed tenocytes (Fig.2-3). None of the controls exhibited neuronal co-existence of glutamate with NMDAR1.

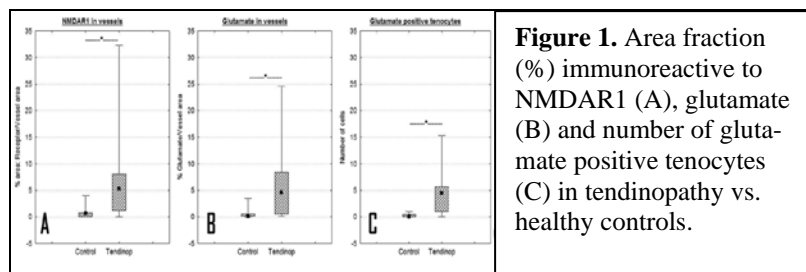


Figure 1. Area fraction (%) immunoreactive to NMDAR1 (A), glutamate (B) and number of glutamate positive tenocytes (C) in tendinopathy vs. healthy controls.

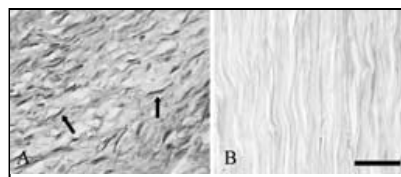


Figure 3. Tendinopathy (A) and control (B) stained for glutamate (arrows). Glutamate positive tenocytes exhibit signs of transformation.

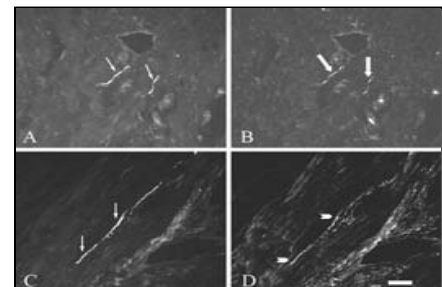


Figure 2. Double staining micrographs of tendinopathy, after incubation with antisera for PGP9.5 (A,C), NMDAR1 (B), glutamate (D)

CONCLUSIONS

This study establishes for the first time that patients with tendinopathy exhibit an elevation of peripheral glutamate receptor NMDAR1, morphologically co-localized with increased glutamate expression. The up-regulated NMDAR1/glutamate system may represent hyper-excitability of the cells – leading to cell proliferative effects observed as angiogenesis, tenocyte transformation, and nerve sprouting. Moreover, the neuronal co-existence of glutamate and NMDAR1 observed in painful tendinosis, but not seen in any of the controls, strongly suggests a role in pain signalling. Future studies will focus on interventional approaches to investigate if modulation of NMDAR1 pathways can ameliorate the symptoms of tendinopathic patients.

Polarization sensitive optical coherence tomography evaluation of intratendinous changes in ruptured and tendinopathic Achilles tendons

Pierre O. Bagnaninchi^{a,b}, Ying Yang^a, Gayle D. Maffulli^a, Alicia El Haj^a, Nicola Maffulli^a

^{a)} Institute for Science and Technology in Medicine, Keele University, Stoke-on-Trent, UK

^{b)} MRC Centre for Regenerative Medicine, University of Edinburgh, Edinburgh, UK

INTRODUCTION

The objectives of this study were to define the diagnostic value of polarization sensitive optical coherent tomography (PSOCT) for the assessment of degenerative changes occurring before Achilles tendon rupture [1], and for the assessment of tendinopathy during exploration. In this study, we compared control tendon samples to ruptured and tendinopathic Achilles tendon samples *ex vivo*.

METHODS

ex vivo PSOCT examinations were performed in 24 tendons (14 ruptured Achilles tendons, 4 tendinopathic Achilles tendon, and 6 controls). Samples were imaged in both intensity and phase retardation modes by PSOCT within 24 hours after surgery, and birefringence was quantified. Samples were fixed and processed for histology immediately after imaging. Slides were assessed twice in a blinded manner to provide a semiquantitative histological score of degeneration. We used a custom-built PSOCT system fitted with a superluminescent diode with a central wavelength of 1310 nm and bandwidth of 52 nm [2]. Each PSOCT scan produced two cross-section images of the specimen, 4 mm long and 1 mm deep in the tissue. An intensity image procures information on the microstructure of the sample, while the phase retardation mode displays information regarding the birefringence of the sample and the associated collagen fibre alignment.

RESULTS

In depth PSOCT microstructural imaging was demonstrated. Collagen disorganization and high cellularity were observable by PSOCT as the main markers associated with pathological features. Quantitative assessment of birefringence and penetration depth found significant differences between non-ruptured and ruptured tendons. No such differences were found for tendinopathic tendons, but abnormalities were observed in the microstructure of 2 out of 4 tendinopathic samples by 3D sample reconstruction. Both Kruskal-Wallis tests on the median values of histological scores and birefringence agree on the group classification, and the methods can significantly measure degenerative changes associated with Achilles tendon rupture.

DISCUSSION

A clear difference was found with PSOCT imaging between tendons with aligned collagen fibres versus tendons from patients with rupture. Both collagen disorganization and high cellularity were observed by PSOCT in respectively phase retardation imaging and intensity imaging. The resolution (15 μ m) of PSOCT does not allow cellular resolution, but an increase of the cell count will limit the light penetration depth into the tissue by raising the scattering coefficient. Quantitative analysis based on birefringence calculation and histological scores failed to distinguish between non-ruptured and tendinopathic tendons. Previous studies have shown that the degree of tendon abnormality is significantly stronger in ruptured than in tendinopathic Achilles tendons [3], although it is unclear whether both pathologies are caused by the same mechanisms. The present study suggests that 3D reconstruction of the tendinopathy samples should be performed. Indeed, for 2 out of 4 samples from Achilles tendinopathy patients showed microstructural abnormality within few in depth cross-sections that could be easily missed by conventional histology. Small regions of advanced and early abnormalities were found, and could be responsible for the tendinopathic nature of the sample.

CONCLUSION

PSOCT has the potential to explore *in vivo* the pathological changes associated with Achilles tendon rupture, and could help to delineate abnormalities in tendinopathic samples.

REFERENCE

- [1] Kannus P, Józsa L. J Bone Joint Surg Am. 1991;73(10):1507-25.
- [2] Yang, Y.; Bagnaninchi, P.O.; Hu, B.; Hampson, K.; El Haj, A.J. IET Optoelectronics. 2008; 2(5):188-194.
- [3] Tallon C, Maffulli N, Ewen S. Med Sci Sports Exerc. 2001;33(12):1983-90.

THE PATHOGENIC ROLE OF TENDON STEM CELLS IN TENDINOSIS

Jianying Zhang, James H-C Wang[#]

MechanoBiology Laboratory, Departments of Orthopaedic Surgery and Bioengineering
University of Pittsburgh, Pittsburgh, PA, [#]wanghc@pitt.edu

INTRODUCTION

Tendinosis is chronic tendon degeneration that affects millions of people in both occupational and athletic settings. Histopathological studies have shown that lipid accumulation, increased amounts of glycosaminoglycans, and calcium deposition are present in tendon lesions, suggesting that cells with diverse phenotypes are present in tendons. We report that rabbit tendons contain multi-potential cells, termed tendon stem cells (TSCs). We suggest that TSCs may play a major role in the development of tendinosis undergoing “wrong” differentiation in response to large mechanical loading conditions.

MATERIALS AND METHODS

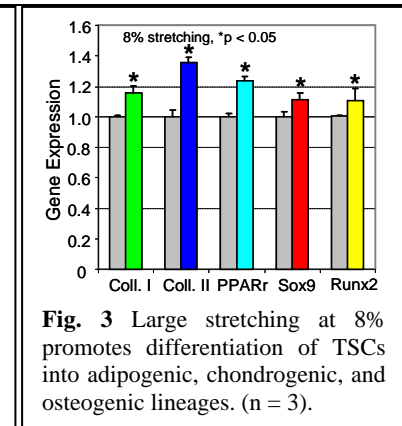
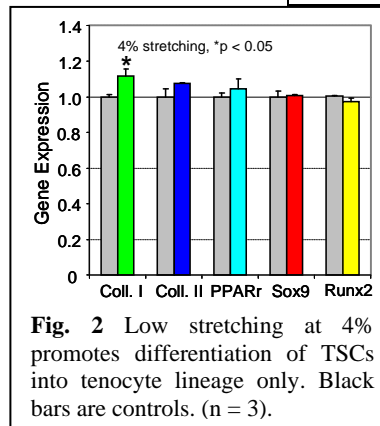
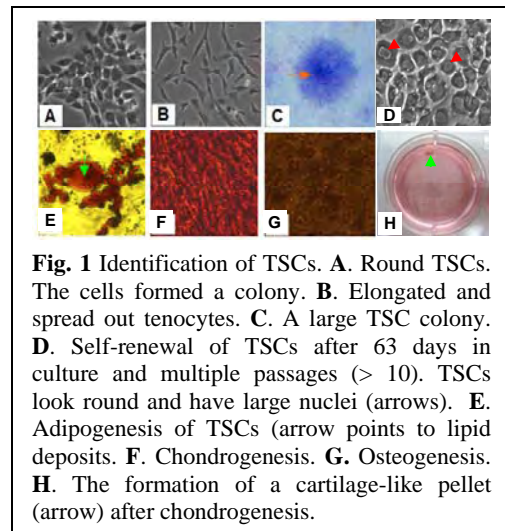
Tendon cells were isolated from both patellar and Achilles tendons of New Zealand white rabbits (female, 4-6 months, 3-4 kgs). These cells were characterized by testing their clonogenicity, self-renewal, and multipotency. The cellular mechanobiological response was examined by subjecting the tendon cells to cyclic mechanical stretching using an custom-made in vitro loading system and profiling marker genes using real time RT-PCR.

RESULTS

We found that these TSCs formed colonies and were round in culture, instead of more elongated like tenocytes, the residential cells in tendons. These cells were also able to self-renew after long-term culture based on the judgment from their round morphology and characteristic large nuclei (**Fig. 1**). In addition, cyclic stretching at 4% significantly increased collagen type I gene expression, but not that of collagen type II, PPAR γ , and Sox-9 (**Fig. 2**); in contrast, stretching at 8% increased expression of all of these genes (**Fig. 3**). Collagen type I, PPAR γ , collagen type II/Sox-9, and Runx2 are marker genes of tenocytes, adipocytes, chondrocytes, and osteocytes, respectively.

DISCUSSION

The tendon cells isolated from rabbit patellar and Achilles tendons were most likely TSCs based on the clonogenicity, self-renewal, and multipotency, three universal criteria for stem cells. The results from cell stretching experiments indicate that small mechanical stretching (4%) may be beneficial in terms of upregulating collagen type I gene expression in TSCs; that is, promoting tenocyte differentiation and hence maintaining tendon homeostasis. However, large mechanical stretching (8%) may be detrimental because it could induce differentiation of TSCs towards “non-tenocyte” lineages (adipocytes, chondrocytes, and osteocytes). Consequently, these “wrong” differentiated cells may cause tendinosis by formation of lipids, glycosaminoglycans, and calcification that are often seen in tendon lesions of tendinosis patients.



REFERENCES

Bi et al., *Nat Med.* 2007 Oct;13(10):1219-27. Epub 2007 Sep 9. Wang and Zhang, 6th ISSCR, p92, 2008.

ACKNOWLEDGEMENT

This work was supported in part by NIH AR049921 and AR049921S1 (JHW).

DEVELOPMENT OF AN IN VITRO MODEL FOR TENDINOPATHY

Jie Qi^{1,2}, Liqun Chi¹, Jian Wang¹, Ruwan Sumanasinghe¹, Michelle Wall¹, Mari Tsuzaki¹ and Albert J. Banes^{1,2}

¹Flexcell International Corp., 437 Dimmock's Mill Rd. suite 28, Hillsborough, NC,

²Joint Department of Biomedical Engineering, University of North Carolina at Chapel Hill, NC and North Carolina State University in Raleigh, NC

INTRODUCTION

Tendinopathy, chronic tendon pathology, is a broad term encompassing painful conditions occurring in and around tendons in response to overuse (1). It is a common disease and difficult to treat because of the lack of knowledge in the development of tendinopathy. Several animal models have been developed which circumscribe two causative mechanisms: 1) changing the mechanical environment (overuse) and 2) exposing tendon to a matrix-degrading agent (2). However, due to the cost, difficulty, invasiveness, reproducibility and time to induce injury, it is difficult to perform routine studies with these models and to test potential mechanisms. In the present study, we developed an in vitro tendinopathy model by exposing low density, human tenocytes in a bioartificial tendon to excessive strain for 1 h/day at 1 Hz for three days (Tissue Train three-dimensional (3D) culture system, Flexcell International Corporation, Hillsborough, NC). It was hypothesized that interleukin-1 β (IL-1 β) could drive a cell survival rather than matrix destructive pathway and spare cells exposed to strain. The results showed that IL-1 β could reverse the expression of marker genes which are up-regulated in "pathologic" tenocytes.

MATERIALS AND METHODS:

Primary human internal fibroblast cells (HTIFs) were isolated from discarded human tendon tissue as described previously (3). HTIFs from passages 2 to 4 were used in this study. HTIF - populated three-dimensional (3D) type I collagen constructs were fabricated in Flexcell's Tissue Train® culture plates (Flexcell International Corporation, Hillsborough, NC) and grown in medium 199 (Invitrogen) containing 2% fetal bovine serum for 48 h. The constructs were then subjected to 3.5% cyclic strain at 1 Hz for 1 hour per day for two days in the presence or absence of 100 pM IL-1 β . Cells were fixed with 3.7% formaldehyde for staining or the total RNAs were collected and real time RT-PCR was performed to determine the expression levels of target genes.

RESULTS: By stretching human tenocytes at low density in 3D collagen gels, a tendinopathy-like environment was simulated. Cells in the control group showed robust actin cytoskeletons and extended cell shapes. The stretched cells rounded up and approximately 90% of the cells died (4) (Figure 1). Even though the mechanism leading to tendinopathy is not clear, the gene expression profile in tendinopathy has been reported (1). In this study, three biomarkers, type I collagen, biglycan and fibronectin, were chosen for monitoring the development of an in vitro "tendinopathy" phenotype. The expression levels of these three genes were elevated in tendons with tendinopathy (1). Results of real time PCR experiments showed that all three marker genes were upregulated in the cells from the stretched group (Figure 2). These results and the change in cell shape indicate that tendinopathy may be induced by the strain regimen used in this study and that this model may be used as an in vitro model for tendinopathy. IL-1 β is released from mechanically-stimulated tenocytes. It was hypothesized that IL-1 β may act as a negative feedback modulator involved in a mechanosensing pathway. Therefore, the role of IL-1 β in the treatment of tendinopathy was further investigated in this study. Results of cytoskeleton staining showed that cells from the stretched group did not round up and die in the presence of IL-1 β . IL-1 β treatment may rescue tenocytes from

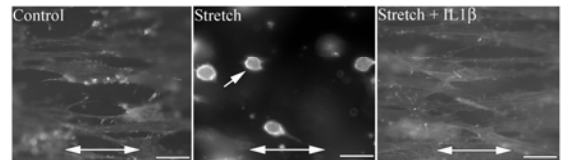


Figure 1. Human tenocytes grown in 3D collagen gels. Cells were fixed and stained with Rhodamine-phalloidin. Scale bar = 50 μ m

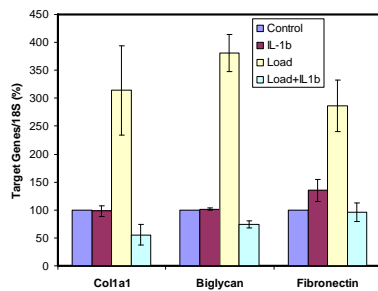


Figure 2. Real time RT-PCR of three tendinopathy marker genes

stretch-induced injury in this model (Figure 1). Real time PCR results showed that IL-1 β treatment also reversed the expression of the three marker genes in the cells from stretch group (Figure 2).

CONCLUSIONS: 1. The tendinopathy-like phenomenon could be induced by stretch in 3D cultures. 2. IL-1 β may play a role in the treatment of tendinopathy

REFERENCES: 1. Riley G. Nature Clinical Practice Rheumatology. 4, 82-89, 2008. 2. Lake SP. Disability and Rehabilitation. iFirst article, 1-12, 2008. 3. Banes AJ, et al. J. Orthop. Res. 6, 83, 1988. 4. Qi J, et al. Tissue Eng. 12(10): 2913-25. 2006.

EXPRESSION OF SENSORY NEUROPEPTIDES IN TENDON PROPER IS ASSOCIATED WITH FAILED HEALING IN CALCIFIC TENDINOPATHY

Pauline Po-yee Lui, Lai-shan Chan, Sai-chuen Fu, Kai-ming Chan

Department of Orthopaedics and Traumatology, The Chinese University of Hong Kong.

The Hong Kong Jockey Club Sports Medicine and Health Sciences Centre, Faculty of Medicine, The Chinese University of Hong Kong.

Introduction:

Recent studies have shown sprouting of substance P (SP)- or calcitonin gene related peptide (CGRP)-positive nerve fibers in clinical tendinopathy samples which were obtained at various stages of the diseases and it was known that the expression of neuropeptides in response to an injury is time-related. This study thus aimed to examine the spatio-temporal expression profiles of these neuropeptides in our established calcific tendinopathy animal model using collagenase injection.

Methods:

Thirty-eight male SD rats were used. Twenty microliters (0.3mg) of bacterial collagenase I or saline were injected into the patellar tendon intratendinously in one limb while the contralateral limb was left untreated. At week 2, 4, 8, 12 and 16 for the collagenase-injected groups and at week 16 for saline-injected group, the patellar tendon was harvested for routine histology and immunohistochemistry (n=6). Semi-quantitative analyses of immunopositive signals of SP and CGRP were done on different cell types in the tendon proper after injury.

Results:

There was increased expression of SP or CGRP in the tendon cells at week 2. The expression in the tendon cells reduced afterwards and increased again at week 16. Their expression in chondrocyte-like cells was observed at week 4, corresponding to the time of first appearance of these cells. The expression in chondrocyte-like cells then decreased at week 8, increased again at week 12 and week 16. Cells embedded in the calcific deposits also showed strong SP or CGRP positive signals. The immunopositivity of SP or CGRP in both cell types together showed a biphasic response, which peaked at week 2 and week 16, with significant increase in expression levels at week 2, 4, 12, 16, but not week 8, compared to that in the saline-injection control.

Discussion:

Our results showed that the spatio-temporal expression profiles of SP and CGRP were very similar. Both neuropeptides were expressed in tendon cells, chondrocyte-like cells and calcified deposits. This indicated that non-neuronal cells also produced neuropeptides, consistent with previous study on clinical specimens that there was a local neuropeptide supply in tendon tissue. The transient reduction in the expression of SP and CGRP at week 8, which corresponded to the transient improvement in histology, was consistent with the hypothesis of failed healing in tendinopathy due to the accumulation of microinjuries. The expression of SP and CGRP in the cells embedded in the calcific deposits suggested that they might have roles in matrix calcification.

Acknowledgement:

This research project was made possible by equipment/resources donated by The Hong Kong Jockey Club Charities Trust.

EVALUATION OF MYOSTATIN INHIBITION IN PRECLINICAL MODELS OF MUSCLE ATROPHY ASSOCIATED WITH ORTHOPEDIC INJURY

Carl A. Morris, Michael St. Andre, Peter Bialek, Jascha Parkington, Adam Root, Jimin Zhang, Gerard Bain, Scott Jelinsky, Paul Yaworsky, & Howard Seeherman
Musculoskeletal Biology, Wyeth Research, Cambridge MA USA

INTRODUCTION

A rapid loss of muscle mass and strength is observed following removal of the normal external load to the affected muscles. This can occur as a result of periods of unloading prior to treatment of tendon rupture or immobilization following bone fracture. The reduction of external load in the former condition and loss of external load in the latter condition is sensed by signaling pathways within the muscle cells, producing observable changes in protein synthesis and degradation. However it is unclear whether these signals are similar for atrophy associated loss of tendon attachment versus immobilization. For example, previous studies have shown matrix metalloproteinase 2 (MMP2) expression to be highly elevated following Achilles tendon transection (Skittone et al., 2007) while only minimal regulation of MMP2 activity was observed following immobilization in rat hindlimb muscles (Reznick et al., 2003). These results suggest different remodeling pathways may be involved during the adaptive response associated with loss of tendon attachment compared to immobilization. Myostatin blockade has been found to be an effective approach to stimulate skeletal muscle growth, as mutations or gene deletions in several species of animals show profound increases in muscle mass during normal development. Although myostatin inhibition clearly stimulates muscle growth, it is less clear if it is effective in limiting muscle loss associated with disuse. The purpose of this study was to characterize two clinically relevant models of muscle atrophy and to determine whether inhibition of myostatin signaling would be effective at attenuating muscle atrophy in these models. Achilles tendon transection was used as a model of unloading and unilateral hindlimb casting was used as a model of immobilization.

METHODS

For the muscle unloading model, the Achilles' tendon bundle from the plantaris, gastrocnemius, soleus muscles of one limb in 8-10 week old male C57Bl/6 mice was isolated from the surrounding fascia and completely transected. For the muscle immobilization model, a fiberglass cast was applied to one hindlimb in similar aged mice, preventing movement of both the knee and ankle joints. In both models, the contralateral limb was untreated. Animals were treated weekly with either IP buffer or 10mg per kg ActRIIb-Fc beginning the day of surgery. Tissue samples were collected at 2, 7, and 14 days post surgery in 8-10 animals per time point for muscle mass, morphological, histological, biochemical, or RNA expression analysis. Procedures were approved by the IACUC.

RESULTS

In the buffer treated animals, both the tendon laceration unloading model and the cast immobilization model resulted in significant atrophy of the gastrocnemius muscle (-23% and -20%, respectively) compared to the contralateral untreated muscle. Although both models produced a similar loss of muscle mass, there is the suggestion that the process may involve distinct mechanisms which was corroborated by global RNA expression profiling. Analysis of MMP-2 mRNA expression showed significant changes 7 and 14 days post-surgery only in the tendon laceration unloading model. No changes in MMP-2 mRNA expression were observed following casting.

Treatment with ActRIIB-Fc was able to completely attenuate the 20-23% loss of mass observed following tendon laceration unloading or cast immobilization. The mass of the ActRIIB-Fc-treated tendon laceration and cast immobilized muscles were similar to the untreated muscles in the buffer treated animals. The mass of the untreated control muscles of ActRIIB-Fc-treated animals was increased significantly (~25-28%) over the untreated muscles of buffer-treated mice.

CONCLUSION

This study demonstrates that unloading due to tendon laceration and cast immobilization leads to significant muscle atrophy in rodents. Global RNA expression profiling and evaluation of MMP-2 mRNA expression demonstrated potential differences in the underlying processes responsible for atrophy. Despite these differences, myostatin inhibition by ActRIIB-Fc was effective in reducing muscle atrophy resulting from unloading due to tendon laceration and cast immobilization. These results suggest that treatment with ActRIIB-Fc at the time of injury or repair may be useful to reduce associated muscle atrophy and shorten rehabilitation times.

EVALUATION OF OSTEOGENESIS OF PHOTO-RESPONSIVE HYDROGEL ENCAPSULATED BONE MORPHOGENETIC PROTEIN-2 AND LIGAMENTUM FLAVUM CELLS

Chih-Hsiang Chang,¹ Chih-Hwa Chen,¹ Chak-Bor Wong,¹ Hsia-Wei Liu,^{1,2} Shu-Wen Whu,¹ Mei-Yun Wu,¹ Jih-Chao Yeh,^{1,3} I-Hsuan Lin,¹ Shi-Hui Chen,¹ and Hsiang-Jou Sun¹

¹Department of Orthopaedic Surgery, College of Medicine, Chang Gung Memorial Hospital-Keelung, Chang Gung University, Keelung, Taiwan

²Material and Chemical Research Laboratories, Industrial Technology Research Institute, Hsinchu, Taiwan

³Department of Biomedical Engineering, Chung Yuan Christian University, Chung Li, Taiwan

⁴Department of Chemical Engineering, National Tsing Hua University, Hsinchu, Taiwan

INTRODUCTION:

Osteogenesis of the ligamentum flavum (LF) is a widely recognized pathophysiologic factor in spinal stenosis and in other pathologic ossifications of the spinal ligament.¹ Bone morphogenetic protein-2 (BMP-2) and the BMP-2 receptor have been reported to be present in the ossification of LF, which suggests a mechanism of osteogenic differentiation of degenerated LF.² The potential for biomimetic constructs with co-immobilized adhesion and rhBMP-2 to induce osteoinduction and osteogenesis was demonstrated in our recent study.³ Ligamentum flavum excised during the decompressive spinal procedure will be sent for histological study or discard. We expect the novel rhBMP-2 tether photopolymerized gel will modified the encapsulated ligamentum flavum cells to be osteogenic and induce osteogenesis. (Shown as Figure 1) This preliminary study will define the role of ligamentum flavum cells in the application of tissue engineering for osteogenesis.

METHODS:

The Ligamentum flavum (LF) tissue was obtained from spinal stenosis patients during surgical spinal decompressive procedures. LF tissue specimens were digested in Neuman-Tytell serumless medium (Gibco BRL) containing 250 U/mL type 1A collagenase (Worthington Biochemical Corp) at 37 C in 5% CO₂ for cell isolation. RhBMP-2 (250 ng/ml) was conjugated to polyethylene glycol (PEG) by reacted with an equimolar amount of acrylate-PEG-*N*-hydroxysuccinimide (ACRL-PEG-NHS, MW 3400Da).³ The soluble rhBMP-2 was incorporated poly (ethylene glycol) diacrylate (PEGDA, MW 3400Da) solution simultaneously for comparison. Immediately before photoencapsulation, LF cells were resuspended in the polymer solution to make a concentration of 10 million cells/ml and gently mixed to make a homogeneous suspension. A 50- μ l aliquot of cell-polymer-photoinitiator suspension was subsequently loaded into disk-shaped molds with a 4-mm internal diameter, followed by photopolymerization with 365 nm UV light to gelate the cell-polymer constructs. The hydrogel constructs were then removed from the molds, washed with sterile PBS containing 1% penicillin-streptomycin, and incubated in 24-well plates for 1, 7 and 14 days. Histological, immunohistochemical and confocal microscopy assays will be tested for the evidence of osteogenesis.

RESULTS AND DISCUSSION:

Most of spindle shape LF cells were harvested, shown as Figure 2. Expression of collagen type I, osteoprotein and alkaline phosphatase (ALP) of LF cells increased with cultured time. Expression of collagen type II and aggrecan of LF cells decreased with cultured time. When LF cells and free rhBMP-2 were incorporated PEDGA, the same expression of collagen type I and alkaline phosphates activity of LF cells at 7 and 14 day was found. Higher expressions of collagen type I, osteoprotein and ALP in PEGDA-PEG-rhBMP-2 gel than one in free rhBMP-2 groups at 14 day was observed. Free rhBMP-2 was lost easily from PEGDA. The LF cells maintained osteogenesis in PEGDA-PEG-rhBMP-2 gel longer due to chemical bond between PEG and rhBMP-2. Ligamentum flavum cells in PEGDA-PEG-rhBMP-2 gel had shown potential in the application of tissue engineering for osteogenesis.

REFERENCES

1. Yoshida M, Shima K, Taniguchi Y, Tamaki T and Tanaka T. Hypertrophied ligamentum flavum in lumbar spinal canal stenosis. *Spine*. 1992;17:1353-1360.
2. Hayashi K, Ishidou Y, Yonemori K, et al. Expression and localization of bone morphogenetic proteins and BMP receptors in ossification of the ligamentum flavum. *Bone*. 1997;21:23-30.
3. Liu HW, Chen CH, Tsai CL, et al. Targeted delivery system for juxtacrine signaling growth factor based on rhBMP-2-mediated carrier-protein conjugation. *Bone*. 2006;39:825-836.

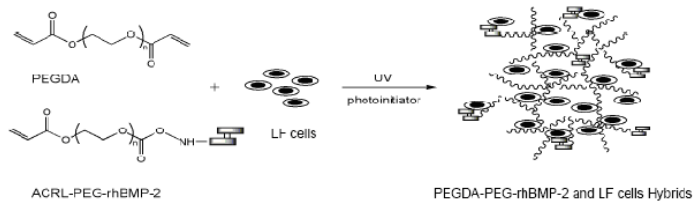


Figure 1. Scheme of LF cells were incorporated PEGDA-PEG-rhBMP-2.



Figure 2. Morphology of LF cells.

NANOFIBER ALIGNMENT REGULATES ADHESION AND INTEGRIN EXPRESSION OF HUMAN MESENCHYMAL STEM CELLS AND TENDON FIBROBLASTS

¹S.P. Kwei, ¹K.L. Moffat, ²W. N. Levine, and ¹H. H. Lu

¹Department of Biomedical Engineering, Columbia University, ²Orthopaedic Surgery, Columbia University, USA

INTRODUCTION: Rotator cuff tendon repair is one of the most common shoulder procedures performed annually in the United States[1]. Failure rates for primary cuff repair have been reported to be as high as 94%[2], and the use of biological grafts has yielded suboptimal results[3]. To improve tendon repair, we have developed a degradable polymer nanofiber-based scaffold system[4], and are currently evaluating the response of human mesenchymal stem cells (hMSC) on this novel scaffold. As an in-depth understanding of the mechanism of cell-material interactions will be essential for the design and optimization of these biomimetic scaffolds, the objective of this study is to compare the adhesion of hMSC and human rotator cuff fibroblasts (hRCF) as a function of nanofiber alignment. It is hypothesized that nanofiber organization will regulate cell adhesion morphology and integrin expression. Moreover, distinct responses are anticipated between the undifferentiated and differentiated cell types.

MATERIALS AND METHODS: *Scaffold Fabrication and Characterization:* Aligned and unaligned nanofiber scaffolds of poly(lactic-co-glycolic) acid (PLGA 85:15, Lakeshore) were produced by electrospinning[4]. Scaffold fiber organization was examined with Scanning Electron Microscopy (SEM, n=3) and confirmed by quantitative alignment analysis[5]. *Cell Culture:* Explant-derived human rotator cuff tendon fibroblasts and hMSC (Cambrex) were seeded on the nanofiber scaffolds at a density of 3.14×10^4 cells/cm² and maintained in fully supplemented medium containing 10% FBS, 1% antibiotics, 1% non-essential amino acids, and 0.1% antifungal. *End-point Analyses (1,3 & 14 days):* Cell adhesion was assessed by Live/Dead assay (n=2) with confocal microscopy on days 1 and 14. Gene expression (n=5) for integrins $\alpha 2$, αV , $\alpha 5$, $\beta 1$, $\beta 3$ and GAPDH was evaluated by RT-PCR.

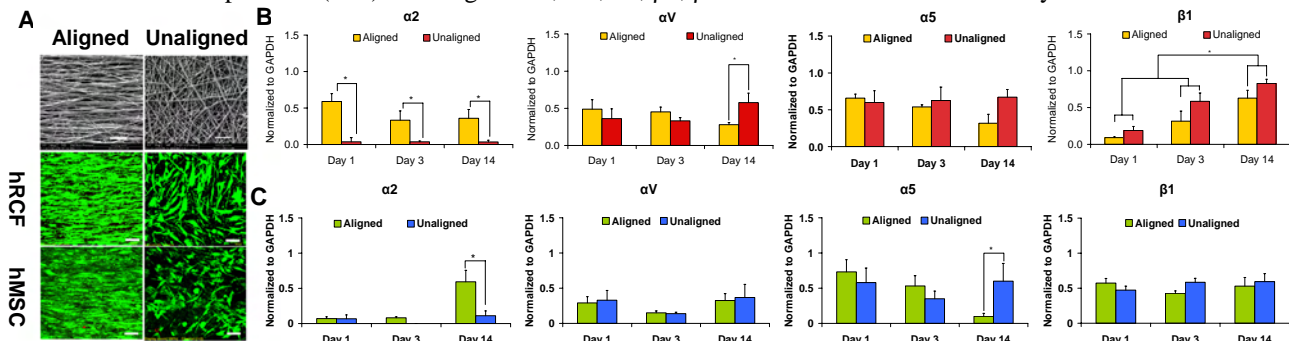


Figure 1: A) SEM of aligned and unaligned scaffolds (top panel, 2000x, bar=20 μ m). Cell viability and morphology on day 14 (20x, bar=100 μ m). Normalized gene expression for integrins $\alpha 2$, αV , $\alpha 5$, $\beta 1$ on unaligned and aligned scaffolds seeded with B) hRCFs and C) hMSCs, (* $p < 0.05$).

RESULTS AND DISCUSSION: The adhesion of both hMSC and fibroblasts was guided by nanofiber alignment, and distinct cell morphologies exhibited on the two types of substrates indicate that these cells recognize differences in fiber organization (Fig. 1A). Interestingly, distinct integrin expression profiles were observed as a function of nanofiber alignment, with significant differences detected between fibroblasts (Fig. 1B) and hMSC (Fig. 1C). Significantly higher expression of $\alpha 2$ and $\beta 1$ (Fig. 1B) were detected for fibroblasts on aligned nanofibers, as these two integrins form a heterodimer that mediates cell attachment to collagen[6], their upregulation on aligned nanofibers suggests that this substrate may better mimic the native tendon matrix. Interestingly, $\alpha 2$ expression in hMSC is upregulated over time on the aligned scaffolds (Fig. 1C), indicating that matrix alignment may promote hMSC differentiation into tendon fibroblasts. As both αV and $\alpha 5$ have been associated with tendon healing[7], their upregulation by day 14 on unaligned scaffolds in both cell types may be more indicative of a scar tissue repair response. It is noted that the scaffolds in this study exhibit similar structural properties (nanofiber diameter, porosity, pore size, permeability)[4]; thus any observed differences in cell adhesion can be attributed largely to nanofiber organization (aligned vs. unaligned). In summary, nanofiber alignment guides hMSC and fibroblast adhesion, with the aligned nanofiber matrix inducing a more biomimetic response. Future work will focus on determining integrin production and the downstream effects of these observed cell responses as a function of nanofiber organization.

REFERENCES: [1] Vitale *et al.*, 2007; [2] Galatz *et al.*, 2004; [3] Sclamborg *et al.*, 2004; [4] Moffat *et al.*, 2008; [5] Costa *et al.*, 2003; [6] Gallant *et al.*, 2007; [7] Harwood *et al.*, 1998.

ACKNOWLEDGEMENTS : NIH/NIAMS R21-AR056459, R01-AR055280 (HHL)

VARIATIONS IN CELL MORPHOLOGY IN THE CANINE CRUCIATE LIGAMENT COMPLEX

K.D. Smith¹, A. Vaughan-Thomas¹, P.D. Clegg¹, D.G. Spiller², J.F. Innes¹, and E.J. Comerford¹

¹Musculoskeletal Research Group, Leahurst Campus, University of Liverpool, Liverpool, U. K.

²Centre for Cell Imaging, University of Liverpool, Liverpool, U. K.

INTRODUCTION

Cruciate ligaments (CLs, anterior, A and posterior, P) aid in stabilising the knee joint. The ACL is twisted around the PCL and each ligament comprises sparse fibroblasts between bundles of collagen fibrils. Although ACL failure is a major source of morbidity, its metabolism and function are poorly understood. Cells in connective tissue can have long cytoplasmic processes which may extend in all directions and contact other cells. These extensive processes suggest the potential to co-ordinate cellular and metabolic responses throughout the tissue through cell-to-cell communication¹. Little is known of variations in cell morphology in the CLs. Rounding of cells is associated with fibrocartilaginous change in the canine ACL². In this study, we detail the previously unreported cell matrix and novel cell morphology in the canine CL complex.

MATERIALS AND METHODS

Four ACLs and 4 PCLs from 2 dogs were fixed in formalin, embedded in paraffin, sectioned at 4µm and stained using H&E. Two ACLs and 2 PCLs from 2 dogs were snap-frozen in isopentane, cryosectioned at 30µm then fixed overnight in cold methanol. Endogenous reactivity was blocked with normal goat serum and then sections were immunostained using two antibodies raised against the cytoskeletal components vimentin and α -tubulin. Secondary fluorophore conjugated antibodies and DAPI allowed image collection using a confocal laser scanning microscope (Zeiss LSM 510 META NLO), and the 3-dimensional reconstruction of cell morphology.

RESULTS

The cells of the epiligament formed a dense meshwork of short, branched processes. An increase in the cellularity of the epiligament was observed in the region of the midsubstance of the ACL in the region of contact with the PCL. A dense meshwork of cells was also seen in the interfascicular regions of the ligament with thick, branching processes of widely varying length, and round nuclei. Cells of the fascicular regions were of three broad types. One group of cells within the ligament had long, thin cytoplasmic processes extending mainly parallel to collagen bundles, long narrow nuclei and some shorter transverse processes. A second group had shorter, thicker, frequently branching processes, with rounder nuclei. Contact with other cell processes was common in these first two groups. The third group were isolated, with rounded nuclei and no cytoplasmic processes. Cell processes were seen to penetrate the interior of collagen bundles. The majority of each ligament comprised either a mixed population of groups one and two, or of group three alone, although juxtaposition of all cell morphologies was also seen. In the midsubstance of the CLs, a decrease in cell density with an increase in the relative proportion of group three cells compared to proximal and distal CLs was noted. Marked local variation in cell density existed, with small areas completely devoid of nuclear or cytoskeletal staining.

DISCUSSION

Confocal images of cells within the ECM of the ligament substance allowed detailed study of their morphology, leading to three broad categories, which may all be variations of the fibroblast. Tension appears important in maintaining cellular processes and a lack of processes and rounded nuclei may be an adaptation to ligament mechanics or physiology³. Local variation in morphology may indicate differences in mechanics between adjacent collagen bundles. Alterations in cell morphology may alter the ability of cells to produce healthy matrix and repair damage through disruption of collagen production. Long cytoplasmic processes provide a mechanism whereby cells apparently distant from blood vessels may acquire nutrients. In the midsubstance, the mechanical environment may make sustainability of cell processes impossible, so the observed decrease in cell density in the midsubstance may reflect lower available nutrition. Areas devoid of nuclear or cytoskeletal staining may mark the initiating event in fibrocartilaginous change.

We have shown marked regional variation in the cell morphology of the canine CL complex and outlined the possible importance of these variations in ligament physiology. The possibility of a three dimensional network of cells has ramifications for cell nutrition, mechanical sensing and coordinated response to injury in the CL complex.

REFERENCES

1. Lo IK, Chi S, Ivie T, Frank CB, Rattner JB. The cellular matrix: a feature of tensile bearing dense soft connective tissues. *Histol. Histopathol. J Anat* 2002 Mar;200(Pt 3):283-96
2. Comerford EJ, Tarlton JF, Wales A, Bailey AJ, Innes JF. Ultrastructural differences in cranial cruciate ligaments from dogs of two breeds with a differing predisposition to ligament degradation and rupture. *J Comp Pathol* 2006 Jan;134(1):8-16
3. Ralphs JR, Benjamin M, Waggett AD, Russell DC, Messner K, Gao J. Regional differences in cell shape and gap junction expression in rat Achilles tendon: relation to fibrocartilage differentiation. *J Anat* 1998 Aug;193(Pt 2):215-22.

FONDAPARINUX DOES NOT INHIBIT TENDON REPAIR.
P. Aspenberg¹; P. Eliasson¹; T. Andersson¹; J. Schilcher¹; T. Lindahl¹
¹University of Linköping, Linköping, Sweden

INTRODUCTION

Heparins fragments inhibit thrombin generation directly and via inhibition of factor Xa. Dalteparin, a low molecular weight heparin (LMWH), inhibits tendon healing in a rat model, but only if applied continuously¹. This may not cause clinical concern, because patients receive intermittent treatment, which was harmless in the model. However, the results suggested that drugs with a continuous effect on thrombin generation can be expected to impair healing also in patients. One such drug is fondaparinux, which exerts its effect indirectly, by inhibiting factor Xa, and lacks most other heparin-like effects. We tested fondaparinux in the same model as before, given continuously at a dose, which produced a relevant effect on factor Xa activity.

MATERIALS AND METHODS

After a series of dose-finding studies, the appropriate dose was found to be 50 µg/h, delivered continuously through a minipump. 20 rats were randomized in two groups: continuous fondaparinux 50 µg/h versus control, 10 rats in each. The anti-factor Xa activity was measured at sacrifice. Results were evaluated by mechanical testing at 8 days.

The Achilles tendon was transected and left unsutured with a gap between the tendon stumps. There was no post-operative immobilization.

The rats were divided into experimental and control groups by a lottery, and the surgeon was blinded. Minipumps (model No. 2001, pumping rate 1.0 µL/hr, Alzet, B&K Universal) were implanted intraperitoneally.

After 8 days, the tendon with the attaching calcaneal bone was removed. Sagittal and transverse diameters were measured with a calliper, and the tendon was pulled at a constant speed of 0.1 mm/s until failure. Mechanical parameters measured were force at failure, stiffness and energy uptake. Transverse area, stress and elastic modulus were calculated. The experiment was approved by the regional animals ethics committee.

RESULTS

One fondaparinux-treated rat had a bleeding in the operated area and was excluded, and one control rat was lost because it gnawed at its wound. The plasma anti-factor Xa activity was increased to a relevant degree (mean 1.1, SD 0.06 U/mL versus control: 0.1 SD 0.01). However, no effect of fondaparinux could be demonstrated. Peak load for the fondaparinux group was 32 N, and for the controls 31 N (Table 1). The 95 % confidence interval for the difference between the mean values of the groups ranges from a decrease by fondaparinux by 6 % to an increase by 16 %. Thus, a relevant negative effect is highly unlikely.

	Fondaparinux		Control	
	Mean	SD	Mean	SD
Peak load (N)	32.0	3.6	30.5	3.9
Stiffness (N/mm)	9.1	1.3	8.2	1.2
Energy uptake (Nmm)	77	15	70	13
Transverse area (mm ²)	10.3	1.8	9.8	1.3
Ultimate stress (Mpa)	3.2	0.7	3.2	0.5
Modulus (Mpa)	14	3.3	14	2.1

Table 1. Mechanical parameters of Achilles tendons after 8 days' healing with or without fondaparinux.

DISCUSSION

In our previous study, the LMWH (dalteparin) decreased force at failure by over 25 %, with high statistical significance¹. Now, with fondaparinux, a decrease of more than 6 % is highly unlikely. Two interpretations are possible: The first would be that the previously reported negative effects of LMWH on tendon repair were neither due to inhibition of prothrombin activation nor inhibition of thrombin activity. The other would be that fondaparinux still allows thrombin generation to a sufficient degree for normal healing. The latter explanation appears less likely, as the whole explanation for the antithrombotic effect of fondaparinux is the inhibition of prothrombin activation via factor Xa, and inhibition of this factor was achieved to the same degree as for dalteparin.

The possibility that LMWHs inhibit healing via mechanisms unrelated to thrombin activation is more easily conceived. Fondaparinux is a pentasaccharide with the same factor Xa-binding saccharide sequence as heparin². Heparins have a wide range of effects on extra cellular matrix biology and cells. They can inhibit fracture repair in several models, and negatively influence bone cells in vivo and in vitro³. In general, these effects become less with decreasing size of the molecule, and in vitro the negative effects of LMWH are not seen for fondaparinux⁴. This suggests that the negative effects of LMWHs on bone are, at least in part, unrelated to factor Xa inhibition, and thereby prothrombin activation. It now appears that the same applies also for the healing of soft collagenous tissue.

The effects apart from thromboprophylaxis of these drugs are complex, and many experiments could be performed to somewhat elucidate the differences between them on various aspects of signaling during repair.

1. Virchenko O et al.. *J Bone Joint Surg Br* 2008.
2. Bauer KA.. *Curr Opin Hematol* 2008.
3. Lindner T, et al.. *Expert Opin Pharmacother* 2008.
4. Handschin et al.. *Br J Surg* 2005.

HISTOLOGICAL, BIOMECHANICAL AND TRANSCRIPTIONAL PROCESSES DURING NORMAL RAT TENDON REPAIR

Scott A. Jelinsky, Li Li, Debra Ellis, Joanne Archambault, Jian Li, Jodie Moreau, Carl Morris, Howard Seeherman
Biological Technologies and WHMSB, Wyeth Research, Cambridge, MA USA

INTRODUCTION

The wound healing process is well-established process that follows a very similar cascade in tendon as in other tissues that include an inflammatory phase, a proliferative phase and a remodeling phase. Typically tendon produced during natural healing has an inferior structural and functional integrity and lower failure force compared to normal tissue due to adhesions and scar tissue that limit range of motion and overall strength. Scar tissue is generally less elastic and more prone to recurring injury. It is therefore critical to understand the signaling mechanism and the complex interaction between the different processes leading to efficient tendon repair. In this study, we asked whether normal tendon healing follows the same molecular mechanism as normal adult wound healing and we determined the timing of the molecular response. Using gene expression profiling, histological evaluation and biomechanical evaluation, we have characterized the changes during normal unaided repair of an Achilles tendon laceration model.

METHODS

Tendon injury was induced through Achilles tendon transection at a point halfway between the musculotendinous junction and the insertion onto the calcaneus while leaving the plantaris muscle and tendon intact. The tendon remained unsutured and was allowed to heal naturally. Tissues samples were collected 3, 7, 10 and 14 days post surgery and analyzed by histology, transcriptional profiling, and biomechanics at days 7 and 14 only. Tissue from the newly formed repair site was separated from the uninjured tendon tissue. Total RNA was isolated, labeled and hybridized to Rat genome RAE230 2.0 arrays (Affymetrix). Statistical identification of significantly regulated biological pathways was implemented using the SigPathway algorithm. Samples harvested for biomechanical analysis were dissected and anchored for Instron testing using custom designed fixtures. Tendons were preconditioned and pulled to failure at 1cm/sec, with final readouts of stiffness and ultimate tensile strength (UTS).

RESULTS

During early healing, the defect region was filled with highly vascularized loose connective tissue infiltrated with mesenchymal stem cells and immune cells. By day 7 to day 10, defect region was filled with dense spindle shaped fibroblast-like cells that loosely aligned with the direction of the force. By day 14, space between spindle shaped cells was completely filled with extracellular matrix produced by the fibroblast-like cells with parallel orientation along with the longitudinal axis of the tendon. Repair tissue had significantly higher UTS and stiffness than those harvested at day 7. We identified 1687 distinct transcripts regulated (Anova $p < 0.01$) during normal tendon repair. Three distinct patterns of expression were observed during normal tendon repair. The three groups consists of genes with high expression early during repair (days 3-7), genes with high expression during days 7-10 and genes with high expression late in the repair process (day 10 –15). Functional characterization of the three groups reveals that early genes are most involved in inflammatory response including IL6 and CXCL6. Genes with high expression during day 7-10 are involved in collagen synthesis and extracellular matrix formation and include Col12a1 and Fibrillin 2. Finally genes induced late in repair include many involved in collagen reorganization and include fibromodulin and tenomodulin. As tendon repair progresses increase expression of tendon and tendon related genes are observed including Col1a1, Scleraxis, Tenomodulin and thrombospondin 4. Global pathway analysis identified the inflammatory response at the most regulated pathway. Concordant with decreased inflammation is a decrease expression of genes involved in cell cycle and cell cycle regulation. This was followed by a shift towards matrix remodeling including increase in extracellular matrix, collagen synthesis, cartilage condensation, cell-to-cell adhesion, and matrix metalloprotease expression. Furthermore genes upregulated during adipocyte differentiation are strongly down regulated through tendon repair including adiponectin and acyl-CoA synthetase 1.

CONCLUSIONS:

We have used a rat model of a tendon defect combined with high throughput transcriptional profiling to determine the molecular processes of normal tendon healing. Through statistical analysis of differential expression and pathway analysis, we have identified genes and pathways regulated in tendon healing and have determined the temporal change in expression. We have shown that many of the processes described for normal unaided wound repair are also occurring during unaided tendon repair.

Characterizing Structure-Function Relationships in Tendon

S Toorani, JC Shelton, HRC Screen

School of Engineering & Materials Science, Queen Mary University of London, UK.

INTRODUCTION: Tendon requirements range from energy storage in highly stressed tendons, to facilitating load or position control during intricate movements^[1]. This study hypothesises that composition and micro-structural organization varies between tendons with different functional roles, in order to optimise their mechanical behaviour. In this study, porcine flexor and extensor tendons were used to provide two tendons with different functional roles for comparison. Understanding tendon structure-function relationships may assist in the optimisation of functional tissue engineering solutions.

METHODS: Fascicles were dissected from porcine superficial digital flexor tendons (SDFTs) and common digital extensor tendons (CDETs) and split into 3 analysis groups. **Mechanical Analysis:** Quasi-static tests to failure were carried out at varying strain rates (10, 20, 45, 60, 100 & 200% min⁻¹) and incremental stress-relaxation tests were completed to 2, 4, 6, 8 & 10% strain with relaxation periods of 600 seconds. **Biochemical Analysis:** Following lyophilisation, fascicles were digested in collagenase to determine water and GAG content. **Structural Analysis:** Fascicles were fixed in 3% glutaraldehyde, wax embedded, sectioned, and stained with Verhoeff's Van Gieson (fibre crimp). Additional fascicles were fixed, resin embedded, sectioned and stained with uranyl acetate & lead citrate for TEM analysis (fibril organisation).

RESULTS: Mechanical Analysis: SDFTs demonstrated a significantly higher UTS and modulus (E) compared to CDETs. Strain rate influenced both groups, with UTS and E values increasing as strain rate increased (fig 1a). This increase was more pronounced in CDETs. The rate and amount of relaxation was consistently greater in CDETs, with CDETs showing completely viscous behaviour beyond 6% strain (fig 1b).

Biochemical Analysis: CDETs contained more water and GAG than SDFTs (fig 2).

Structural Analysis: Histology highlighted more tightly packed fibres with a significantly sharper crimp angle in SDFTs (fig 2). No traces of elastin were seen in any samples. TEM highlighted more tightly packed fibrils covering a higher percentage area in SDFTs (fig 2 "cover"). Also smaller fibril diameters were measured in SDFT (145.2nm) than CDET (187.5nm). SDFT fibrils were additionally 10% more circular in shape (fig 2).

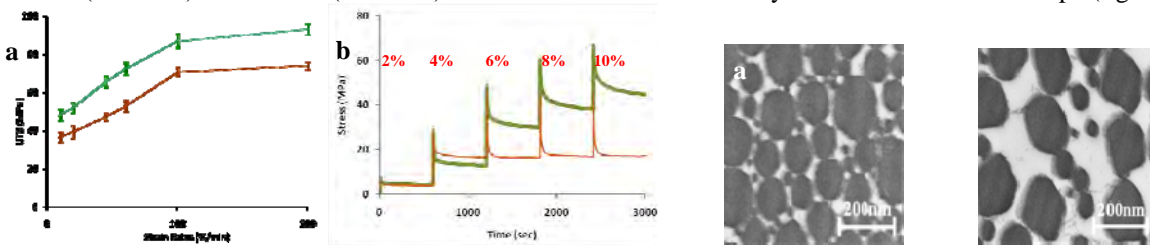


Fig 1:(a) Effects of strain rate (b) Incremental stress relaxation Fig 2: TEM images & data analysis (a)SDFT & (b)CDET

DISCUSSION: This study has identified relative differences in the mechanical, biochemical and structural characteristics of two tendons with different functional requirements. The higher UTS and E values recorded for SDFTs could be an adaptation to the larger stresses they experience *in vivo*. Structurally this behaviour may result from the more tightly packed, smaller diameter SDFT fibrils, which provide a larger surface area for enhanced interfibrillar binding^[2]. The sharper crimp angle observed in SDFTs may explain the lower stresses recorded during the toe-region. This sharper crimp angle may be important for SDFTs as it may facilitate their energy storage capabilities.

The viscoelastic nature of tendon was apparent from the changes in properties with increasing strain rates. The greater viscoelastic response of the CDETs could also be an adaptation to allow more intricate position and pressure control. Biochemically, the higher water and GAG content of CDETs may elicit their more viscous behaviour^[3] and may also be responsible for the larger fibril diameters recorded in TEM^[3]. The increased rate and amount of relaxation in CDETs beyond the 6% strain increment indicates that there may be partial failure at 6% strain. SDFTs appear more resistant to this failure, possibly owing to their greater interfibrillar binding.

The reason for the more circular fibrils observed with SDFTs is unclear. However, this could be due to the higher fibril density within the SDFTs and also the higher tensile stresses they experience. This study supports the hypothesis that tendons use subtle micro-structural difference to optimise their mechanical behaviour to best suite their functional role.

REFERENCES: [1] Ker RF *et al.*, (1988) *J. Zool.* 216:309-324. [2] Franchi M *et al.*, (2007) *Sci. World J.* 7: 404-420. [3] Robinson PS *et al.*, (2005) *J. Biomech. Eng.* 27(1)181-185.

LONG TERM FOLLOW-UP OF ANTERIOR CRUCIATE LIGAMENT RECONSTRUCTION WITH AN IMMUNOCHEMICALLY MODIFIED PORCINE XENOGRAFT

Stone KR; **Turek TJ; ***Walgenbach AW; **Galili U

*The Stone Clinic, San Francisco, USA, **CrossCart, San Francisco, USA, ***Univ. of Mass., Worcester, USA

INTRODUCTION

Clinical ACL reconstruction with synthetic and non-human tissue based devices has led to failure due to a range of factors including material property mismatch, fatigue, abrasion, particulate shedding, poor fixation, anatomical placement, and immunologic rejection. The objective of our investigations was to develop an immunocompatible, dynamic bio-implant xenograft for ACL reconstruction with characteristics matching homologous human tissue. Primate studies have shown that treatment of porcine tissues with α -galactosidase enzyme effectively attenuates host to graft immune recognition by α -Gal epitope cleavage and have demonstrated gradual graft remodeling and long term ACL function as assessed at 2, 6 and 12 months [1,2]. Additional evaluations supporting development have included static and dynamic biomechanical testing, biomaterials biosafety/biocompatibility, toxicology, sterility and viral inactivation. This study is the first long-term human clinical evaluation of ACL reconstruction with an immunochemically modified porcine patellar tendon device.

METHODS

This was an FDA and IRB approved pilot clinical investigation in 10 patients requiring ACL reconstruction. A mixed complex patient population was enrolled to challenge the device in a safety and implantability study. Porcine bone-patellar tendon-bone grafts were processed using α -galactosidase, low-level glutaraldehyde and terminally sterilized with 17.8 kGy radiation. All patients received the porcine xenograft. The patient population was extremely athletic with mean age of 41 years (range 21-51), mean pre-injury Tegner Score of 8 (range 6-10). Primary study endpoints were knee stability, serology and MRI findings. Secondary endpoints included subjective measurements of activity level, function and quality of life.

RESULTS

Safety and Implantability: Intra-operative surgical and technical feasibility objectives were met with device handling comparable to human patellar-tendon allografts. Four subjects failed due to non-device related events: (two by non-compliance and trauma; two by graft impingement). One subject failed due to intermittent effusion and was revised at 24 months. Five of six evaluable subjects met success criteria and were athletic and stable at 60 months.

Clinical Outcomes: Initial postoperative effusions resolved by six months. All stability assessments including KT-1000, Lachman's, anterior drawer and pivot shift demonstrated significant improvement ($p < 0.05$) over the study period (Fig 1.). Secondary outcome measures of patient self-evaluations also improved over the study period for Tegner Activity, IKDC and SF-36 measures (Fig 2.).

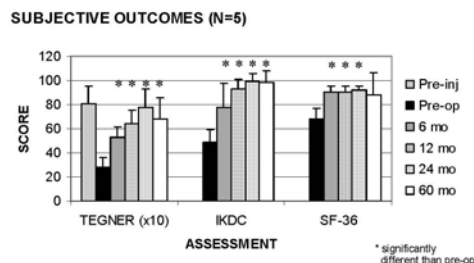
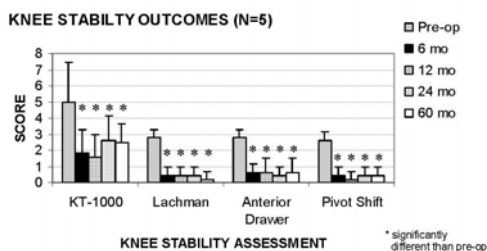


Fig. 1. Ave. knee laxity assessments, N=5, mean + SD.

Fig. 2. Ave. subjective assessments, N=5, mean + SD.

* $p \leq 0.05$ pre-op. vs. 6,12, 24 and 60 months post-op.

* $p \leq 0.05$ pre-op. vs. 6,12, 24 and 60 months post-op.

Serological Outcomes: Antibody response is consistent with primate studies and shows a low anti-Gal titer with transient increase at 2-mo. ($< 1/20^{\text{th}}$ of untreated tissue) and resolution to pre-implant range by 12 to 24-mo. A lower antibody response to other pig antigens (anti-non-Gal) peaked at 6-months, and resolved to pre-implant range by 24-mo. in parallel with completion of graft remodeling. No adverse clinical response could be attributed to serological findings.

CONCLUSION

ACL reconstruction with immunochemically modified porcine grafts lead to successful outcomes in compliant patients. Graft long-term function, histopathology, MRI assessments and serology demonstrates host remodeling (ligamentization) of the treated grafts and supports the development of immunocompatible dynamic bioimplants from xenograft sources. 1. Galili U *et al. Proc Natl Acad Sci U S A.* 1991;88:7401. 2. Stone KR *et al. Arthroscopy.* 2007;4:411.

THE COMPARISON OF *in vivo* KNEE KINEMATICS BETWEEN KNEE OSTEOARTHRITIS PATIENT AND YOUNG HEALTHY SUBJECT DURING NORMAL GAIT ~ APPLICATION OF POINT CLUSTER TECHNIQUE ~

¹Naito K., ²Nagano Y., ²Fukano M., ³Ida H., ⁴Torii S., ¹Nakazawa K., ¹Akai M. and ⁴Fukubayashi T.

¹National Rehabilitation Center for persons with Disabilities, Tokorozawa, Japan
²Graduate School of Sports Sciences, Waseda University, Tokorozawa, Japan
³Human Media Research Center, Kanagawa Institute of Technology, Atsugi, Japan
⁴Faculty of Sports Sciences, Waseda University, Tokorozawa, Japan

INTRODUCTION

Because degenerative change of knee cartilage is closely connected to mechanical stress, exact understanding of knee kinematics and kinetics in weighted environment is very important in treatment of knee osteoarthritis (OA) patients. However, the detailed property of knee kinematics during normal gait in knee OA patients is still unknown. Especially, dynamic kinematics of tibial rotation is unclear because of technical problem, such as marker noise in traditional 3D motion analysis technique. Against this problem, the Point Cluster Technique (PCT) was established as a useful method that allow for description of the *in vivo* knee kinematics of six degrees of freedom without marker noise (Andriacchi TP. et al. 1998). This method might be useful in understanding of the movement of knee OA patients. The purpose of this study was to compare the *in vivo* knee kinematics between knee OA patient and healthy young subject using the PCT.

METHODS

Six healthy young subjects (HY) and 6 knee OA patients (OA) were participated in this study. Subjects of both groups underwent three-dimensional (3D) gait analysis using an eight-camera motion capture system synchronized with three force platforms. They were asked to walk on the 10 m walkway with self-selected speed. The motion and force data were recorded at 200 Hz and 1000 Hz, respectively. For each subject, twenty four reflective markers of 9 mm diameter were secured to the lower limb (Ten markers were the thigh cluster markers, 6 were shank cluster markers, and 8 were bony landmark markers.). The markers were used to implement the PCT. For the calculation of knee joint kinematics of six degrees of freedom, we developed our algorithm of the PCT following the procedure described by Andriacchi et al (1998). In each trial, we calculated the angular displacements (flex/ext, abd/add and int/ext tibial rotation), as well as the translational displacements (A/P, S/I and L/M tibial translation) using the PCT. The reference position for these measurements was obtained from the data of static trial.

RESULTS

The tibial rotation angle of HY group shows acute internal rotation after heel contact. And, after 20 % of stance phase, gradually shift to external rotate position (see Fig. 1 : thin line). This pattern was consistent in most of the HY group. In contrast, although the kinematic pattern of tibial rotation in OA group is similar with HY, the amount of internal rotation immediately after heel contact was small in OA group (see Fig. 1 : thick line). Moreover, the kinematic pattern was not consistent in OA patients as opposed to HY subjects. Remarkable difference between groups was not seen in the other parameters.

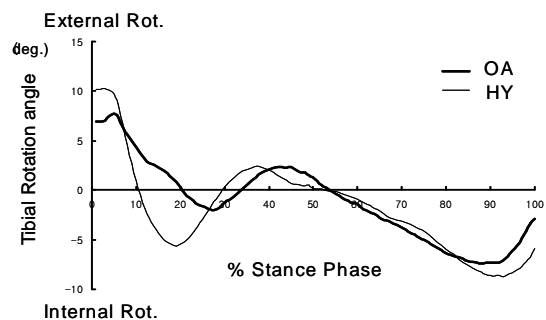


Fig. 1. The tibial rotation angle during stance phase

DISCUSSION

The main finding of this study was difference in motion of tibial rotation between knee OA patients and young healthy subjects. It is relevant to think that the internal rotation after heel contact, seen in HY subjects, which implies natural tibial rotation associated with knee flexion, called screw-home movement. Nevertheless, this natural joint motion was impaired in the OA patients. We speculated that this abnormal motion of tibial rotation in OA patients might be induce additional mechanical stress on knee joint cartilage.

Reference

Andriacchi TP et al. A point cluster method for *in vivo* motion analysis: applied to a study of knee kinematics. J Biomech Eng 1998;120:743-9.

Effect of Lubricin on the Attachment and Proliferation of Tenocytes

¹Sun, Y-L; ¹Zhao, C; ²Jay, G D; ¹An, K-N; ⁺Amadio, P C

¹Mayo Clinic College of Medicine, Rochester, MN, USA, ²Rhode Island Hospital and Brown University, Providence, Rhode Island, USA
Senior Author: pamadio@mayo.edu

INTRODUCTION:

Lubricin, also known as superficial zone protein (SZP) and proteoglycan 4 (PRG4), serves as a boundary lubricant in joints^{1,2}. It also limits the attachment and healing of cartilaginous tissues, and inhibits integrative cartilage repair^{3,4}. Lubricin has also been found in tendon⁵⁻⁷, and shows similar lubricating ability in tendon as it does in joints. The removal of lubricin from the surface of flexor digitorum profundus (FDP) tendons results in increased friction⁸, while the addition of lubricin on the surface of peroneus longus tendon reduces friction⁹. It is unclear, though, whether lubricin is detrimental to the attachment or healing of tendons. The purpose of this study was to investigate the effects of lubricin on the attachment and proliferation of tenocytes in vitro.

METHODS:

Bovine synovial fluid was aspirated percutaneously from the lateral aspect of radiocarpal joints of freshly slaughtered cattle with sterile 18 gauge needles after cleaning the skin with alcohol swabs. The cattle were 1 year old and were of both sexes. Purification of lubricin from synovial fluid was performed as described previously¹⁰.

Tendon cells were harvested from canine FDP tendons for culture using a modification of a collagenase digestion technique described previously¹¹. A 24-well plate was coated with the mixture of 1% hyaluronic acid, 10% gelatin, 1% EDC, and 1% NHS (cd-HA-gelatin). 0.2 ml of saline solution, containing lubricin at a concentration of 0, 10, 25, 50, 100, 250 or 500 µg/ml was then added to the wells, with three wells were used for each concentration. After overnight incubation, the wells were washed with PBS and MEM. 1×10^4 tenocytes were planted in each well and cultured at 37°C with 5% CO₂ for 5 days. The morphology of cells was observed microscopically (Olympus).

RESULTS:

Tenocytes attached and proliferated on wells plated with cd-HA-gelatin and cd-HA-gelatin treated with lubricin at concentrations of 10, 25, 50 and 100 µg/ml. However, tenocytes in the wells treated with lubricin in the concentrations of 250 and especially 500 µg/ml did not attach, but instead assembled into round clusters (Figure 1).

DISCUSSION:

Lubricin has been found in synovial fluid, the superficial zone of articular cartilage, tendons and ligaments^{1,2,5-7,12}. Its concentration in synovial fluid is 200-450 µg/ml^{13,14}. The secreted lubricin in synovial fluid inhibits synovial overgrowth with integrative cartilage repair^{4,15}. Lubricin at a concentration of 250 µg/ml also reduces integrative cartilage repair capacity³. In this study, we found that similar concentrations of lubricin (≥ 250 µg/ml) inhibited the attachment and proliferation of tenocytes.

Articular cartilage, anterior cruciate ligament (ACL) and FDP tendon all exist in an intrasynovial environment. All also encounter difficulty in healing clinically. This study provides evidence that lubricin affects attachment and proliferation of tendon cells, and thus may be a factor affecting tendon healing in a synovial environment. Restricting exposure to lubricin during the healing period could be useful in improving the healing of repaired FDP tendon as well as cartilage and ligament.

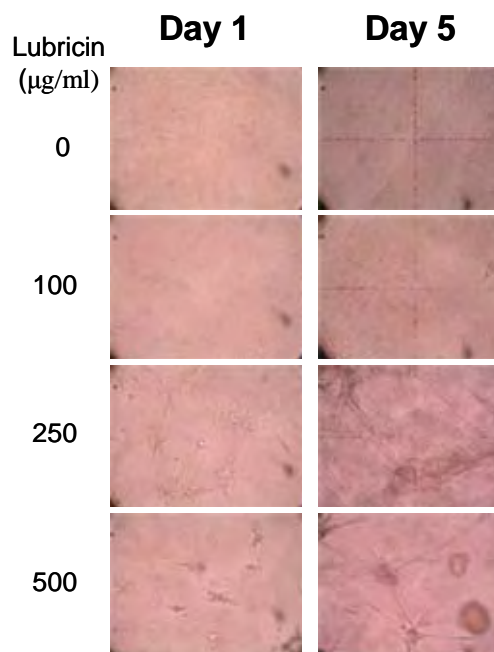


Figure 1. Tenocytes on cd-HA-gelatin, which was coated with lubricin with the concentration of 0, 100, 250 and 500 µg/ml after 1- and 5-day culture.

ACKNOWLEDGEMENTS:

This study was supported by a grant from NIH (AR44391).

REFERENCES:

1. Swann, D. A. et al. *Arthritis Rheum.* **24**, 22-30 (1981).
2. Jay, G. D. *Connect Tissue Res* **28**, 71-88 (1992).
3. Schaefer, D. B. et al. *Biorheology* **41**, 503-8 (2004).
4. Englert, C. et al. *Arthritis Rheum.* **52**, 1091-9 (2005).
5. Rees, S. G. et al. *Matrix Biology* **21**, 593-602 (2002).
6. Sun, Y. L. et al. *J. Orthop. Res.* **24**, 1861-1868 (2006).
7. Funakoshi, T. et al. *J. Bone and Joint Surg.* **90A**, 803-14 (2008).
8. Sun, Y. L. et al. *J. Orthop. Res.* (2008).
9. Taguchi, M. et al. *J. Bone and Joint Surg.* **90A**, 129-135 (2008).
10. Jay, G. D. et al. *J. Rheumatol.* **27**, 594-600 (2000).
11. Banes, A. J. et al. *J. Orthop. Res.* **6**, 83-94 (1988).
12. Sun, Y. L. et al. *Connect Tissue Res* **47**, 215-221 (2006).
13. Elsaid, K. A. et al. *Arthritis Rheum.* **52**, 1746-55 (2005).
14. Nugent-Derfus, G. E. et al. *J. Orthop. Res.* **25**, 1269-76 (2007).
15. Rhee, D. K. et al. *J. Clin. Invest.* **115**, 622-631 (2005).

MECHANICAL FUNCTION OF THE THREE BUNDLES OF THE ANTERIOR CRUCIATE LIGAMENT IN RESPONSE TO EXTERNALLY APPLIED LOADS

Shoji Fukano¹, Hidenori Otsubo², Tomoyuki Suzuki², Konsei Shino³, and Hiromichi Fujie¹

¹Biomechanics Laboratory, Department of Mechanical Engineering, Kogakuin University, Tokyo, Japan

²Sapporo Medical University, Sapporo, Japan

³Osaka University Medical School, Osaka, Japan

INTRODUCTION:

The surgical technique of the anterior cruciate ligament (ACL) reconstruction had been improved in the last decade. However, current reconstruction techniques still neither reproduce normal knee kinematics nor fully restore the functions of the ACL. For more successful clinical results, it is required to obtain the detailed information regarding the normal ACL and to assess reconstruction techniques. For these purposes, a novel robotic system, developed in our laboratory for mechanical testing of human knee joint in multi-degrees of freedom (DOF), was applied to the determination of the forces in the anteromedial, intermediate, and posterolateral bundles in response to anterior force, internal moment, and hyperextension to moment the knee.

METHODS:

A novel robotic system¹⁾, consisted of a 6-DOF manipulator, servo motor controllers, control computer, and a universal force-moment sensor (UFS) was utilized in the present study. A previous test revealed that the clamp-to-clamp stiffness of the system is better than 312 N/mm. The system is controlled by a custom-made PID-hybrid position/force control software on the LabView (version 8.0, National Instruments). It is possible to simultaneously control the both displacement of, and force/moment applied to, the human knee joint in 6-DOF.

Four human cadaveric knee specimen were utilized. With a laser digitization system, the knee joint coordinate system²⁾ was fixed to the knee. Three-dimensional paths of the intact knee in response to the anterior force (up to 100 N), internal moment (up to 5 Nm), and hyperextension moment (up to 5 Nm) to the knee were recorded. Then the ACL was separated to anteromedial (AM), intermediate (IM), and posterolateral (PL) bundles following a previous study³⁾. The cross-sectional area of the IM bundle and AM bundle was approximately 11.3 and 11.5 mm², respectively, which the area of the PL bundle was 15.7 mm². After the AM bundle was transected the 3-D paths of intact knee motion were reproduced. The intact paths were reproduced after the transection of the IM bundle and then the PL bundle. Force data measured with the UFS were used to determine the in-situ forces in the bundles in response to the above-mentioned force/moment applications⁴⁾.

RESULTS & DISCUSSION:

Results revealed that the three bundles have clearly distinguished mechanical functions in response to the applied loads. At hyperextension, the force in the PL bundle was much higher than those in the AM and IM bundles. At full extension, the force in the PL bundle was larger than those in the AM and IM bundles in the anterior drawer test. At 15 and 30 degree of flexion, the force in the PL bundle was decreased while that in the AM bundles were increased. When the flexion angle was larger than 30 degree the force in the AM bundle was slightly decreased while the force in the IM bundle was increased. In response to internal moment, the functions of the three bundles were similar to those in response to anterior force, however, the force in the IM bundle is more important than in response to anterior force.

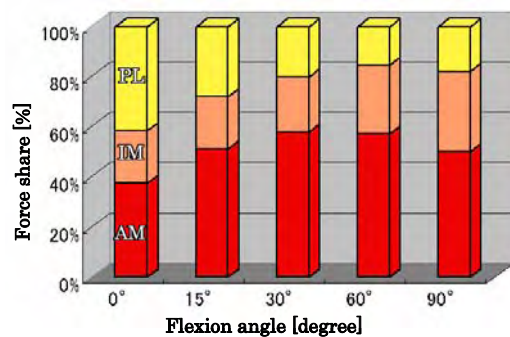


Fig.1: In-situ forces in the three ACL bundles in response to 100 N of anterior force.

REFERENCES:

1) Fujie et al., *JBME* 2004., 2) Grood & Suntay, *JBME* 1983., 3) Norwood and Cross, *AJSM* 1979., 4) Fujie et al., *JBME* 1995.

ACKNOWLEDGMENT:

This study was financially supported by the Grant-In-Aid for Scientific Research (C) (#20591766) from MEXT, and by Biomedical Engineering Research Center, Kogakuin University (2008-2012) (supported in part by the MEXT).

BIOMECHANICAL EVALUATION OF THREE DIFFERENT SUBSCAPULARIS TENDON REPAIRS

Fan Chia Wang, Geoffrey S. Van Thiel, Vincent Wang, Shane Nho, Dana Piasecki, Anthony Romeo
Department of Orthopaedic Surgery, Rush University Medical Center, Chicago, IL, USA

INTRODUCTION

The standard deltopectoral approach for shoulder arthroplasty requires compromise of the subscapularis tendon for insertion of prosthetic components, requiring repair of the tendon back to its insertion at the conclusion of the procedure. Postoperative rupture of this repair is an increasingly recognized postoperative complication, and one that significantly impairs outcomes once it occurs¹. While a number of techniques have been described for repairing the tendon after component insertion^{2, 3}, few studies have tested the biomechanical strengths of these repairs. The purpose of this study was to biomechanically evaluate a combined tendon and bone repair, tendon to bone repair, and a lesser tuberosity osteotomy.

METHODS

Twelve pairs (i.e. 24 total) fresh-frozen cadaver shoulders were dissected down to the capsule. The subscapularis muscle was then elevated off the scapula and the humerus was detached from the glenohumeral joint with the subscapularis intact. Shoulders were randomly divided into three groups; a combined repair, tendon to bone repair, and a lesser tuberosity osteotomy as proposed by Gerber³. Prior to the repair, the humerus was prepared for a press-fit humeral component and the prosthesis was inserted (Aequalis[®] TSR set). The subscapularis muscle belly was then fixed in a freezing clamp and the humerus was fixed in an angled holder. The entire construct was mounted in an MTS (MTS Insight 5, Eden Prairie, MN, USA) machine and positioned in the anatomic plane of the subscapularis pull. Three columns of spatial markers were placed on either side of the repair construct to aid in analysis of cyclic and failure testing with a digital imaging system. Each specimen was preloaded to 10 N for 1 minute to establish initial distance. Cyclic loading testing was between 10 N and 100 N at rate of 0.5 Hz for 150 cycles, followed by a pull to failure test applied at 1 mm/s.

RESULTS

Eighteen specimens have been tested. In the tendon to bone repair group the average bone mineral density (BMD) was 0.70 and the average displacement after 150 cycles was 3.45±2.16 mm with a load to failure of 457±152 N. In the combined group the average BMD was 0.58 with a displacement after 150 cycles of 4.22±2.3 mm and a load to failure of 473±63.6 N. The Gerber technique had an average BMD of 0.57 with a displacement of 3.65±0.72 mm and a load to failure of 567±213 N. ANOVA calculations revealed no significant differences between the groups. Independent T-tests also revealed no significant differences between the paired groups.

DISCUSSION

Shoulder arthroplasty is increasing in prevalence and the contribution of an intact subscapularis tendon to good postoperative results has repeatedly been borne out in the contemporary literature. However, there remains no consensus as to the best way to repair the tendon after it has been mobilized for implantation of the prosthesis. A recent biomechanical study by Ahmad et al² has suggested that a combined method of repair is the most resilient. However, Gerber et al³ has suggested an osteotomy procedure is the best way to repair the tendon. The results from our study do not support one technique over another from a biomechanical standpoint. However, it is noteworthy that the Gerber technique produced cyclic loading results with a substantially lower standard deviation; suggesting that it may be a more reproducible technique. Nonetheless, this study illustrates that biomechanically all constructs are equally robust and the question of durability is more a result of healing potential than construct. Each of these methods represents a different mode of healing. The osteotomy requires bone to bone and the tendon repairs require both tendon to bone and tendon to tendon healing. Perhaps, the small amount of displacement in the osteotomy group is less tolerable than the tendon repair groups due to micromotion leading to a non-union. However, these observations are speculative at this point and require further clinical research.

1. **Miller BS et al.**, *J Shoulder Elbow Surg.* 2005
2. **Ahmad CS et al.**, *J Shoulder Elbow Surg.* 2007
3. **Gerber C et al.**, *J Bone Joint Surg Am.* 2006

**DETERMINATION OF THE MECHANICAL PROPERTY OF THE PATELLAR TENDON
FROM BIGLYCAN KNOCKOUT MICE :
APPLICATION OF A NOVEL ALL-IN-ONE MICRO TENSILE TEST SYSTEM**

Toshifumi Imai¹, Hiroshi Amano², Wataru Ando², Norimasa Nakamura² and Hiromichi Fujie¹

¹ Biomechanics Laboratory, Department of Mechanical Engineering, Kogakuin University, Tokyo, Japan

² Department of Orthopaedic Surgery, Osaka University Medical School, Osaka, Japan

INTRODUCTION:

Tendon proteoglycans (PGs) play important roles for matrix assembly and organization, cell metabolism, and mechanical properties. However, little is known with regard to the effect of the PGs on tendon healing process although it has been determined that the PGs affect the mechanical properties of intact patellar tendon (PT) in knockout mouse studies¹. We have been investigating the significance of specific PG, biglycan (Bgn), which is overexpressed in healing ligament tissues². The objective of the present study was to investigate the mechanical properties of intact and healing tendons from Bgn knockout (BKO) mice.

MATERIAL AND METHOD:

The BKO mice (C57BL/6) were obtained from the NIDR (Dr. M. Young) and were subjected to the experiment at the age of 12 weeks. The midsubstance of the PTs of 2-3 mm in longitudinal length were surgically removed, followed by cage activity for 4 or 8 weeks. The healing PTs and intact PTs (without surgery) were harvested from the mice with patella and tibial bone block. The patella-1/3 healing PT-tibia complex was fixed to a novel all-in-one micro tensile test system developed in our laboratory⁴). In the system, The actuator, load transducer and two clamps were aligned vertically and connected by aluminum alloy plates. The clamps were allowed to rotate about a vertical axis in a range of 180 degrees using a ball bearing connected between the plates. Using this mechanism, the transverse width of the 1/3 PT was measured at every 10 degrees of rotation using a dimension analyzer system with a CCD camera (CV-3500, Keyence, Japan). Reconstruction of the cross-sectional shape and area of the 1/3 PT was performed. After two small gauge markers were adhered to the midsubstance, tensile test was performed for the complex at a rate of 0.01 mm/s soaked in physiological saline solution. Tensile load and strain at midsubstance were measured with a load transducer (LUR-A-50NSA1, Kyowa, Japan) and the dimension analyzer, respectively. The stress-strain relationship of the healing PT was obtained, and the tangent modulus and tensile strength were calculated. For comparison, PTs from normal mice were subjected to the experimental procedure similar to that for BKO mice. All experimental procedures were approved by the Institutional Animal Care and Use Committees of Osaka University Medical School.

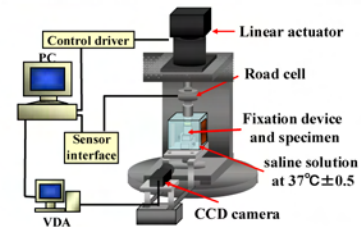


Fig.1: All-in-one micro tensile test system

RESULTS and DISCUSSION:

The stress-strain relationships of the intact PT from BKO mice, and intact and healing PTs from normal mice were indicated in Fig.2. In normal mice, the tangent modulus and strength were very high (189 MPa and 10 MPa, respectively) in intact PTs, but they were decreased to 16 MPa and 2.6 MPa, respectively, in the healing PTs. The result was similar to a finding by Dressler et al that the modulus and strength were decreased in the healing PTs as compared with the intact PTs in the rabbit⁵). In the BKO mice, the modulus was higher than that in the normal mice, while strength was lower than that. Robinson et al reported that the modulus of the intact PT was higher in BKO mice than in normal mice, which was similar to the present study. However, the modulus and strength regarding the intact PTs from normal and BKO mice were much lower in the present study than in their study although we are not sure about the reason for the difference. The modulus and strength of the healing PTs from BKO mice are under investigation, and will be presented at the symposium.

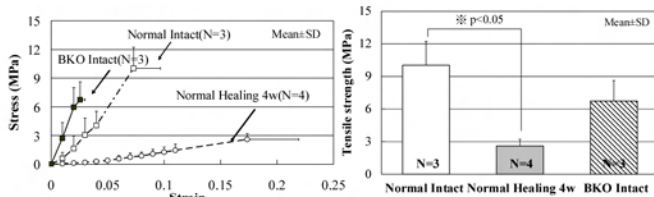


Fig.2: Stress-strain relationship (left) and tensile strength (right) of intact PTs from BKO mice, as compared with those of intact and healing PTs from normal mice

REFERENCES:

- 1) Robinson PS, et al. J Biomech Eng (ASME), 127 (2005), 181-185.
- 2) Boykew R, et al. Matrix Biol, 17 (1998), 371-378.
- 3) Fujie H. et al. Proceedings of the 53rd ORS, 2007.
- 4) Imai T, et al. Proceedings of the 8th ISLT, 2008.
- 5) Dressler MR, et al. J Biomech, 39 (2006), 2205-2212.

MRI of the Posterolateral Corner of the Knee using microscopy coil

H. Ishigooka^{1,4}, T. Sugihara¹, T. Satoh¹, S. Miyamoto¹, Y. Kawana¹, H. Fujiya², K. Kitsukawa³, T. Lee⁴, M. Beppu¹

¹Department of orthopedic surgery, St. Marianna University School of Medicine, Kanagawa, Japan

²Department of Sports Medicine St. Marianna University School of Medicine, Kanagawa, Japan

³Department of Radiology, St. Marianna University School of Medicine, Kawasaki, Kanagawa, Japan

⁴Department of orthopedic surgery, University of California Irvine

INTRODUCTION: Recently, popliteofibular ligament (PFL) is considered to be the most important element of the posterolateral corner (PLC) of the knee. Sufficient manual maneuver in the acute stage, for the diagnosis that the PFL injury is combined with or without the PLC injury, is difficult due to pain. There have been very few detailed studies on the MRI examination for the PLC and the standardized PLC visualized technique also hasn't been established. The purpose of this study is to create visualization that evaluates two methods: the double oblique (DO) and the 3D MRI technique for the PLC.

MATERIALS AND METHODS: There were 18 healthy volunteers (22 knees), consisting of 15 males and 2 females aging from 22 to 54 years old (mean, 33.9 years) used as subjects for the DO method. One fresh frozen cadaveric knee was used for the DO, the 3D MRI and anatomical examination. Imaging was performed using a 1.5T MRI system and a 47 mm in diameter microscopy coil (fig.1). Prescans were taken of the anterior inclination angle of the popliteal tendon (PLT) in the sagittal plane and the rotation angles of the PFL in the axial plane for determining both angles. The final scan of the PFL was done in the same manner as the DO method, and included the connection of the head of fibula to PLT that was performed. The DO method, the 3D MRI was performed using the cadaveric knee PFL was confirmed as well as anatomical result.



and the PFL was to PLT and the Fig.1

Microscopy coil

RESULTS: In this study, visualization of the PFL including the head of the fibula to PLT, by MRI was performed with 95.5% accuracy (21/22) using normal knees (Fig. 2). The average rotation angle in the axial plane of the PFL was rotated 0.3 degrees internally (40 degrees internal to 29 degrees external) (Fig. 3). It took 1/2 the time to visualize the PLC using the 3-D method (Fig. 4, 5). The measured angle of the PFL, using the cadaveric knee, was the same in both the MRI data and the anatomical investigation (Fig. 6)



Fig.2 DO method

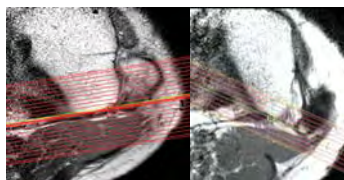


Fig.3 variation of axial rotation

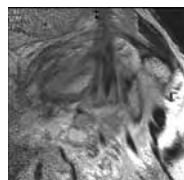


Fig.4 DO method

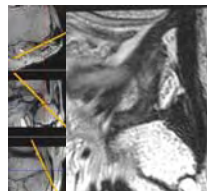


Fig.5 3D MRI



Fig.6 anatomical result

DISCUSSION: There were substantial morphological variations in the angle of the PFL, in the axial plane, among individuals. Therefore, it is difficult to visualize the PFL by the routine MRI method. Since the PFL is thin (about 2.1 mm)¹, imaging using conventional coil for the knee joint is difficult due to limitations in resolution.

Therefore, it is necessary to use microscopy coil with high resolution, for the visualization of this ligament. The scan of the anterior inclination angle and rotation angle to each knee were adjusted and confirmed so that the PFL connection between the PLT musculotendinous junction and the head of the fibula were both visualized simultaneously.

Using the DO method, visualization of the PFL is possible. Using 3D method makes the time of examination shorter. Using a microscopy coil and a 3D MRI makes certain the diagnosis of the PLC, if it is available. If it is not available, the DO method should be used.

REFERENCE 1) Ishigooka. H, Sugihara. T et al. Anatomical study of the popliteofibular ligament and surrounding structures. J Orthop Sci 2004;9(1):51-8.

Rabbit Subscapularis Model for Studying Rotator Cuff Pathology and Repair

Thay Q Lee, PhD

Orthopaedic Biomechanics Laboratory, VA Long Beach Healthcare System, Long Beach, CA and
Department of Orthopaedic Surgery, University of California, Irvine, CA

INTRODUCTION:

Recent studies demonstrated that the rabbit subscapularis tendon complex may serve as a practical model for studying human supraspinatus pathology and repair. This is based on anatomic similarities in bony architecture and proportionate footprint dimensions between the rabbit subscapularis and human supraspinatus tendon, as well as similar histological changes following damage.¹ We further investigated this model for tendon excursion and biomechanical properties of different repair techniques and compared these with previously published human data.²

METHODS:

Tendon Excursion: Nine New Zealand White rabbit shoulders were mounted on a custom testing jig (Figure 1) that permitted muscle loading and glenohumeral flexion/extension to simulate a normal rabbit forelimb range of motion. Each specimen was manually ranged from 20° of flexion to 10° of extension for five cycles and analyzed with a video digitizing system (WINalyze, Mikromak, Berlin, Germany). With the specimen securely mounted, markers were placed on the surface of the coracobrachialis, coracoid process, and subscapular tendon for video digitizing analysis. Tendon excursion was defined as the difference in movement between two markers, one on the lateral subscapular tendon and one on the coracobrachialis in the same horizontal plane. To verify the true tendon excursion, the coracobrachialis muscle was removed and tendon deformation was calculated to ensure the tendon was moving through the tunnel and not simply deforming.

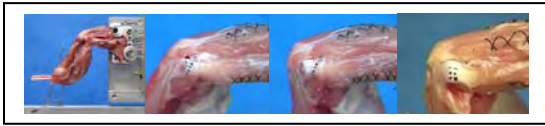


Figure 1: Photographs showing the custom testing jig and rabbit shoulders with the markers for tendon excursion and strain measurements.

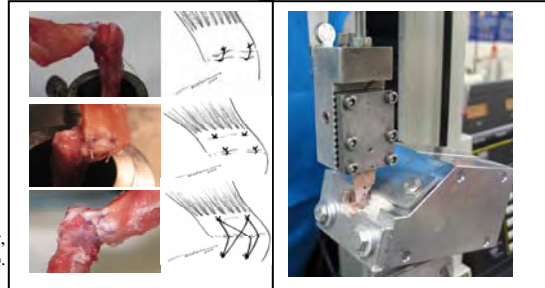


Figure 2: Photographs showing single row repair, double row repair, transosseous equivalent repair and the testing setup.

Tendon Repairs: Biomechanical testing was performed on 21 fresh frozen New Zealand White rabbit subscapularis tendon complexes using an Instron testing system. The specimens were surgically repaired with either a single row repair, double row repair, or transosseous equivalent repair (n=7 for each group). The constructs were subjected to uniaxial tensile loading to failure at a rate of 10 mm/min (Figure 2). WINalyze video digitizing software was used to quantify deformation of the tendon at the repaired footprint.

RESULTS:

Tendon Excursion: Average tendon excursions of the superior and middle rabbit subscapularis tendon were 2.63mm and 2.06mm respectively (p <.05). Post-coracobrachialis resection, average tendon deformation in response to extension along the superior, middle and inferior tendon region was 0.08mm, 0.09mm and 0.03mm respectively and not significantly different from one another (p >.04). Tendon length ranged from 7.24mm to 9.55mm (mean 8.11mm, SD 0.69mm).

Tendon Repairs: A statistically significant difference was noted for the yield (p = 0.02) and ultimate (p = 0.03) loads between the single row and double row groups with double row group showing greater structural properties. However, there were no statistically significant differences in linear stiffness (p = 0.12), deformation at yield load (p = 0.33), deformation at ultimate load (p = 0.50) and energy absorbed to failure (p = 0.07) between the single row and double row groups. The relative ratios of these values were compared to previously published data for the human supraspinatus.² (Table). For double row and transosseous equivalent groups, a statistically significant difference was noted for the ultimate load (p = 0.02), ultimate deformation (p = 0.01) and energy absorbed to failure (p < 0.01) with transosseous equivalent group showing greater structural properties. There were no statistically significant differences in linear stiffness (p = 0.79), yield load (p = 0.17), and deformation at yield (p = 0.19). The relative ratios of these values were compared to previously published data for the human supraspinatus.³ (Table).

Table 1: Ratio of single row (SR) to double row (DR) and double row (DR) to transosseous equivalent (TOE) rotator cuff repair biomechanical properties

	SR / DR Ratio		DR / TOE Ratio	
	Kim et al. ² Human Supraspinatus	Rabbit Subscapularis	Park et al. ³ Human Supraspinatus	Rabbit Subscapularis
Linear Stiffness	0.69	0.68	1.00	1.06
Yield Load	0.72	0.66	0.82	0.82
Ultimate Load	0.68	0.70	0.68	0.72
Energy Absorbed to Failure	0.59	0.67	0.37	0.57

DISCUSSION:

The rabbit subscapularis tendon passes under the tuberculum supraglenoidale and coracobrachialis to insert on the lesser tubercle of the humerus in a manner analogous to the human supraspinatus tendon passing under the coracoacromial arch. In addition, its footprint size and recent findings that the rabbit subscapularis and human supraspinatus undergo similar characteristic patterns of fatty infiltration and atrophy following resection¹ suggest that the rabbit subscapularis is a good model to study rotator cuff pathology and repair strategies. The findings from these subsequent studies demonstrate that the rabbit subscapularis tendon experiences tendon excursion similar to that of the human supraspinatus through their respective bony-ligamentous/muscular tunnels. The findings from this study also demonstrate that complex rotator cuff repair techniques of the human supraspinatus tendon can be simulated in the rabbit subscapularis tendon and the biomechanical properties of these repairs are similar in proportion to previously published human data for supraspinatus tendon repair.

REFERENCES:

1. Gupta, R. and Lee, TQ. *JSES*. 2007; 2. Kim, DH et al. *AJSM*. 2006; 3. Park, MC et al. *JSES*. 2007

ACKNOWLEDGEMENTS:

Ranjan Gupta, MD; Karimdad A Otarodifard; Jeffery E Wong; Charlie Preston, MD; Sam Galle; Kenneth Lee; Pooya Javidan; Tony Lin, MD; Maxwell C Park, MD; James E Tibone, MD; Neal S ElAttrache, MD
VA Rehabilitation Research & Development, VA Medical Research, California Orthopaedic Research Institute, and John C. Griswold Foundation

Mesenchymal stem cells in the bursa subacromialis

- Implications for a rotator cuff repair mechanism

Steinert AF, Stehle J, Rolf O, Jakob F, Nöth U, Gohlke F

University of Wuerzburg, Dep. of Orthopaedic Surgery, Brettreichstr. 11, 97074 Wuerzburg, Germany

PURPOSE

Uthoff and colleagues first described the healing potential of the subacromial bursa in rotator cuff repairs. Although this was confirmed by several other studies, the cellular and molecular mechanism of this finding has not been clarified yet. The purpose of this study was to characterize the cells that are present in subacromial bursa tissue and to evaluate their potential to differentiate into the various mesenchymal lineages compared to marrow-derived mesenchymal stem cells.

MATERIAL AND METHODS

Cells were isolated from 10 bursae subacromiales (BSCs) by collagenase digestion and mesenchymal stromal cells from bone marrow aspirates (BMSCs) were recovered by adherent culture from 10 different donors. Tissues and aspirates were retrieved from patients undergoing rotator cuff repair surgery or total hip arthroplasty after informed consent and local IRB approval. Monolayer cultures of BSCs and BMSCs were analyzed by using cell proliferation assays (cell counts, ATP test), immunohistochemistry, flow cytometry and differentiation into the main mesenchymal lineages (adipogenic, osteogenic, chondrogenic) was induced for three weeks using standard culture conditions.

RESULTS

BSCs and BMSCs appeared adherent and mainly fibroblastic shaped upon light microscopy with BSCs showing elevated cell proliferation rates compared to MSCs. BSCs and revealed similar positive stainings for CD73, 90, 105, 106 and 166 in immunohistochemistry and flow cytometric analyses. Both cell types were negative for CD34, 53, 133 and 144. Following three weeks of differentiation culture, BSCs and BMSCs revealed a strong chondrogenic, adipogenic and osteogenic potential, as shown by the respective histological, immunohistochemical and RT-PCR analyses in contrast to the negative control cultures for both cell types.

CONCLUSION

Our findings indicated that BSCs fulfil the minimal criteria of a mesenchymal stem cell according to the International Society for Cellular Therapy. This knowledge can be harnessed in order use BSCs to improve functional healing of the rotator cuff. Our findings may also help to explain the lower success rates of arthroscopic rotator cuff repairs compared to open techniques with preserved bursa tissue, especially in elderly patients and massive tears.

A BIOMECHANICAL ANALYSIS OF ANTERIOR BANKHART REPAIR WITH CAPSULAR PLICATION USING SUTURE ANCHORS

Rachel M. Frank¹, Geoffrey S. Van Thiel¹, Shane J. Nho¹, Fan Chia Wang¹, Vincent M. Wang¹, Matthew T. Provencher², Augustus D. Mazzocca³, Anthony A. Romeo¹, Nikhil N. Verma¹

¹Department of Orthopaedic Surgery, Rush University Medical Center, Chicago, IL, USA

²Department of Orthopaedic Surgery, Naval Medical Center San Diego, San Diego, CA, USA

³Department of Orthopaedic Surgery, University of Connecticut, Farmington, CT, USA

INTRODUCTION:

There have been a variety of techniques proposed for the arthroscopic repair of anterior Bankart lesions. Fixation to the glenoid with suture anchors is currently the most commonly used technique. However, there remains a paucity of data regarding the strength of many of these anchor constructs. The purpose of this study is to compare the biomechanical properties of commercially available single loaded and knotless suture anchors.

METHODS:

Ten fresh frozen shoulders with a mean age of 54.6 years (range, 48 to 63) were dissected down to the glenohumeral capsule, disarticulated from the humerus, and an anterior Bankart lesion was created. The shoulders were randomly divided into groups using either single loaded suture anchors or knotless suture anchors to achieve capsulolabral plication of the anteroinferior quadrant. Each shoulder was loaded into a Mechanical Testing System (MTS) and the construct was preloaded at 5 N for 1 minute and then loaded to failure at 25 mm/min (48 Hz). Two markers were placed 1 cm apart on the glenoid and capsule tissue, and optical tracking was measured via Digital Motion Analysis System (DMAS) software to determine the amount of displacement of the capsule from the fixed glenoid.

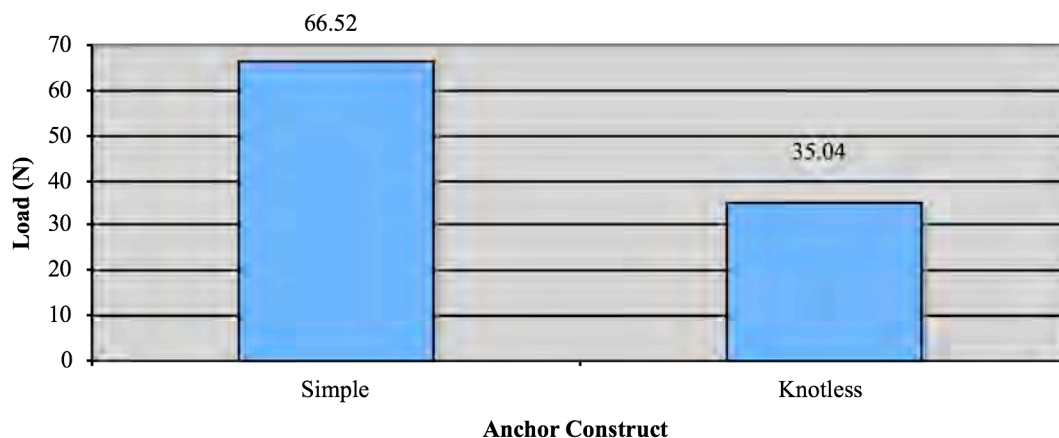
RESULTS:

There was no statistical difference in ultimate load to failure between the single loaded suture anchor group (173.1 ± 45.3 N) and the knotless suture anchor group (167.9 ± 42.3 N). The single loaded suture group experienced significantly greater load at 2 mm displacement (66.5 ± 21.7 N) compared to the knotless suture anchor group (35.04 ± 12.5 N; $P = 0.04$). In the single loaded suture anchor group, suture failure caused 3 failures (60%) while anchor failure accounted for 2 (40%). In the knotless suture anchor group, suture failure caused 4 failures (80%) while the anchors failed in 1 case (20%).

DISCUSSION:

The ultimate strength of anterior Bankart repair constructs is similar among single loaded suture anchors and knotless suture anchors. However, knotless suture anchors provide a significantly weaker repair than single loaded suture anchors at 2 mm of displacement, an amount often considered to cause clinical failure. Repair of anterior shoulder instability due to Bankart lesions may be more stable when single loaded suture anchors are used as opposed to knotless suture anchors.

Table 1. Average Load at 2 mm Displacement (p = 0.04)



SHOULDER ROTATIONAL PROPERTIES OF THROWING ATHELETES WITH AND WITHOUT ARM INJURY HISTORY

N. Zheng¹ and K. Eaton²

¹University of North Carolina at Charlotte, NC

²Tampa Bay Rays, Tampa, FL

INTRODUCTION

Shoulder pain is a frequent phenomenon among baseball pitchers, regardless of age or level of play. Pain experienced during throwing results in an inability to throw with velocity, causing a dead arm syndrome. The cause of pain and injury may be due to overuse of the pitching arm, inadequate rest and poor pitching mechanics. Shoulder rotational laxity is often checked and compared bilaterally. However, current exam may not be adequate to catch any signs of potential injuries. Computer assisted exam may provide us more detailed and quantitative shoulder rotational properties. The purpose of this study is to compare differences of shoulder rotational properties, measured during computer assisted exams, of throwing athletes with and without arm injury history.

METHODS

One hundred baseball pitchers from professional and collegiate teams were recruited for the study. After having signed IRB approved consents and filled out injury questionnaires, they were examined using a custom-made wireless device. The wireless system was calibrated and validated with errors less than 1° for orientation and 1 N for force measurement. The arm orientation and force applied during testing were recorded at 100 Hz. Subjects were tested on both shoulders in external and internal rotations (Fig. 1). Five trials were collected for each condition and a total of 20 trials were collected from each subject. A 15-second pause was taken between trials. The resistance onset angle (ROA) and end-point angle (EPA) were determined when the rotational force applied reached 2 N and 40 N, respectively (Fig. 2). Both free range of motion (fROM) and end range of motion (eROM) were determined. The shoulder rotational flexibility (SRF) was determined as the amount of rotation caused by a unit rotational torque. The rotational torque was calculated using the forearm mass, length, orientation and the force applied. Bilateral differences were compared among three groups (players without injury history, with surgery history and with injury history but no surgery) using multivariate analysis with alpha set at 0.05 (SPSS, Chicago, IL).



Fig. 1 Shoulder rotational tests (a) external, (b) internal, (c) shoulder rotational angle in degrees (top) and applied force in N (bottom).

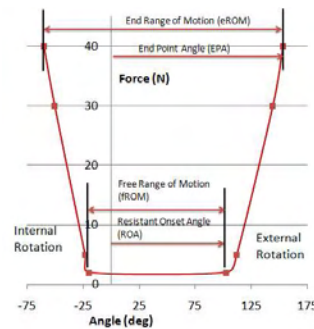


Fig. 2 Variables of shoulder rotational properties.

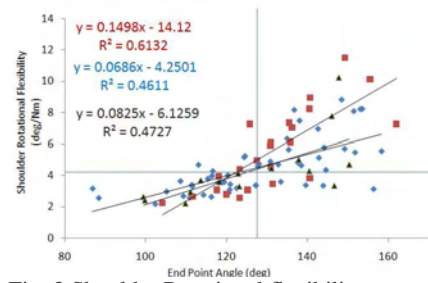


Fig. 3 Shoulder Rotational flexibility vs. EPA in uninjured (♦), injured with surgery (■) without surgery (▲).

RESULTS AND DISCUSSION

All subjects filled out injury questionnaires. Ten were injured at the time of test and did not participate in the laxity test. Twenty three had surgeries performed on their throwing arm. Fifteen had throwing arm injuries in the past year but did not have surgery. The dominant arm had significantly lower internal ROA ($p=.000$), internal EPA ($p=.000$) and internal SRF ($p=.003$), but significantly higher external ROA ($p=.000$), external EPA ($p=.000$) and external SRF ($p=.002$) than the non-dominant arm. There were no significant differences in fROM and eROM between the dominant and non-dominant arms. For the throwing arm, subjects with greater EPA had greater SRF (Fig. 3). Although not significant ($p=0.09$) the injured group had greater external SRF of the throwing arm ($1.02 \pm 0.5^\circ/\text{Nm}$). No significant differences were found among three groups for the throwing arm. However, when the bilateral differences were compared, the players with surgery history had greater bilateral differences in fROM ($11 \pm 4^\circ$, $p=0.02$) and eROM ($7.5 \pm 3^\circ$, $p=0.06$) than the players without injury history. Posterior contracture is related to the internal rotation deficit of the throwing arm. Greater external SRF may be related to throwing arm injuries, both on the elbow and shoulder. Findings of this study may lead us to effective preventive measures of throwing arm injuries.

Acknowledgement: This study is funded by a Clinical Research Grant from the Major League Baseball.

EFFECT OF INTERNAL ROTATOR MUSCLES ON SHOULDER INTERNAL IMPINGEMENT:
A CADAVERIC STUDY

Teruhisa Mihata^{***}, Bong Jae Jun^{*}, Yu-Jen Chen^{*}, Michelle H. McGarry^{*}, Samuel E Galle^{*}, Mitsuo Kinoshita^{**},
Thay Q Lee^{*}

^{*}Orthopaedic Biomechanics Laboratory, VA Long Beach Healthcare System and UC Irvine

^{**}Department of Orthopaedic Surgery, Shoulder&Elbow Biomechanics Laboratory, Osaka Medical College, Japan

INTRODUCTION

Shoulder internal impingement is described as a contact between the undersurfaces of the supraspinatus and infraspinatus tendons with the greater tuberosity, superior labrum, and glenoid rim. In some overhead-throwing athletes, this repetitive and forceful contact in the late cocking phase of the throwing motion leads to articular-side partial thickness rotator cuff tears and superior labral lesions. Several studies have reported that external-to-internal rotator muscle force ratios are lower in a baseball player’s dominant extremity than in the non-dominant extremity. This lower ratio on the dominant side results from an increased strength in internal rotation without concomitant increase in external rotation strength. In addition, an electromyographic study showed that in throwing athletes those with shoulder pain elicited at the apprehension position had decreased activity of the subscapularis and pectoralis major muscles in the late cocking phase of throwing. Therefore, we hypothesized that changes in the internal rotator muscle force have a strong influence on the magnitude of forceful internal impingement in the late cocking position. The objective was to quantify the effects of internal rotator muscle force on glenohumeral contact pressures and the internal impingement area.

METHODS

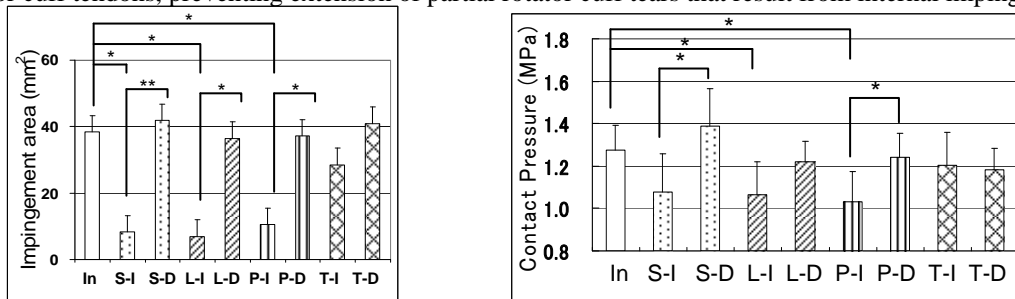
Seven fresh frozen cadaveric shoulders were tested in the simulated late cocking position, with loading of deltoid, pectoralis major, latissimus dorsi, teres major, and all rotator cuff muscles. Glenohumeral contact pressure at maximum external rotation position were measured using Tekscan. The location of the rotator cuff insertion on the greater tuberosity relative to the glenoid was digitized and tracked. The area of overlap between this insertion and the glenoid represented the area of internal impingement. The impinged area was then reconstructed and calculated with Rhinoceros software program. Muscle forces were determined from previous published studies using the maximum muscle potential force from the physiological cross-sectional area of each muscle and shoulder muscle activity during throwing. To assess the effect of internal rotator muscles, all data were compared among conditions with increased and decreased muscle force of the subscapularis, pectoralis major, latissimus dorsi, and teres major. Data were analyzed using Fisher’s post hoc test ($p < 0.05$).

RESULTS

The impinged area was significantly increased with decreased force of the subscapularis ($P < 0.01$), pectoralis major ($P < 0.05$), and latissimus dorsi ($P < 0.05$). Glenohumeral contact pressure was significantly increased with decreased subscapularis muscle force ($P < 0.01$) and with decreased pectoralis major muscle force ($P < 0.05$). The changes in glenohumeral contact pressure and impingement area between decreased and increased muscle forces among all the internal rotator muscles were the largest for the subscapularis.

DISCUSSION

Internal impingement area and glenohumeral contact pressure increased significantly with decreased force of internal rotator muscles of the shoulder joint. Of the internal rotator muscles, the subscapularis may be the most influential in shoulder internal impingement. These results suggested that strengthening of the internal rotator muscles, especially the subscapularis, may prevent forceful internal impingement; it may therefore also protect the rotator cuff tendons, preventing extension of partial rotator cuff tears that result from internal impingement.



Left: Internal impingement area. Right: Glenohumeral contact pressure. In: initial, S-I and S-D: subscapularis increased and decreased, L-I and L-D: Latissimus dorsi increased and decreased, P-I and P-D: Pectoralis major increased and decreased, T-I and T-D: Teres major increased and decreased. * $p < 0.05$

NANOFIBER COMPOSITE FOR TENDON-TO-BONE INTERFACE TISSUE ENGINEERING

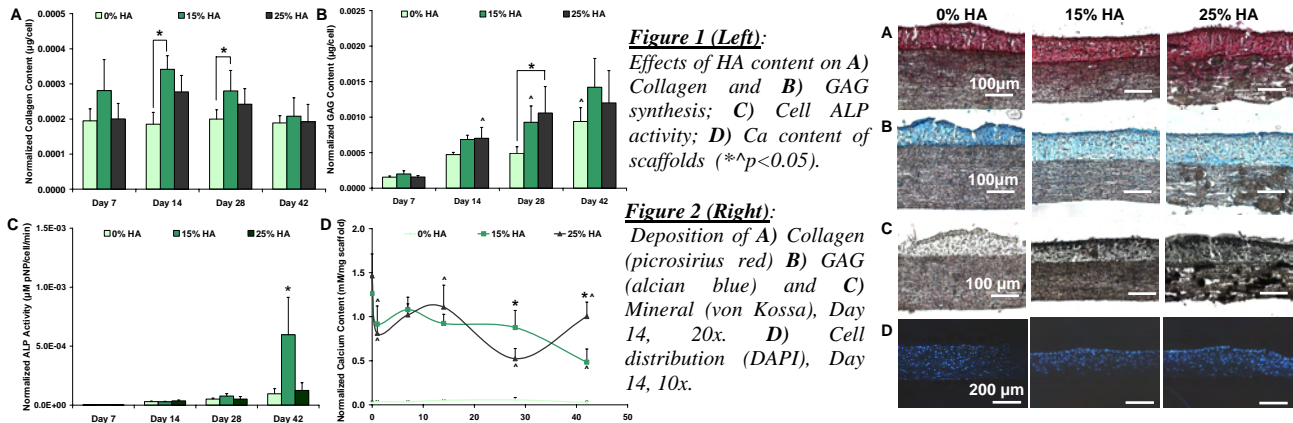
¹K. L. Moffat, ¹Y. Kim, ¹S. D. Subramony, ²S. B. Doty, and ¹H. H. Lu

¹Department of Biomedical Engineering, Columbia University; ²Hospital for Special Surgery, New York, NY

INTRODUCTION: Injuries to the rotator cuff tendons often occur at the tendon-to-bone insertion site[1], which consists of a continuous fibrocartilaginous transition divided into non-calcified and calcified regions containing chondrocyte-like cells[2-6]. Regeneration of this interface is a prerequisite for the biological fixation of tendon grafts. Our approach to tendon-bone integration focuses on the design of biomimetic nanofiber-based scaffolds that will enable interface regeneration and promote osteointegration. The **objective of this study** is to evaluate the effects of hydroxyapatite (HA) nanoparticle content on chondrocyte differentiation on composite nanofiber scaffolds of poly(lactide-co-glycolide) (PLGA) and HA (PLGA-HA). It is hypothesized that nanofiber HA content will regulate chondrocyte biosynthesis and mineralization.

METHODS: *Scaffold Fabrication:* Aligned nanofiber scaffolds of PLGA (85:15, Lakeshore) and HA nanoparticles (Nanocerox) with varying HA content (0-25% w/w) were formed via electrospinning[7,8]. *Cells & Cell Culture:* Full-thickness articular chondrocytes from the tibial plateau of neonatal bovine were enzymatically digested, seeded on scaffolds at a density of 3.14×10^4 cells/cm², and cultured in ITS media+10% FBS. *End-Point Analyses (1, 7, 14, 28, & 42 days):* Cell penetration into the scaffold was evaluated by DAPI stain (n=2). Cell growth (n=5) was assessed by a total DNA assay. Glycosaminoglycan (GAG) and collagen deposition were evaluated by histology (n=2) and quantified by DMMB and Sircol assay (n=5), respectively. Alkaline phosphatase (ALP) activity (n=5) was determined by a colorimetric assay and scaffold Ca content (n=5) was quantified by an alizarin red assay.

RESULTS: *Cell Growth and Biosynthesis:* Chondrocytes proliferated and deposited a matrix rich in both collagen and GAG on all scaffolds tested (Figs. 1,2). Scaffold GAG content significantly increased over time and chondrocytes on PLGA-HA (25%) synthesized significantly more proteoglycan than those on 0% HA scaffolds (Fig. 1B). Similarly, collagen production was significantly greater on the PLGA-HA (15%) scaffolds compared to PLGA (0%, Fig. 1A). These observations were confirmed by histology, which also revealed enhanced matrix deposition penetrating the depth of the scaffold with increasing HA content (Fig. 2). *Mineralization:* While chondrocyte ALP activity was the highest at day 42 on the 15% HA scaffolds (Fig. 1C), a significant increase in Ca content was detected on 25% HA scaffolds on both days 14 and day 42 (Fig. 1D). In contrast, Ca content of the 15% HA scaffolds decreased significantly over time. Mineral deposition is confirmed by von Kossa staining (Fig. 2C).



DISCUSSION AND CONCLUSIONS: These findings demonstrate that the incorporation of HA in PLGA nanofibers result in significant changes in chondrocyte biosynthesis and mineralization. Proteoglycan and collagen deposition increased on the PLGA-HA scaffolds. As such, these differences were not modulated by increasing mineral content. In contrast, HA content modulated chondrocyte mineralization, with significant cell-mediated mineralization observed on the 25% HA scaffolds compared to the 15% HA and 0% HA control. Scaffold degradation is also modulated by HA content. In summary, these results show that PLGA-HA nanofibers promote chondrocyte-mediated formation of a mineralized proteoglycan- and collagen-rich matrix. Future studies will evaluate the potential of this calcified fibrocartilage-like matrix in promoting tendon-to-bone integration *in vivo*.

REFERENCES: [1]Iannotti *et al.*, 1994; [2]Woo *et al.*, 1987; [3]Benjamin and Ralphs, 1998; [4]Cooper and Misol, 1970; [5]Kumagai *et al.*, 1994; [6]Thomopoulos *et al.*, 2003; [7]Reneker and Chun, 1996; [8]Moffat *et al.*, 2008.

ACKNOWLEDGEMENTS: NIH/NIAMS R21-AR056459 (HHL); R01-AR055280 (HHL)

THE INFLUENCE OF ALIGNED POLY(ϵ)CAPROLACTONE NANOFIBRE MESHES ON THE GENE EXPRESSION AND CELLULAR ORIENTATION OF TENDON FIBROBLASTS

S.E. Taylor¹, L. Bosworth², A. Vaughan-Thomas¹, S. Downes², R.K.W. Smith³ and P.D.Clegg¹

¹Veterinary Clinical Sciences, University of Liverpool, Leahurst, South Wirral., ²Biomaterial Science, University of Manchester, Manchester. ³Royal Veterinary College, University of London, Hawkshead, Hertfordshire.

INTRODUCTION: Tendon has a poor intrinsic repair capacity therefore tissue engineering approaches are being studied to improve the functional repair of this tissue. Electrospinning of synthetic polymers allows the fabrication of fibres with a diameter < 1 μ m (nanofibres). The diameter and orientation of these fibres can be varied by changing the type of polymer solution and the collecting plate respectively (1). This work aimed to identify whether (a) tendon fibroblasts (TF) retain viability and proliferate on poly(ϵ)caprolactone (PCL) nanofibre meshes (b) cellular orientation was influenced by nanofibre alignment and (c) differential changes in gene expression occur in response to aligned and randomly orientated scaffolds.

MATERIALS & METHODS: The superficial digital flexor tendon (SDFT) was collected from horses subjected to euthanasia for non-orthopaedic disease. A 1cm³ section of tissue taken from the mid-metacarpal SDFT was subjected to overnight collagenase digestion (0.1%). TF were plated at 5000 cells/cm² and grown to confluence in DMEM containing 10% FCS, penicillin/streptomycin and amphotericin. Cells were released from flasks with 0.05% trypsin EDTA and seeded at 0.5 x 10⁵ cells per scaffold. PCL nanofibre meshes were fabricated through electrospinning to form random meshes, aligned meshes and bundles. All scaffolds were anchored within low binding 6 well plates using ScaffoldexTM inserts and soaked in 10% DMEM 24 hours prior to cellular seeding. Cells were grown on the different scaffolds for 14 days changing the media every 3-4 days. Samples were collected at three time points (1 day, 5 days and 14 days) to allow calculation of cellular proliferation (picoGreen DNA assay) and to evaluate gene expression (qPCR) and cellular morphology (scanning electron microscopy-SEM).

RESULTS: TF remained viable and proliferated on both random and aligned PCL nanofibre meshes as well as on PCL nanofibre bundles. Whilst cell proliferation was slowest on the bundles in the first 5 days, by 14 days the bundles demonstrated the highest level of cell proliferation of any construct. TF grown on randomly orientated PCL nanofibres spread and showed no orientation whereas TF grown on aligned PCL meshes tended to orientate along the axis of the PCL nanofibre with an elongated morphology (Figure 1). Expression levels of COL1A2, COL3A1 and COL5A1 were greatest on aligned nanofibre meshes (Figure 2). Biglycan and decorin expression were greatest on the aligned PCL nanofibres but tenascin-C expression was greatest on the bundles of PCL nanofibres.

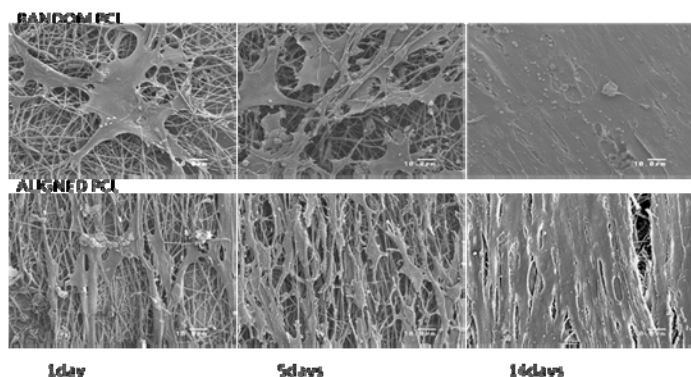


Figure 1: SEM images of cells on random and aligned nanofibre scaffolds.

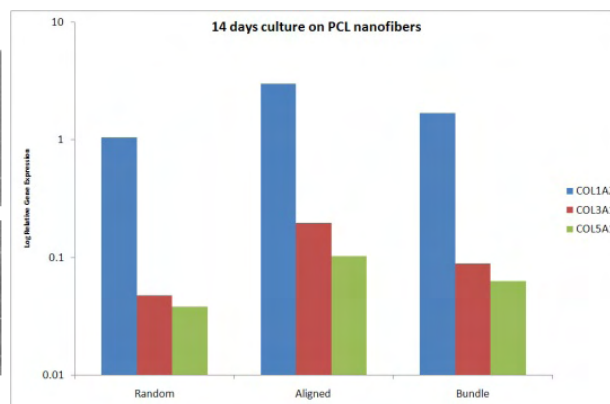


Figure 2: Collagen gene expression.

DISCUSSION AND CONCLUSIONS: This work demonstrates that TF are able to survive and proliferate on PCL nanofibre scaffolds. Additionally cellular orientation can be manipulated to achieve an elongated fibroblastic appearance similar to that found in natural tendon tissue by using aligned nanofibrous scaffolds. Increased collagen type-I expression has been identified previously when bone marrow derived stromal cells were cultured on randomly orientated PLGA (2). This work demonstrates that COL1A2 expression can be further increased by manipulating the orientation of the nanofibres. Future work will focus on determining the mechanical properties of cell seeded scaffolds to determine if PCL nanofibres are able to provide the functional support and necessary stimuli to promote tendon regeneration.

REFERENCES:

1. Kumbar, S.G., James, R., Nukavarapu, S.P., and Laurencin, C.T. Electrospun nanofiber scaffolds: engineering soft tissues. *Biomed Mater* 3, 034002, 2008.
2. Sahoo, S., Ouyang, H., Goh, J.C., Tay, T.E., and Toh, S.L. Characterization of a novel polymeric scaffold for potential application in tendon/ligament tissue engineering. *Tissue Eng* 12, 91, 2006.

ACKNOWLEDGEMENTS: S. E. Taylor is funded by the Horserace Betting Levy Board and L. Bosworth is funded by the EPSRC.

In vivo study of ACL regeneration using silk scaffolds in a pig model

Haifeng Liu¹, Hongbin Fan¹, Siew Lok Toh^{2,3}, James C.H. Goh^{1,2*}

1. Department of Orthopedic Surgery, National University of Singapore, Singapore

2. Division of Bioengineering, National University of Singapore, Singapore

3. Department of Mechanical Engineering, National University of Singapore, Singapore

Although most in vitro studies indicate that silk is a suitable biomaterial for ligament tissue engineering, in vivo studies of implanted silk scaffolds for ligament reconstruction are still lacking, especially in a big animal. The objective of this study is to investigate anterior cruciate ligament (ACL) regeneration using mesenchymal stem cells (MSCs) and silk scaffold in a pig model. The scaffold was fabricated by incorporating microporous silk sponges into knitted silk mesh, which mimicked the structures of ligament extracellular matrix (ECM). In vitro culture already demonstrated that MSCs on scaffolds proliferated vigorously and produced abundant collagen. The MSCs/scaffold was implanted to regenerate ACL in a pig model. After 24 weeks, histology observation showed that MSCs were distributed throughout the regenerated ligament and exhibited fibroblast morphology. The key ligament ECM components including collagen I, collagen III, and tenascin-C were produced prominently. The tensile strength of regenerated ligament also met the mechanical requirements. In conclusion, the results imply that silk scaffold has great potentials in future clinical applications.

NOVEL 3D TENSILE CULTURE SYSTEM FOR LIGAMENT TISSUE ENGINEERING WITH MESENCHYMAL STEM CELLS

D.M. Doroski¹, M.E. Levenston², and J.S. Temenoff¹

¹Coulter Department of Biomedical Engineering, Georgia Tech and Emory University, Atlanta, GA, USA

²Department of Mechanical Engineering, Stanford University, Stanford, CA, USA

INTRODUCTION

Tensile strain has been employed to stimulate differentiation of mesenchymal stem cells (MSCs) toward a ligament fibroblast phenotype [1], and thus may be an important part of tissue engineering approaches for ligament regeneration. We have developed a strain-controlled, tensile culture bioreactor to study the effects of mechanical stimulation on MSCs encapsulated in a well-defined 3D environment consisting of our novel oligo(poly(ethylene glycol) fumarate (OPF) hydrogels. This study was designed to determine if a hydrogel environment presenting tethered adhesive RGD ligands would promote long-term cell viability, and to examine effects of static 5% strain on MSCs embedded in these 3D constructs compared to MSCs cultured in two dimensions over 1 week in vitro.

METHODS

OPF with a poly(ethylene glycol) chain of molecular weight 3KDa was combined (1:1 wt/wt) with poly(ethylene glycol) diacrylate (nominal M_n 3,400) and 1.14 μmol GRGDS adhesion peptide/g swollen hydrogel. Polymers were cross-linked (thin disks: 7mm dia, 0.7 mm thick) using N,N,N',N'-tetramethylethylenediamine and ammonium persulfate thermal radical initiators (0.018M, 10min, 37°C) with human MSCs (hMSCs, Lonza) encapsulated at 10E6 cells/ml (control: no cells). At 1, 3, 7, 14, and 21d hydrogels were stained with LIVE/DEAD (molecular probes) to image viability. Additional constructs (12.5x9.5x1.6mm thick) of the same seeding density were cultured at 5% strain in our tensile culture system, and analyzed at 1, 3, and 7d. The PicoGreen assay ($n \geq 3$) was used to find double stranded DNA content, which can be correlated to cell number, and the hydroxyproline assay ($n \geq 3$) was used to measure hydroxyproline, which can be used to estimate collagen content. Results were normalized to day 1 and compared to data from hMSCs plated for the same time period on 6-well plates. Significance was determined using ANOVA followed by Tukey's Multiple Comparison Test ($p \leq 0.05$).

RESULTS

LIVE/DEAD images revealed green staining indicating a majority of live cells after 3 weeks of culture (Fig. 1). OPF hydrogels with encapsulated hMSCs held under 5% strain maintained DNA content over 7 days (Fig. 2), while hMSCs plated on tissue culture polystyrene showed a statistically significant increase in DNA content after seven days of culture (Fig. 2). The hydroxyproline assay did not demonstrate any significant increase over 7 days in either the strained 3D constructs or on 2D surfaces (Fig. 3).

DISCUSSION

Conservation of DNA content in 5% strain constructs suggests that cell numbers in the constructs was relatively constant. In conjunction with the positive viability results seen in the LIVE/DEAD assays through 3 weeks of culture, this indicates that hMSCs grown in our constructs maintain cell numbers while remaining viable over multiple weeks of culture. Although the hydroxyproline assay showed only a small amount of collagen produced in the 3D constructs, this may be due to the assay's early timepoints. While further work, particularly in the area of dynamic culture, remains to be completed, these preliminary studies demonstrate the utility of this tensile bioreactor/hydrogel construct system for studying the effects of combinations of biomechanical and biochemical stimuli on MSC differentiation for ligament tissue engineering applications.

REFERENCES

[1] Altman, G., et al., *Cell differentiation by mechanical stress*. FASEB J, 2002. **16**(2): p. 270-2.

ACKNOWLEDGEMENTS

Arthritis Foundation Investigator Award (JST); NIH R21 EB8918-1

Fig. 1: LIVE/DEAD staining of hMSCs encapsulated in OPF hydrogels after three weeks of culture (10e6 cells/ml). Scale bar = 100 μm . A majority of cells stained green indicating live cells

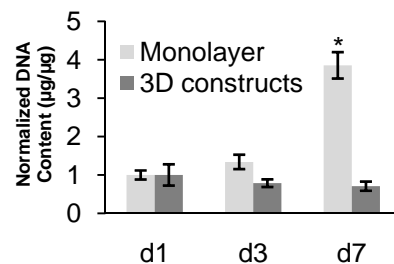
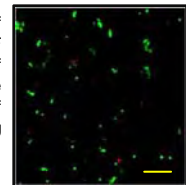


Fig. 2: PicoGreen assay (DNA content) of hMSCs in monolayer and 3D constructs ($n \geq 3 \pm \text{SD}$, * $p < 0.05$ compared to d1).

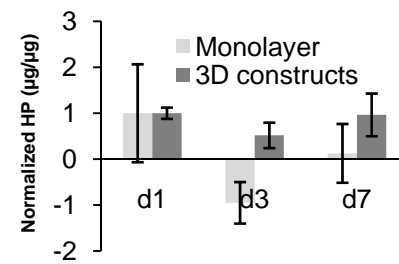


Fig. 3: Hydroxyproline assay (collagen content) of hMSCs in monolayer and 3D constructs ($n \geq 3 \pm \text{SD}$, * $p < 0.05$ compared to d1).

Cyclic tensioning culture strengthens a stem cell-based self-assembled tissue (scSAT) derived from synovium

*Saito K., *Ogawa A., **Ando W., **Nakamura N., and +*Fujie H.

+*Biomechanics Laboratory, Department of Mechanical Engineering, Kogakuin University, Tokyo, Japan

** Department of Orthopaedic Surgery, Osaka University Medical School, Osaka, Japan

INTRODUCTION:

It is well known that various fibrous tissues such as tendons and ligaments functionally adapt to dynamic and static loads. Although a variety of biomechanical studies have been done so far to determine the mechanism of remodelling in fibrous tissues, it was difficult to obtain detailed information because of complicated constitution of the tissues. Meanwhile we have developed a stem cell-based self-assembled tissue (scSAT) for tissue engineering. Since the scSAT is consisted of synovium-derived mesenchymal stem cells (MSCs) and their native extracellular matrix, it is a good experimental model to determine the process of remodelling of fibrous tissues. Therefore, the effects of cyclic tensioning and its duration on the mechanical property of the scSAT were investigated in the present study.

MATERIALS AND METHODS:

Stromal cells obtained from the synovial membranes of human knee joints were cultured in DMEM in monolayer. After the cell density reached to 4.0×10^5 cells/cm², 0.2 mM of ascorbic acid 2-phosphate was injected to promote the biosynthesis of extracellular matrix. Thirty five days after the injection, synthesized matrices were carefully detached from culture plate and then cultured for 1 hour to develop scSATs¹⁾. Then the scSATs were subjected to cyclic tension with the range of 4.0-8.0 mN was applied to the scSAT for 1 or 3 days in DMEM using a cyclic tensioning apparatus²⁾ in an incubator at 37 °C (loaded groups). In each day, the load was applied to the scSAT for 1 hour followed by an unloaded condition for 23 hours. In addition, the scSAT specimens were cultured with no load for 3 days in an incubator (control group). The scSATs were then subjected to a tensile testing at a rate of 0.05 mm/s in PBS at 37 °C using a custom-made micro tensile tester²⁾. Morphological observation of the surface of the scSATs was performed using a scanning electron microscope (VE-8800, KEYENCE).

RESULTS and DISCUSSION:

Scanning electron microscopic observation indicated that the loaded scSATs exhibited fibrous structures oriented to the loading direction (Figure 1). All the relationships between stress and strain exhibited J-shaped curves, although they were almost linear in high strain region in the 3 day loaded group. Tangent modulus in 5-10% of strain and tensile strength were indicated in Fig.2. In the 1 day loaded group, the modulus became significantly higher but the strength was almost same as compared with the non-loaded control group. In contrast, in the 3 day loaded group, the modulus was almost same but the strength became significantly higher as compared with the non-loaded control group. It was suggested that, in the 1 day loaded group, the collagen-like fibrous structure in the scSAT was re-organized so that the fiber was aligned parallel to tensioning direction. This may be the reason for higher modulus but similar strength as compared with the non-loaded control group. However, in the 3 day loaded group, the modulus was similar but the strength was significantly higher as compared with the non-loaded control group. It is suggested that not only structural re-organization but also some bio-synthesis or crosslink of collagen fibers were occurred in response to the applied 3 day cyclic tensioning. In conclusion, the obtained results imply that the remodelling phenomenon possibly occurs in a simple tissue constitution composed of cells having differentiation ability and their native extracellular matrix. The cyclic tensioning of 4-8 mN (5-10 kPa) with approximately 16-22% strain for 1 hour a day for total 3 days significantly increases the strength of the scSAT.

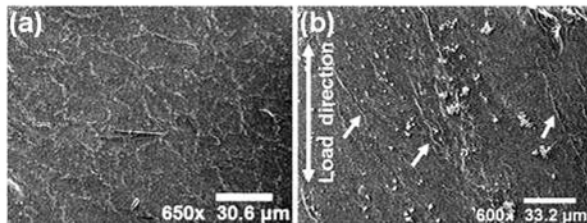


Fig.1. Scanning electron microscope observation of the non-loaded control (a) and the 3 day loaded scSATs (b).

REFERENCES:

- 1) Ando W. et al. Proceedings of the 52st ORS, 2006.
- 2) Kumagai K. et al. Proceedings of the 8th ISLT, 2008.

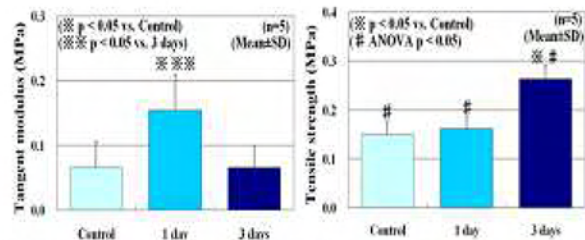


Fig.2. Tangent modulus (left) and tensile strength (right) of the loaded and control scSATs

ACKNOWLEDGMENT

The present study was financially supported in part by the Research Project from the Ministry of Education, Science, Culture and Technology, Japan (BERC, Kogakuin University)

EFFECT OF NATIVE LIGAMENT EXTRACELLULAR MATRIX ON HUMAN ADIPOSE STEM CELLS

Little, D.¹, Blount, A.N.², Guilak, F.^{1,2}, Ruch, D.S.¹

¹Division of Orthopaedic Surgery, Department of Surgery, ²Department of Biomedical Engineering, Duke University, Durham, NC, USA

INTRODUCTION:

Current surgical methods for repair of the anterior cruciate ligament (ACL) do not provide long term benefit in prevention of osteoarthritis. Furthermore, up to 10% of reconstructions fail in the short term due to factors such as failure of re-cellularization and ligamentization, stress shielding and mechanical insufficiency. Extracellular matrix scaffolds from a variety of sources have been used to supplement tendon and ligament repair but provide inadequate mechanical stability during healing. Use of a tissue engineered scaffold seeded with autologous adipose-derived stem cells (hASCs) is an appealing strategy; however the challenge remains to facilitate cellular differentiation, proliferation and matrix synthesis before the underlying scaffold loses mechanical strength and fails. *We hypothesize that* the extracellular matrix of native ligament has will enhance the differentiation and proliferation of hASCs. *The objective of this study* was to evaluate lyophilized porcine ACL powder prepared in two different ways for its ability to induce proliferation, differentiation and matrix synthesis in hASCs seeded in collagen gel.

METHODS:

Porcine ACL from mature female pigs was minced then pulverized. The pulverized tissue was stirred in either phosphate buffered saline pH7.4 (PBS) or 0.1% peracetic acid (PA) overnight at 4°C then frozen and lyophilized. The lyophilized ACL was pulverized, and the powder sterilized before use. hASCs from 3 female donors were seeded at a density of 1×10^6 /ml in Type I Rat Tail Collagen (2mg/ml) \pm PBS or PA treated ACL powder (25mg/ml) and scaffolds were maintained in culture. Cell-seeded and unseeded scaffolds were harvested at Day 0,7,14 and 28 for assessment of double-stranded DNA (dsDNA), sulfated glycosaminoglycans (sGAG), collagen content and gene expression. Data were analyzed using analysis of variance (ANOVA). Fisher's least significant difference test was used to determine differences between treatments following ANOVA. $p \leq 0.05$ was considered significant for all analyses.

RESULTS:

dsDNA in unseeded scaffolds decreased significantly by Day 7, and in seeded scaffolds increased over time and was significantly greater in PA treated scaffolds than in scaffolds containing collagen gel alone, (Figure 1a,b). There was significantly more sGAG in scaffolds containing PA treated powder than in constructs containing PBS treated powder, and in seeded scaffolds both of these groups contained more sGAG than scaffolds containing collagen gel alone. In unseeded scaffolds, sGAG decreased over 28 days, but in seeded scaffolds, sGAG was maintained through the same period, (Figure 1c,d). Collagen content was greater in scaffolds containing PA treated powder than in constructs containing PBS treated powder, or collagen gel alone, and collagen content did not change over time in culture. There was significant upregulation of Tenomodulin (TNMD), Tenascin C (TNC) and Type III Collagen (COL3) expression at Day 7 compared to Day 0. Decorin (DCN) expression was upregulated at Day 7 and 14, whereas Biglycan (BGN) expression was unchanged. Gene expression was not different between PA or PBS powder treated scaffolds and those treated with collagen gel alone.

DISCUSSION:

These data suggest that lyophilized native ligament extracellular matrix powder has the ability to enhance cellular proliferation and extracellular matrix synthesis by hASCs, but that method of matrix preparation is critical. The increase in TNMD and TNC expression, sustained increase in DCN expression and lack of detected change in BGN expression seen is consistent with ligament development rather than healing. These data support further evaluation of ligament extracellular matrix and hASCs as a component of tissue-engineered ligament constructs.

ACKNOWLEDGEMENTS:

Supported by an unrestricted fellowship grant from Synthes.

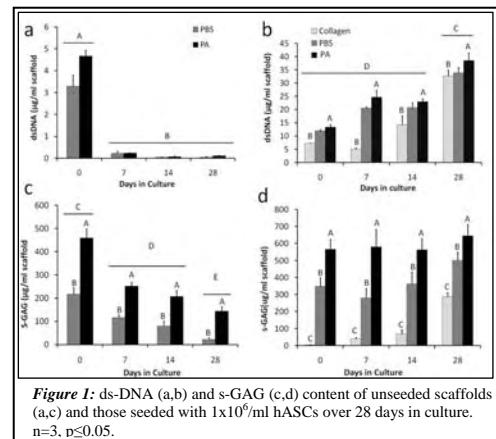


Figure 1: ds-DNA (a,b) and s-GAG (c,d) content of unseeded scaffolds (a,c) and those seeded with 1×10^6 /ml hASCs over 28 days in culture. $n=3$, $p \leq 0.05$.

ELECTROSPUN SCAFFOLDS TO SUPPORT CELLULAR DIFFERENTIATION FOR LIGAMENT TISSUE ENGINEERING

R.D Shaffer¹, L.A. Dahlgren² and A.S. Goldstein¹

1. School of Biomedical Engineering and Sciences, 2. Large Animal Clinical Sciences, Virginia-Maryland Regional College of Veterinary Medicine, Virginia Tech, Blacksburg, VA

INTRODUCTION

An estimated 100,000 anterior cruciate ligament (ACL) tears or ruptures occur each year, making it among the most common knee injuries in the United States [1]. Current reconstruction strategies are not sufficient for successful long-term clinical outcomes and a new method to repair the ACL-deficient knee is needed. Efforts to develop tissue engineered ligament replacements are numerous and are focused on the use of a biomaterial scaffold and cell source to create a neoligament. However, providing the ideal environment to promote the differentiation of stem cells and development of organized extracellular matrix (ECM) remains a challenge. Biomaterial architectures have been shown to alter stem cell differentiation, cell growth and morphology [2]. In these studies, an elastomeric poly(ester urethane urea) (PEUUR) is electrospun into fibrous scaffolds with a tailored fiber diameter and orientation. The purpose of this study was to evaluate ECM deposition and evidence of mesenchymal stem cell differentiation towards a ligament phenotype on oriented or unoriented scaffolds of varying fiber diameter.

METHODS

PEUUR was electrospun from a 4 – 17 wt% solution, to vary the fiber diameter, in hexafluoroisopropanol onto glass coverslips. Orientation was achieved using a mandrel rotating at 9.5 m/s. C3H10T1/2 cells, a mesenchymal stem cell line, were seeded onto supported scaffolds and evaluated after one week and two weeks of culture. Cells were assessed for total DNA content, expression of collagen type I α I, decorin and scleraxis using real-time PCR and deposition of collagen type I using immunohistochemistry. Controls were smooth, spincoated polymer surfaces.

RESULTS

Total DNA (cell number) was significantly reduced on the largest fiber diameter at day 3 (Figure 1). Gene expression of collagen type I α I and decorin was significantly reduced on the largest fiber diameter relative to spincoated control at day 7. Decorin and scleraxis expression increased over time in culture while collagen type I α I expression remained at similar expression levels (Figure 2). Interestingly, if the fibers were oriented within the scaffold, gene expression was largely unchanged on the differing fiber diameters.

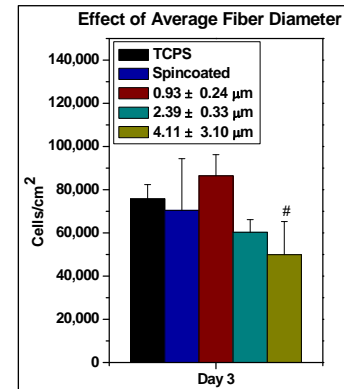


Figure 1: Cell density on scaffolds of varying fiber diameter (n=3). Mean ± std dev. # significant from smallest fiber diameter (p<0.05).

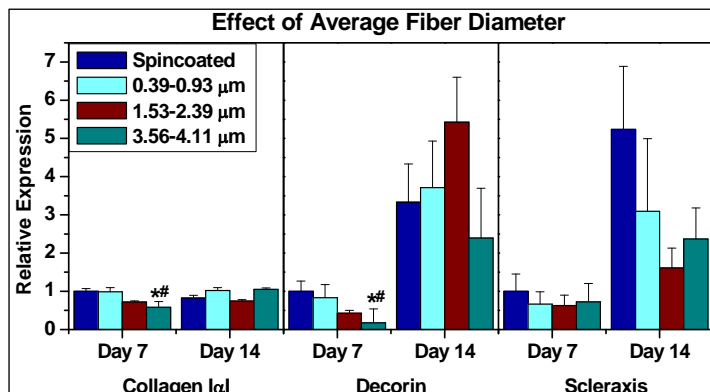


Figure 2: Gene expression of ligament ECM proteins on scaffolds of varying fiber diameter (n=6). Mean ± std dev. * significant from spincoated, # significant from smallest fiber diameter (p<0.05)

DISCUSSION

By tailoring the architecture of the biomaterial scaffold to enhance cellular responses, a suitable tissue engineered ligament replacement can be developed. The ideal ligament scaffold will have fiber morphology that maximizes ECM gene expression and protein deposition while supporting cellular growth. These studies suggest that smaller diameter fibers (< 3 μm) may be more suitable for a ligament scaffold.

REFERENCES

1. Beynon, B.D., et al., Am J Sports Med, 2005
2. Lim, J.Y. and H.J. Donahue, Tissue Eng, 2007

Notes

Notes

International Symposium on Ligaments & Tendons - IX

Las Vegas, NV

February 21, 2009

7:30 - 8:00 AM	Registration & Check-In
8:00 - 8:20 AM	Opening Ceremony, Welcome & Announcements Savio L-Y. Woo, PhD
8:20 - 9:05 AM	Podium Session 1 ACL Reconstruction Moderators: Mario Lamontagne, PhD & Giuliano Cerulli, MD
9:05 - 10:05 AM	Podium Session 2 Knee Kinematics & Mechanics Moderators: Michael Torry, PhD & Harukazu Tohyama, PhD
10:05 - 10:35 AM	Break and Poster Session 1 Moderators: Sinan Karaoglu, MD & Christos Papageorgiou, MD
10:35 - 12:05 PM	Podium Session 3 Ligament & Tendon Healing & Mechanics Moderators: Louis Soslowsky, PhD & David Butler, PhD
12:05 - 1:05 PM	Lunch and Poster Viewing
1:05 - 2:25 PM	Podium Session 4 Tendinopathy Moderators: James Wang, PhD & Albert Banes, PhD
2:25 - 3:10 PM	Podium Session 5 Biology & Biochemistry Moderators: Chih-Hwa Chen, MD & Catherine Kuo, PhD
3:10 - 3:40 PM	Break and Poster Session 2 Moderators: Stavros Thomopoulos, PhD & David Corr, PhD
3:40 - 4:25 PM	Podium Session 6 Shoulder Moderators: Evan Flatow, MD & Zong-Ming Li, PhD
4:25 - 5:40 PM	Podium Session 7 Functional Tissue Engineering-Bioscaffolds Moderators: Martha Murray, MD & Helen Lu, PhD
5:40 - 5:50 PM	Closing Remarks Savio L-Y. Woo, PhD
6:45 PM	Banquet